UNIVERSITY OF BIRMINGHAM

wellcome trust

HEPATITIS C TRANSMISSION USING LYMPHOCYTES AS VECTORS: MECHANISM AND THERAPEUTIC INTERVENTIONS

AND

NEUTROPHIL RECRUITMENT TO MICROVASCULAR ENDOTHELIUM: THE IMPACT OF MESENCHYMAL STEM CELLS

by Kristina Petrovic

A thesis submitted to the University of Birmingham for the degree of
Masters by Research (MRes)

School of Immunity and Infection
College of Medical and Dental Sciences
University of Birmingham
May 2014

UNIVERSITY OF BIRMINGHAM

HEPATITIS C TRANSMISSION USING LYMPHOCYTES AS VECTORS: MECHANISM AND THERAPEUTIC INTERVENTIONS

by Kristina Petrovic

This project is submitted in partial fulfilment of the requirements for the award of the MRes

wellcome trust

School of Immunity and Infection
College of Medical and Dental Sciences
University of Birmingham
May 2014

ABSTRACT

Hepatitis C virus (HCV) causes hepatitis C, a chronic liver condition that represents a global health burden with no optimal therapeutic agents and no vaccine available. Recent findings suggest that, apart from infecting hepatocytes directly, HCV can be transmitted from B-lymphocytes to hepatocytes in a process called trans-infection. This project characterises trans-infection further by examining the receptors and cell components involved in HCV transmission from B- and T-lymphocyte cell lines to hepatoma cells. Our results suggest both lymphocyte classes are equally capable of trans-infection, which can be significantly reduced in the presence of HCV entry receptor inhibitors or HCV-specific neutralising antibodies. The actin cytoskeleton of the target hepatocyte is also involved, although seemingly not through uptake of either live or dead lymphocytes. Further work is needed to fully characterise lymphocyte-mediated HCV infection of liver cells. This would provide us with crucial new insights into the varied modes of HCV transmission, with a view to designing more effective therapeutic approaches in the future.

ACKNOWLEDGEMENTS

I would like to thank my supervisor, Dr Zania Stamataki, for the immeasurable support, guidance and wealth of knowledge she provided me with during this project. I also extend my thanks to all the staff and students at the Centre for Liver Research who took their time to assist me in my very first scientific research study.

Table of Contents

List of figures and tables

FIGURES

TABLES

1. INTRODUCTION

Hepatitis C virus (HCV) is the cause of multiple chronic liver-associated pathologies with a huge impact on the sufferers' quality of life on a global scale. Current antiviral treatments are suboptimal, and there is no vaccine yet that could confer protection against its numerous and highly variable strains. HCV gains entry into the liver in a complex process which researchers have yet to elucidate fully (Lindenbach & Rice 2013), and ever increasing evidence suggests that the virus is also able to infect by direct cell-to-cell transmission (Timpe *et al.* 2008). Recent work has highlighted yet another mechanism of transmission – trans-infection of liver cells by HCV-carrying B-lymphocytes – but little is known about the receptors and factors involved in this process (Stamataki *et al.* 2009). This project aims to investigate the mechanism of lymphocyte-mediated HCV trans-infection in further detail, and discover whether T-lymphocytes can also be vehicles for HCV transmission to liver cells.

1.1 HCV importance, structure and cell culture systems

HCV infects approximately 170 million people, or ~3% of the global population (Mittapalli *et al*. 2011; Meredith *et al*. 2012). While HCV infection can be acute, around 60-80% of all cases progress onto chronic hepatitis C, which can in turn lead to liver steatosis, cirrhosis, hepatocellular carcinoma and liver failure within 10-30 years of initial infection. This makes HCV a top indicator for liver transplantations worldwide (Meredith *et al*. 2012; Wilson & Stamataki 2012; Lindenbach & Rice 2013; Rupp & Bartenschlager 2014). Despite the slow progression of HCV-mediated liver damage, newly transplanted livers become re-infected with circulating HCV within weeks, eventually leading to graft failure and, consequently, reduction in patient

survival (Ciesek & Wedemeyer 2012; Wilson & Stamataki 2012). Furthermore, the mainstay of current HCV therapy – pegylated interferon-α with ribavirin – is not equally effective in all patients and carries substantial risk of side effects such as haemolytic anaemia and psychiatric disorders (Meredith *et al*. 2012; Rupp & Bartenschlager 2014). New direct-acting antivirals (DAA), the first ones of which were telaprevir and boceprevir, were approved in 2011 and directly targeted viral proteins necessary for the HCV life cycle. These led to higher rates of sustained virological response (SVR) in patients, but mainly in those infected with HCV genotype 1; in addition, they showed greater propensity towards side effects and development of viral resistance (Rupp & Bartenschlager 2014). It is not surprising, therefore, that much effort is going into developing new antiviral treatments and vaccines. For these efforts to succeed, reliable models of HCV replication *in vitro* and *in vivo*, together with a better understanding of the life cycle of the virus, are both needed.

HCV is the sole member of the *Hepacivirus* genus within the *Flaviviridae* family of viruses. It is highly variable – its naturally occurring forms exhibit at least six major, distinct genotypes (Lindenbach *et al*. 2005), with genotypes 1 and 2 being distributed worldwide (Kato *et al*. 2003). HCV is an enveloped, positive-strand RNA virus, the genome of which is translated into a single polyprotein subsequently cleaved into individual structural or non-structural (NS) proteins (Lindenbach & Rice 2013). The structural proteins are an integral part of the virus particle and include the ‘core’ protein, which forms the capsid, and the two glycoproteins, E1 and E2. The NS proteins, on the other hand, do not integrate into the virus, instead performing

functions related to HCV replication inside the host cell. These are p7, NS2, NS3, NS4A and NS5A and –B (Lindenbach & Rice 2013).

1.1.1 The evolution of the HCV cell culture system

The study of the complex life cycle of HCV *in vitro* has historically been hampered by the inability to reproduce its many aspects in cell culture. The first functional complementary DNA (cDNA) clone of HCV genotype 1a was synthesised in 1997, and its RNA transcripts exhibited viral replication in the liver of a chimpanzee after direct intrahepatic injection (Yanagi *et al*. 1997; Kolykhalov *et al*. 1997). This was followed by generation of 'subgenomic replicons', or units of HCV RNA capable of autonomous replication. While these allowed for examination of HCV replication in cell culture, productive infection was not established (e.g. reviewed in Lohmann 2009). Infectious (pseudo)-virus was first produced by displaying HCV glycoproteins E1 and E2 onto a retro- or lentiviral core, generating the so-called HCV pseudo-particles (HCVpp). These were capable of entering primary hepatocytes and allowed for examination of putative receptors for HCV cell entry, but were not able to establish a spreading infection (Bartosch *et al*. 2003). It was not until 2005 that a full-length HCV genome, capable of both replication and transmission of infection in cell culture (HCVcc), was generated (Lindenbach *et al.* 2005; Wakita *et al.* 2005). Lindenbach *et al.* also demonstrated that the newly produced HCVcc infectious clone, which they named J6/JFH, established productive infections in chimpanzees and in immunodeficient mice with human liver grafts (Lindenbach *et al*. 2006).

Most studies of HCVcc are performed on the Huh-7 hepatoma cell line which, while supportive of HCV replication (Blight *et al*. 2002), lacks some of the key features of primary hepatocytes, such as the ability to polarise or to form tight junctions (Mee *et al*. 2008). As such, it is unclear how representative the *in vitro* results are of the *in vivo* infection. The ideal study system is the liver itself, although its complexity and the activation of non-hepatocytes (e.g. endothelial cells, Kupffer cells) during inflammation introduces problems into the design of representative *in vitro* models (Meredith *et al*. 2012). There have, however, been advances in this field, such as co-cultures of primary human hepatocytes and supportive stroma which were able to support HCV replication (Ploss *et al*. 2010). Suitable small animal models are also in development. For example, a recent study found that genetically humanised mice with blunted antiviral immunity were able to sustain HCV viraemia for several weeks, and even produce new infectious particles inhibited by DAA treatment (Dorner *et al*. 2013).

Regardless of the difficulties surrounding the study of the full HCV life cycle, the conserved nature of the first step in the cycle – host cell entry – has generated great interest due to its potential as a therapeutic target (Meredith *et al*. 2012). Studying it further will provide us with valuable insight into the complex mechanism employed by HCV to establish a productive infection.

1.2 Mechanism of HCV cell entry

While circulating in the blood, HCV comes into contact with the basolateral surface of hepatocytes, where its attachment and entry is initiated (Lindenbach & Rice 2013).

The attachment happens *via* interaction of the virus with low-density-lipoprotein receptor (LDLR) and glycosaminoglycans (GAG) on the hepatocyte cell surface, as evidenced by anti-LDLR antibody and desulfation of GAG both significantly reducing HCV adsorption *in vitro* (Germi *et al*. 2002). In addition, five surface molecules are needed for HCV to gain entry: CD81, scavenger receptor class B type I (SR-BI), claudin-1 (CLDN1), occludin (OCLN) and Niemann-Pick C1-like-1 (NPC1L1) (Lindenbach & Rice 2013) **(Figure 1)**. Following successful attachment, the virus is internalised through the process of clathrin-mediated endocytosis. This was shown by inhibition of HCVcc entry into Huh-7 by either small interfering RNA (siRNA)-mediated clathrin heavy chain depletion, or chlorpromazine-mediated inhibition of clathrin-coated pit formation (Blanchard *et al*. 2006). HCV also requires acidification of its endosomal compartment in order to fuse with the endosomal membrane and expel its genetic material into the cytosol (Tscherne *et al*. 2006). For example, pre-treating Huh-7 or Huh-7.5 cells (Huh-7 cells cured with interferon as described by Blight *et al*. 2002) with bafilomycin A1, a vacuolar ATPase inhibitor known to impact endosome acidification, inhibited HCVcc entry into the host cell (Blanchard *et al*. 2006; Tscherne *et al*. 2006).

1.2.1 The roles of CD81 and SR-BI in HCV entry

The first HCV receptor to be discovered was CD81, a tetraspanin (surface protein containing four membrane-spanning domains) ubiquitously expressed in the body, including on hepatocytes and B-lymphocytes (Pileri *et al*. 1998). It was found to bind to the HCV glycoprotein E2; furthermore, HCV-neutralising antibodies *in vivo* also inhibited virus attachment to CD81 *in vitro* (Pileri *et al*. 1998). While it is located on

the surface of many different cell types and thus makes an inherently poor drug target, CD81 may help define HCV species preference, or tropism, for human hepatocytes. For example, mice expressing human CD81 and OCLN in the liver became infected with HCV (Dorner *et al*. 2013). On the other hand, it has been shown that, while necessary, CD81 alone is not sufficient for HCV cell entry (Bertaux & Dragic 2006). Through a series of genetic mutations and imaging techniques, researchers demonstrated that CD81 associates with CLDN1 on the basolateral surface of the polarised HepG2 cell line in order to mediate HCV entry (Harris *et al*. 2010). In addition to its clearly diverse roles, CD81 may prime HCV glycoproteins for activation by low endosomal pH, as shown by the ability of soluble CD81 to sensitise virus particles to acid (Sharma *et al*. 2011).

SR-BI is highly expressed on hepatocytes, where it has a significant role in cholesterol uptake from its transport lipoproteins (Acton *et al*. 1996). It was identified as an important co-receptor for HCV entry when recombinant HCV E2 was shown to bind to it on HepG2 cells which do not express CD81 (Scarselli *et al*. 2002). Moreover, this interaction was highly selective, as neither the closely related human scavenger receptor CD36 nor mouse SR-BI were found to bind to E2 (Scarselli *et al*. 2002). This, coupled with its high expression levels in the liver, may help define HCV hepatotropism (Lindenbach & Rice 2013). SR-BI is also responsible for initial HCV attachment *via* binding to viral apolipoproteins (e.g. apolipoprotein E, apoE), and initiates lipid transfer required for productive infection to be established (Dao Thi *et al*. 2012). It is only after this that the SR-BI/E2 interaction takes place and causes a conformational change in E2 that allows HCV to bind to CD81 (Dao Thi *et al*. 2012).

This is another example of the surface receptors communicating in order to mediate viral entry.

1.2.2 HCV cell-to-cell transmission

The HCV entry model shown in Figure 1 constantly changes to accommodate the ever-expanding knowledge on the process. For example, recent evidence has emerged of the capacity of HCV for direct cell-to-cell transmission, thus enabling it to evade the host's humoral immune response (Timpe *et al.* 2008; Carloni *et al.* 2012; Meredith *et al.* 2012). The first report of this phenomenon *in vitro* described the HCV-infected, human B lymphoblastoid TO.FE cell line transmitting the virus to co-cultured human HepG2 hepatoma cells through direct cell contact (Valli *et al*. 2006). HepG2 did not express LDLR or CD81 and were thus non-permissive to cell-free HCV infection; this model, therefore, showed that hepatoma HCV permissiveness can be achieved by cell-to-cell contact with infected human B-lymphocytes (Valli *et al*. 2006). CD81, SR-BI, CLDN1 and OCLN were all found to be necessary for the cell-to-cell route of infection in Huh-7.5 cells (Brimacombe *et al*. 2011). In addition, SR-BI inhibition by antibodies and small molecules preferentially inhibited HCV cell-to-cell transmission, highlighting the significance of this surface receptor in this particular transmission route (Brimacombe *et al*. 2011).

The studies above clearly show the mechanisms of HCV transmission are varied and complex, potentially presenting problems in the design of new therapeutic agents. Moreover, the ability of the virus to infect hepatocytes by transmission from B-lymphocytes, as initially demonstrated by Valli *et al.* in 2006, has recently received

more attention as another potentially inhibitable route this virus takes in the body. This infection of a cell by contact with another, infected cell rather than the infectious agent (i.e. virus) itself has been termed *trans-infection*.

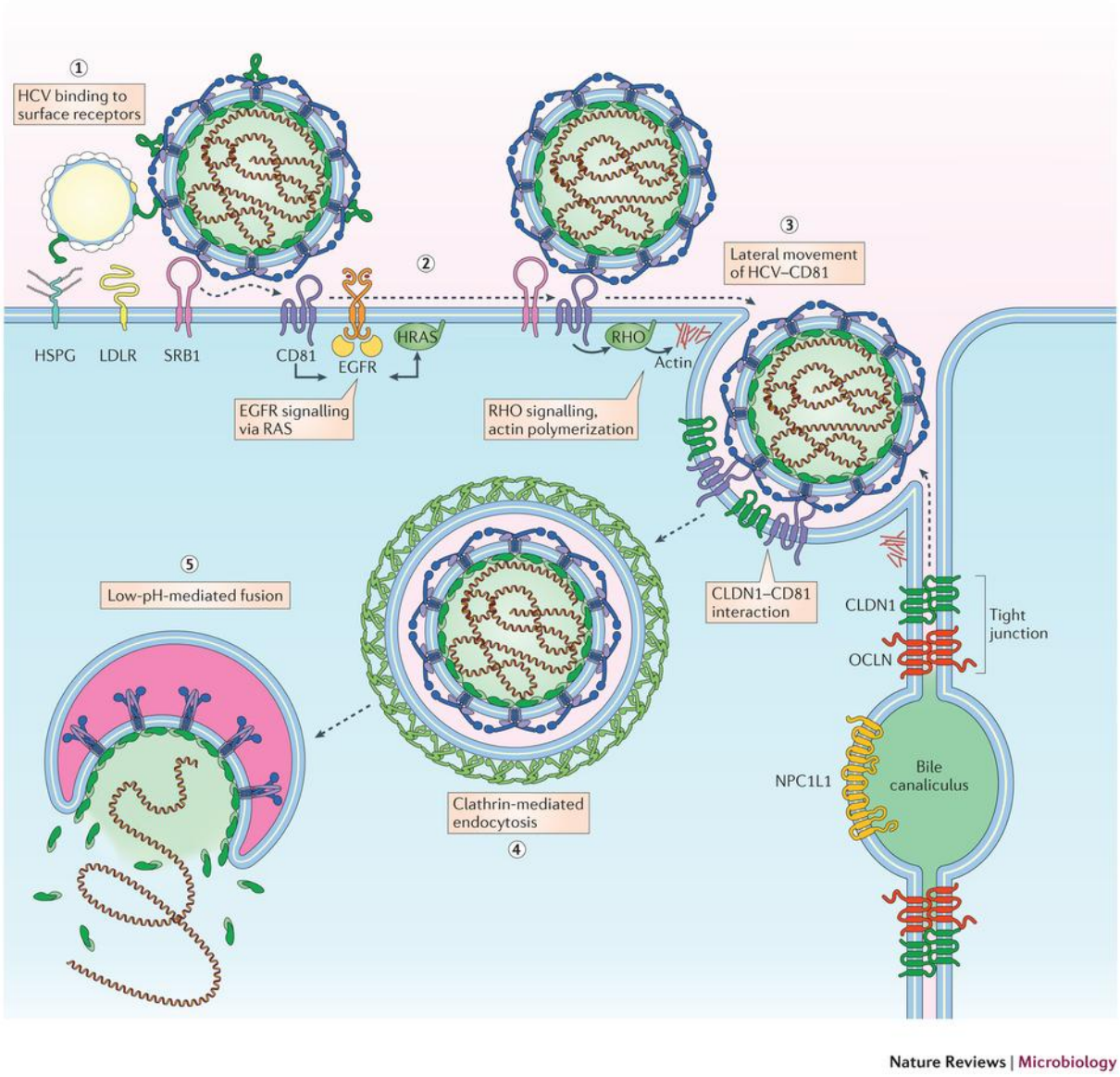

Figure 1 – The integrated model of HCV cell entry.
HCV engages in a series of temporally and spatially ordered interactions with several entry factors in order to enter hepatocytes. Lipoprotein-associated viral particles interact with SR-BI, LDLR and GAG present on heparan sulphate proteoglycans (HSPG) to mediate initial attachment. SR-BI then engages in lipid transfer to possibly dissociate HCV from its lipoproteins, which exposes the CD81-binding domain on the HCV E2 glycoprotein. This activates signal transduction through epidermal growth factor receptor (EGFR), HRAS GTPase and RHO GTPases, which remodel actin filaments to allow CD81-bound virus to be transported laterally to tight junctions. Here HCV-CD81 and CLDN1 interact to induce clathrin-mediated endocytosis. E2-CD81 interactions within the endosome may prime the glycoprotein response to low endosomal pH, inducing HCV fusion with the endosomal membrane and the release of its RNA into the cytosol, ready for translation to viral protein. The roles of OCLN and NPC1L1 in the entry process are not fully understood yet.

1.3 Lymphocyte-mediated HCV trans-infection

The viral infection of and transmission between lymphocytes is not a new concept. Rappocciolo *et al.* demonstrated that both HIV-1 and human herpesvirus-8 (HHV-8) could infect activated B-lymphocytes by endocytosis mediated by dendritic cell-specific ICAM-3 grabbing nonintegrin (DC-SIGN) expressed on B-lymphocyte surface. In the case of HIV-1, this process further led to trans-infection of T-lymphocytes with the virus (Rappocciolo *et al*. 2006; Rappocciolo *et al*. 2008). Pre-treating B-cells with anti-DC-SIGN antibody blocked both HIV-1 trans-infection of T-cells and HHV-8 infection of B-cells (Rappocciolo *et al*. 2006; Rappocciolo *et al*. 2008). In the case of HCV, however, it was shown that HCVcc failed to replicate in primary B- and T-lymphocytes, and HCVpp did not infect a B-cell line that expressed high levels of CD81, SR-BI and CLDN1 (Marukian *et al*. 2008). Despite its inability to establish a productive infection in lymphocytes, it was found that B-cell-associated HCV readily infected hepatoma cells with increased specific infectivity (ratio of infectious virus particles to genomic RNA) compared to cell-free infection (Stamataki *et al*. 2009). Antibody neutralisation of SR-BI and C-type lectins DC-SIGN and L-SIGN on B-lymphocyte surface significantly reduced B-cell-mediated HCV trans-infection, while HCV-specific neutralising antibodies failed to do the same. This was consistent with HCV being internalised by B-lymphocytes in this process (Stamataki *et al*. 2009). The internalisation was confirmed in a further study when anti-CD20 antibody rituximab, which causes B-cell lysis, led to an increase in infectious HCV released from these cells *in vitro* (Stamataki *et al*. 2011).

Recent work carried out by our group suggests that T-lymphocytes may also facilitate *in vitro* trans-infection of permissive Huh-7 and polarised HepG2-CD81 hepatoma cell lines (Stamataki *et al.* 2013, manuscript in preparation). There is, however, a paucity of information regarding the mechanism of trans-infection using lymphocytes as vectors. Speculation is further complicated by our lack of knowledge of the molecular processes that govern lymphocyte-hepatocyte interactions. Unanswered questions that stem from recent work include: i) Is lymphocyte-hepatocyte contact required for virus transmission? ii) Is trans-infection an active process and iii) is it receptor-mediated? iv) Can we inhibit trans-infection by virus-specific neutralising antibodies? Elucidation of why HCV B- and T-lymphocyte-mediated trans-infection offers an advantage for HCV infection of hepatomas compared to cell-free virus is a worthwhile avenue of further research.

1.4 Hypothesis and aims

Building on the work described above, we aimed to characterise the mechanism of lymphocyte trans-infection of hepatomas by HCVcc. We hypothesised that trans-infection was an active process, which would be sensitive to therapeutic interventions. Our specific objectives were the following:

- To compare live and dead B- and T-lymphocyte cell lines as vectors for HCVcc transmission to Huh-7;
- To investigate if viral entry receptors CD81 and SR-BI on hepatomas play a role in trans-infection;
- To examine the effect of HCV-specific neutralising antibodies on HCV trans-infection of Huh-7 by B- and T- cell lines;

- To establish the effect of chemical and cytokine treatment on HCV trans-infection of Huh-7 by live or dead B- and T-lymphocyte cell lines.

2. MATERIALS AND METHODS

2.1 Culture of hepatoma and lymphocyte cell lines

Huh-7 hepatoma cells were cultured in Dulbecco's modified Eagle medium (DMEM) supplemented with 10% foetal bovine serum (FBS), 1% penicillin with streptomycin, 1% non-essential amino acids and 1% L-Glutamine (all Gibco, Life Technologies, Paisley, UK). The cells were incubated at 37°C in 5% CO_2 when not in use and passaged two to three times a week to maintain viability and optimal growth conditions.

Four B-lymphocyte (L3055, Raji, DG75 and KEM) and one T-lymphocyte cell line (Jurkat) were used. These were all cultured in Roswell Park Memorial Institute (RPMI) medium (Gibco) supplemented in the same way as DMEM above. They were kept in the same conditions and passaged with approximately the same frequency as Huh-7.

2.2 HCVcc trans-infection and lymphocyte entry assays

Before each experiment, Huh-7 cells were incubated with 0.25% trypsin-EDTA solution (Gibco) for four minutes to detach them from the flask. 10% FBS/DMEM was subsequently added to neutralise trypsin and prevent permanent cell damage. Cells were counted using a haemocytometer, with the addition of trypan blue (Sigma-Aldrich, Poole, UK) to visualise dead cells. The amount of Huh-7 needed for each experiment was then removed from suspension and diluted to the appropriate volume with 10% FBS/DMEM before being seeded in 24- or 96-well plates as

required. The seeding density was chosen so as to give the cells enough space to grow and multiply for 48-72h. Previous lab experience showed that the adequate quantities for this were $3x10^4$ and $0.75x10^4$ Huh-7/well for a 24-well and 96-well plate respectively.

B- and T-lymphocytes were counted in the same way as Huh-7 (trypsin-EDTA was not used as these cells do not adhere to plastic). The required quantities were either left viable or heat-killed by being exposed to a temperature of 56°C on a heat block for 30 minutes. Live or dead lymphocytes were subsequently incubated with HCVcc and added to Huh-7 (see **section 2.2.1**), or alternatively added directly to hepatoma cells (see **section 2.2.2**). The number of lymphocytes added per well was $0.5\text{-}1x10^6$ or $0.25x10^6$, depending on whether Huh-7 were seeded in 24- or 96-well plates, respectively.

2.2.1 Trans-infection assays and fluorescent imaging

After seeding in 96-well plates, Huh-7 were incubated at 37°C for 24h to allow the cells to adhere to the plastic. After 24h various treatments with inhibitors, cytokines or antibodies (see **section 2.3**) were added to the cells for 1h before being washed off and replaced with 10% FBS/DMEM. At the same time, both live and dead B- and T-lymphocytes were incubated with the SA13/JFH strain of HCVcc at 37°C for 2h in the category 3 containment level laboratory to allow the lymphocytes to take up the virus. Infected cell suspensions were then washed five times using 10% FBS/RPMI to remove any viral particles that did not bind. These HCVcc-carrying lymphocytes, or the virus alone for comparison, were subsequently added to the pre-treated Huh-7.

The whole plate was incubated for 48h to allow hepatoma infection, or for 72h to allow infection and virus spread to surrounding hepatomas. At the end of the incubation, the cells were fixed by adding ice-cold methanol for 5 minutes before replacing it with phosphate-buffered saline (PBS; Gibco). In order to visualise infected Huh-7, the following labelling protocol was performed:

1) Primary mouse immunoglobulin G3 (IgG3) antibody binding to HCV NS5A protein (gift from Jane McKeating, University of Birmingham) was added for 30 minutes before being washed off;
2) Secondary anti-mouse IgG3 antibody conjugated to Alexa Fluor® 488 green dye (Invitrogen, Life Technologies, Paisley, UK) was added for 30 minutes before being washed off and replaced with PBS.

The plate was then ready for examination using a Nikon fluorescent microscope. The number of green-fluorescing clusters of infected cells, called focus-forming units (FFU) (**Figure 2**), was determined for each well, and means were calculated from two or three replicates for each condition.

2.2.2 Lymphocyte entry assays and confocal imaging

A series of assays on lymphocyte entry into hepatomas was run in parallel with trans-infection assays in order to establish a possible correlation between the mechanisms of entry and trans-infection. For this set of experiments we only used Jurkat T-lymphocytes. To visualise their entry into hepatomas, Huh-7 cells and Jurkat T-cells were labelled using CellTracker™ Green CMFDA and CellTracker™ Red CMTPX (both Invitrogen) respectively. Briefly, the cells would be placed in 5μM CellTracker™ solution in serum-free media (SFM) for 45 minutes, after which SFM would be

replaced with 10% FBS/DMEM to quench the labelling reaction. Once all the cells were appropriately labelled, Huh-7 were seeded onto glass coverslips in a 24-well plate and placed in SFM for 1h, while Jurkat T-cells were either left alive or heat-killed as described. Following serum starvation of Huh-7, reagents that either boosted or inhibited lymphocyte uptake by hepatomas (see **section 2.3**) were added to the wells for 1-2h before being washed off and replaced with 10% FBS/DMEM. Live or dead T-lymphocytes were then incubated with Huh-7 for 2-4h to allow their entry into the hepatomas. The cells were subsequently fixed with methanol or 1% paraformaldehyde (PFA; Sigma-Aldrich, Poole, UK) as described in section 2.2.1.

We left some wells lymphocyte-free to help us visualise the actin cytoskeleton and the nuclei of the hepatomas and thus gain a better understanding of the action of the reagents on these cell components. To do this, we added 0.3% Triton™-X 100 (Sigma-Aldrich) in PBS to PFA-fixed Huh-7 for 5 minutes to render them permeable to dye. The detergent was then removed and a PBS solution of red Alexa Fluor® Phalloidin 568 (Life Technologies, Paisley, UK) applied for approximately 1h to allow phalloidin to bind to F-actin inside the cell. This was also removed and followed by application of the blue nuclear stain, DAPI (Life Technologies) in PBS for 5 minutes. Once the staining was complete, the glass coverslips were mounted onto slides using Fluorescence Mounting Medium (Dako, Ely, UK) and examined using a confocal microscope (LSM780, Carl Zeiss). The images were obtained and analysed using ZEN software (**Figures 3 and 4**).

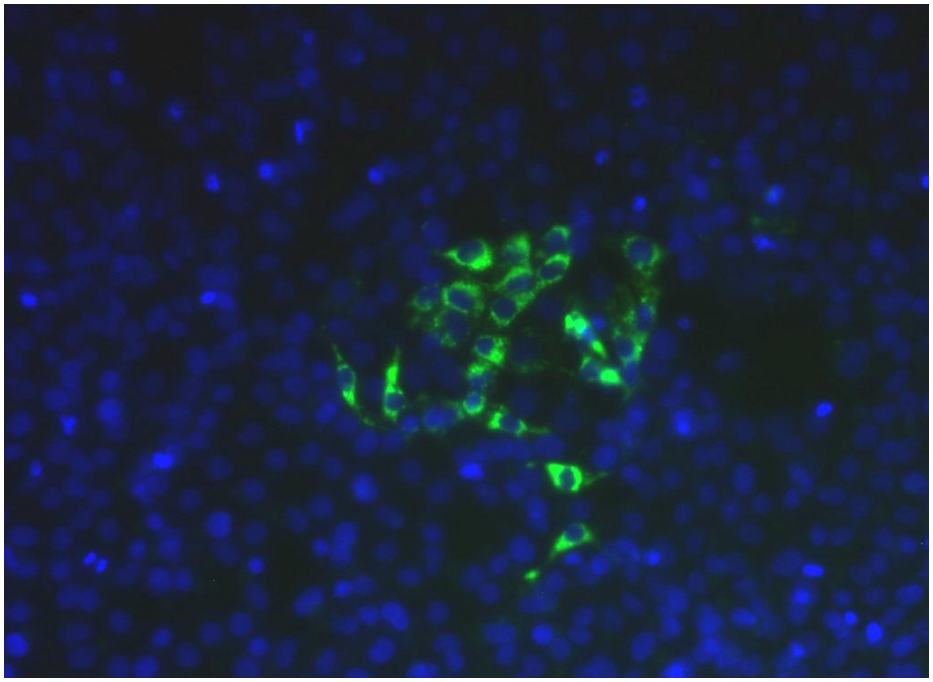

Figure 2 – Defining a focus-forming unit of HCVcc-infected Huh-7 cells.
Huh-7 cells were incubated with live or dead HCVcc-carrying B- or T-lymphocytes for 72h. The cells were subsequently fixed with methanol and stained using primary mouse anti-NS5A IgG3 and secondary anti-mouse IgG3 conjugated to Alexa Fluor 488 green dye. The cells were then studied using a Nikon fluorescent microscope. Cell nuclei can be seen in blue (DAPI). Clusters of infected cells called focus-forming units (FFU) were apparent when Huh-7 successfully transmitted the infection to neighbouring cells. Single infected cells were also observed when transmission was poor (not shown).

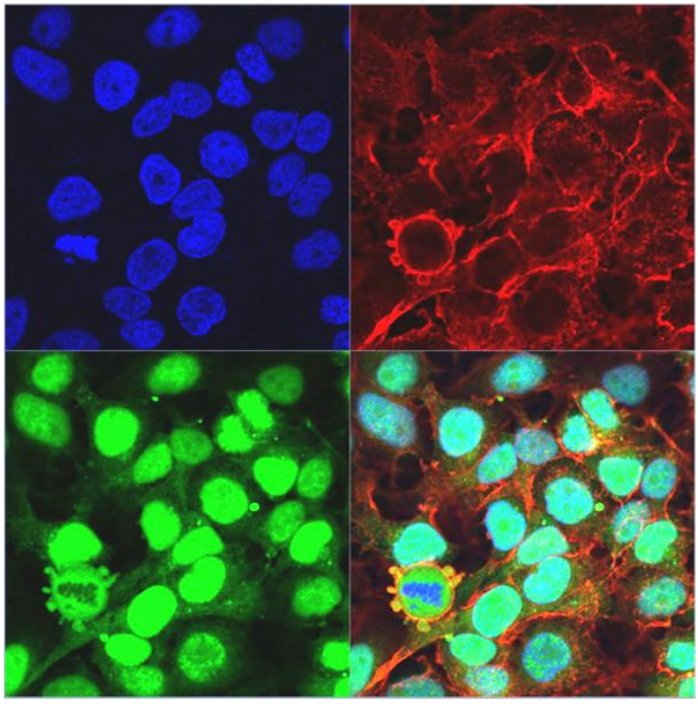

Figure 3 – Imaging F-actin in Huh-7 cells.
Huh-7 cells were stained using CellTracker™ Green CMFDA, and their actin cytoskeleton and nuclei visualised with red Alexa Fluor Phalloidin 568 and blue DAPI dye, respectively. From top left: Huh-7 nuclei (blue), actin cytoskeleton (red), cytoplasm (green) and merged image of a Huh-7 monolayer.

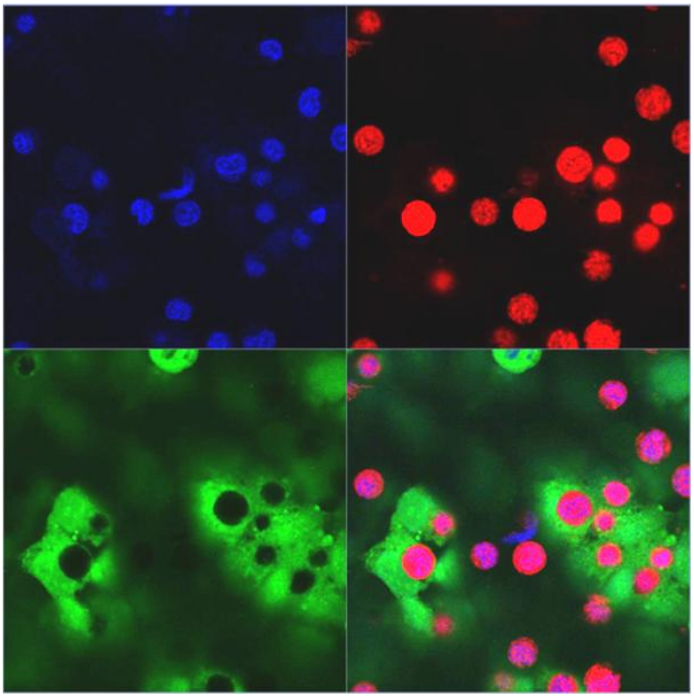

Figure 4 – Imaging phagocytosis of dead lymphocytes in Huh-7 cells.
Huh-7 and Jurkat T-cells were stained using CellTracker™ Green CMFDA and CellTracker™ Red CMTPX respectively before being incubated together to allow the lymphocytes to enter the hepatoma cells. The nuclei of all cells were visualised with blue DAPI dye. From top left: cell nuclei (blue), dead Jurkat T-lymphocytes (red), Huh-7 cytoplasm (green) with obvious vacuoles where T-lymphocytes have internalised, and merged image showing phagocytosis of dead Jurkat T-cells by the hepatoma cells.

2.3 Reagents

As part of trans-infection assays, Huh-7 were treated with chemicals and cytokines that could impact on their ability to take up extracellular material – in this case, lymphocytes and viral particles. Additionally, a SR-BI inhibitor and antibodies against HCV itself or CD81 were also tested. The specific reagents, their exact functions and concentrations are listed in **Table 1**.

In addition to some of the reagents above, actin polymerisation inhibitors were added to Huh-7 in lymphocyte entry assays, with the aim of assessing the impact this had on the ability of hepatomas to engulf lymphocytes. These inhibitors and their working concentrations are listed in **Table 2**.

2.4 Statistical analysis

All data were analysed using GraphPad Prism 5 and expressed as mean ± standard error of the mean (SEM). Analysis of variance (ANOVA) was used to assess variation between multiple conditions and Bonferroni post-tests to compare individual treatments, as appropriate. Statistical significance was assumed if $P < 0.05$. Where ANOVA did not show statistical significance for any of the parameters, no mention of it was made in the figure legends.

Table 1 – Chemical treatments, cytokines and antibodies added to Huh-7 cells during trans-infection assays

Reagent	Function	Manufacturer	Working concentration
Chemicals/cytokines			
Amiloride	Macropinocytosis inhibitor	Sigma-Aldrich	0.5mM
Bafilomycin A1	Endosome acidification inhibitor	Sigma-Aldrich	100nM
ITX5061	SR-BI inhibitor	iTherX, San Diego, California, USA	10-20µM
Secretory leukocyte protease inhibitor (SLPI)	Phagocytosis potentiator	PeproTech, Rocky Hill, New Jersey, USA	1µM
Tumour necrosis factor α (TNFα)	Phagocytosis potentiator	"	10ng/mL
Antibodies			
Anti-CD81 clones 2-s131 and 2-s337	Anti-CD81 IgG	McKeating, University of Birmingam, UK	5µg/mL
BT003	HCV-specific polyclonal human IgG	Biotest, Solihull, UK	100µg/mL
BT001	Non-specific polyclonal human IgG (isotype control for BT003)	"	100µg/mL
Nanobody	Broadly neutralising HCV-specific heavy-chain antibody	The University of Nottingham, UK	100µg/mL

Table 2 – Actin polymerisation inhibitors added to Huh-7 cells during lymphocyte entry assays

Inhibitor	Manufacturer	Working concentration
Cytochalasin-D	Cambridge Bioscience, Cambridge, UK	10µM
Latrunculin-A	"	1µM

3. RESULTS

3.1 HCVcc-carrying dead lymphocytes can lead to efficient trans-infection of hepatoma cells

Previous work from our laboratory has shown that B-cells (Stamataki *et al.* 2009) and T-cells (unpublished) can transmit HCVcc *in trans* to hepatoma cells *in vitro*. We first set out to investigate if the lymphocytes needed to be alive for this trans-infection to occur. We added live or dead HCVcc-carrying B-lymphocytes to Huh-7 cells seeded in a 24-well plate, allowed infection to occur for 72h and then fixed and stained cells for viral protein to measure infection. Four different B-lymphocyte cell lines – Raji, L3055, DG75 and KEM – were used for comparison, and infection was quantified as FFU/well (**Figure 5A**). Trans-infection by live cells indicated that Raji cells and, to a lesser extent, DG75 cells, but not L3055 or KEM cells were capable of trans-infection. Interestingly, heat-killed lymphocytes apart from KEM cells all transmitted HCVcc infection at similar levels – about two-fold less than transmission seen by live Raji cells. Live or dead KEM cells did not transmit infection, indicating that this cell line may not capture HCV. This experiment shows that heat-killed lymphocytes can transmit HCVcc infection to hepatomas *in vitro*.

To further characterise the infection established by each type of B-lymphocyte, the size of the foci was also measured. Since FFU consisting of two cells were most likely derived from one infected cell which subsequently underwent division, the foci which contained more than two fluorescing cells at 72h post-infection were considered to show actual transmission of the virus. These large, or ‘transmitting’

foci, were counted for each type of B-lymphocyte apart from KEM (see above), and their number compared to the total number of foci in order to get an estimate of percentage of transmission (**Figure 5B**). This was close to 40% for all but the live L3055. Importantly, the difference in transmission between live and dead B-cells was not significant for any of the three cell lines, showing that the presence of dead lymphocytes in co-culture with hepatomas can also lead to efficient HCVcc transmission.

Raji and L3055 cells, showing the highest and lowest trans-infection potential respectively, were used for further studies. The same set of experiments was repeated with these two cell lines and the Jurkat line of T-lymphocytes, in order to compare the trans-infection potential of B- and T-cells. Huh-7 were seeded in a 96-well plate in this and all subsequent trans-infection assays, resulting in lower numbers of lymphocytes used per well – this is reflected in the results.

Consistent with previous findings, the presence of live Raji cells resulted in significantly greater numbers of infected FFU compared to dead Raji (**Figure 6**). L3055, on the other hand, transmitted the infection to Huh-7 to approximately the same extent whether live or dead. Jurkat T-cells exhibited a very similar trans-infection pattern to that of the Raji. Even though the number of infected foci was not high for any of the dead cell lines examined, it was still significant enough to establish a successful infection. This indicated, once again, that the presence of virus-carrying lymphocytes can result in successful HCVcc infection of Huh-7 even when the vehicles for that infection have been killed.

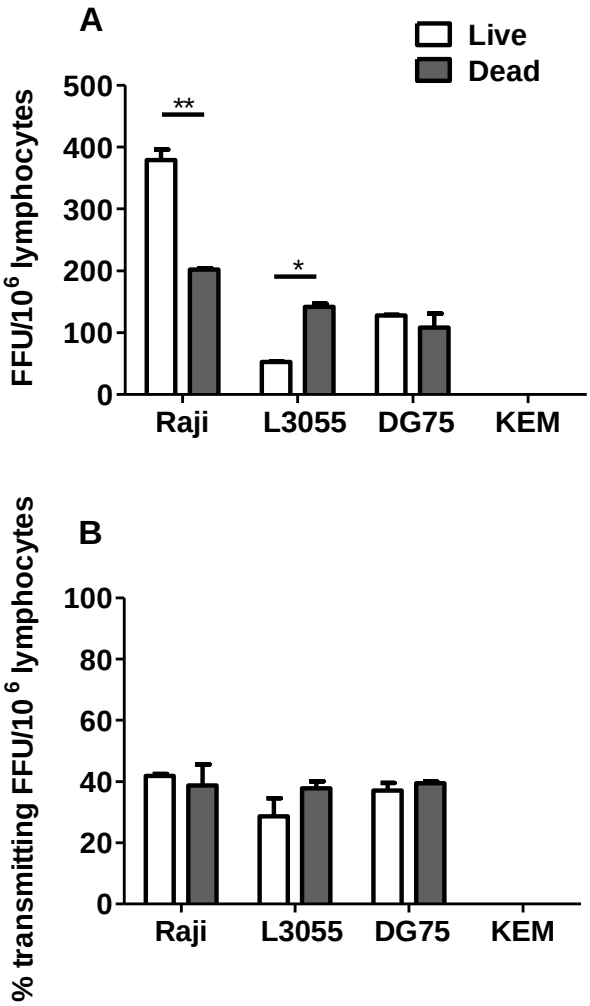

Figure 5 – Dead lymphocytes can trans-infect Huh-7 cells with HCVcc.
Four different B-lymphocyte cell lines (Raji, L3055, DG75 and KEM) carrying HCVcc were added to Huh-7 (10^6 lymphocytes/well) to assess the potential of lymphocytes to transmit HCV infection to hepatomas. Infection was allowed to occur for 72h and was measured by NS5A staining. **(A)** Average number of infected focus-forming units (FFU)/well after treatment with either live or dead B-lymphocytes of each cell line. Two-way ANOVA showed a significant effect of both B-lymphocyte type ($P<0.0001$) and viability ($P<0.05$) on trans-infection. * = $P<0.05$ and ** = $P<0.01$ by Bonferroni post-tests. **(B)** Average percentage (from total FFU) of FFU showing transmission (>2 infected cells/focus) after treatment with either live or dead B-lymphocytes of each cell line. Two-way ANOVA showed a significant effect of B-lymphocyte type ($P<0.01$), but not viability, on trans-infection. Data are mean ± SEM from two replicates, n=1.

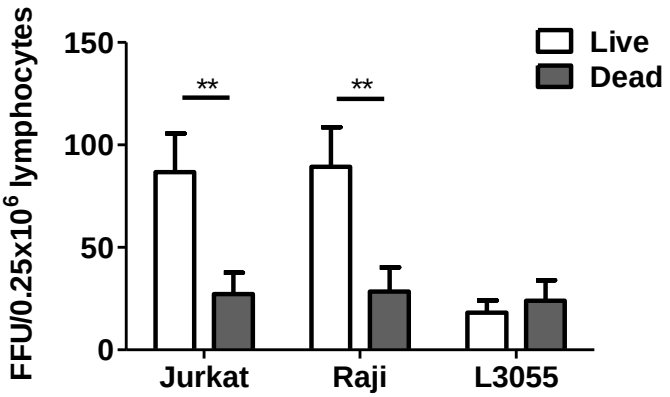

Figure 6 – Live and dead T-lymphocytes as well as B-lymphocytes can trans-infect hepatomas with HCVcc.

Jurkat T-lymphocytes and Raji and L3055 B-lymphocytes carrying HCVcc were added to Huh-7 ($0.25x10^6$ lymphocytes/well) to assess the potential of lymphocytes to transmit HCV infection to hepatomas. Infection was allowed to occur for 48h and was measured by NS5A staining. The average number of FFU/well was plotted for Huh-7 treated with either live or dead lymphocytes of each cell line. Two-way ANOVA showed a significant effect of lymphocyte viability ($P<0.01$), but not type, on trans-infection. ** = $P<0.01$ by Bonferroni post-tests. Data are mean ± SEM, n=5.

3.2 HCVcc transmission to hepatomas by lymphocytes is receptor-dependent

To elucidate the importance of HCV attachment receptors CD81 and SR-BI in lymphocyte-mediated HCVcc infection, we treated Huh-7 with two different clones of anti-CD81 antibody (2-s131 or 2-s337), or the SR-BI inhibitor ITX5061, before the addition of virus-carrying lymphocytes or virus alone (**Figure 7**). Both clones of anti-CD81 were more potent inhibitors of HCVcc infection than ITX5061, although the differences in the extent of neutralisation achieved with these two treatments were not statistically significant. Anti-CD81 antibodies were less successful in inhibiting the infection when live L3055 were present, with 2-s337 not achieving any neutralisation in this lymphocyte subset. ITX5061 appeared to work better when dead lymphocytes were the carriers of infection. Overall, however, the levels of neutralisation for all three inhibitors were similar in the presence of live or dead lymphocytes. The capacity of the inhibitors to neutralise cell-free infection (i.e. without lymphocytes) was also examined for comparison (**Figure 7C**). All three were very effective, with ITX5061 achieving almost 80% and the two anti-CD81 antibodies virtually 100% neutralisation.

CD81 inhibition was therefore highly efficient for both cell-free virus and trans-infection, however ITX5061 was not as efficient in preventing trans-infection compared to cell-free virus infection. Taken together, this work shows that trans-infection by live and dead lymphocytes uses receptor-mediated mechanisms for HCVcc infection of hepatomas.

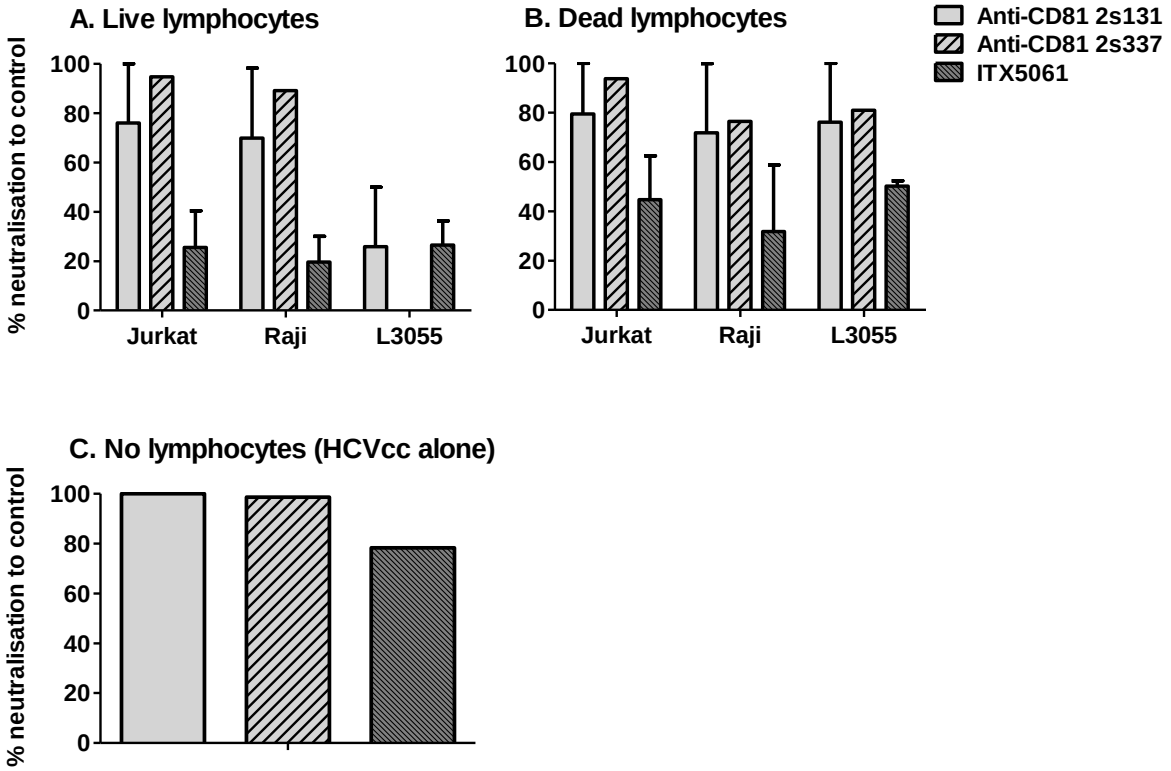

Figure 7 – Trans-infection by live and dead lymphocytes is receptor-mediated.
Huh-7 cells were left untreated or pre-treated with one of two clones of anti-CD81 antibody, or the SR-BI inhibitor ITX5061, before HCVcc-carrying lymphocytes (live or dead) or virus alone were added to them. Infection was allowed to occur for 48h and was measured by NS5A staining. The average numbers of FFU/well were compared between each treatment and controls (isotype-matched antibody for anti-CD81 or DMSO vehicle for ITX5061) and plotted as % FFU that were neutralised relative to control-treated Huh-7 for **(A)** live lymphocytes, **(B)** dead lymphocytes and **(C)** no lymphocytes (HCVcc alone). Data are mean ± SEM. n=2 for anti-CD81 2-s131 and ITX5061 in live and dead lymphocytes. n=1 for anti-CD81 2-s337 and for all treatments with no lymphocytes present.

3.3 HCVcc trans-infection is sensitive to neutralisation by virus-specific antibodies

To test if lymphocyte-transmitted virus was susceptible to neutralising antibodies, we used BT003, a HCV-specific polyclonal human IgG, and a HCV-specific nanobody (Tarr *et al.* 2013) to treat Huh-7 before adding the virus-infected lymphocytes or virus alone (**Figure 8**). Both antibodies, and especially the nanobody, showed effective inhibition of HCVcc infection across the board. The smallest effect was once again seen in live L3055 cells. BT003 seemed to work somewhat better in the presence of dead lymphocytes compared to live cells. For comparison, when the two antibodies were tested against hepatoma infection caused by HCVcc alone, both displayed virtually 100% inhibition (**Figure 8C**). The data obtained therefore showed that, like cell-free infection, HCV trans-infection by live and dead lymphocytes can also be successfully inhibited by HCV-specific antibody neutralisation.

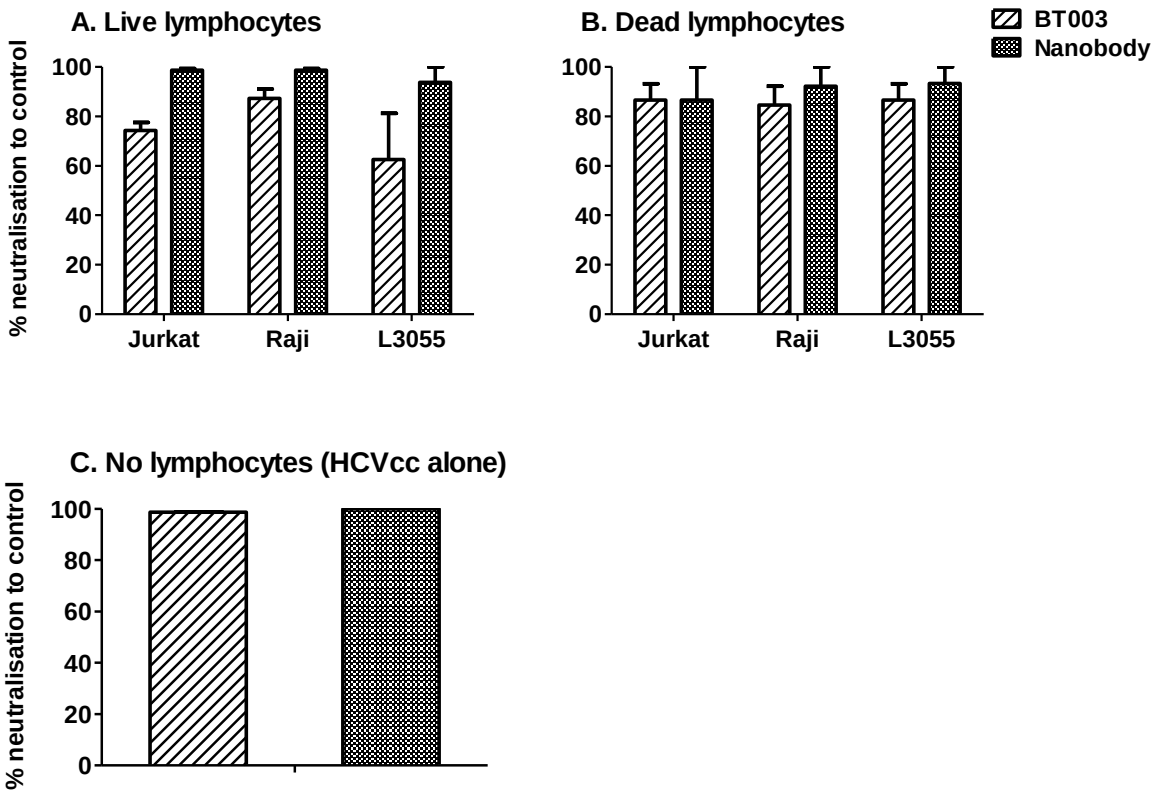

Figure 8 – Trans-infection by live and dead lymphocytes is susceptible to antibody neutralisation.

Huh-7 cells were pre-treated with HCV-specific polyclonal human IgG (BT003) or HCV-specific nanobody before virus-carrying lymphocytes (live or dead) or virus alone were added to them. Infection was allowed to occur for 48h and was measured by NS5A staining. The average numbers of FFU/well were compared between each treatment and controls treated with non-specific polyclonal human IgG, and plotted as % FFU that were neutralised relative to control for **(A)** live lymphocytes, **(B)** dead lymphocytes and **(C)** no lymphocytes (HCVcc alone). **(A)**, two-way ANOVA showed a significant effect of the type of neutralising antibody ($P<0.01$), but not lymphocyte type, on trans-infection. Data are mean ± SEM from three replicates, n=1.

3.4 Defining the mechanism of trans-infection by live and dead lymphocytes

Hepatocytes are phagocytic cells and internalise dead lymphocytes as early as 1h following co-culture (effect seen in Figure 4). We wanted to establish if phagocytosis played a role in HCVcc entry to hepatomas, or if trans-infection by live and dead T-cells was mechanistically comparable. In the absence of specific inhibitors for phagocytosis, we set out to establish the role of acidification and macropinocytosis mechanisms in trans-infection. We treated Huh-7 with bafilomycin A1, an endosomal acidification inhibitor that prevents viral fusion with the endosome and pH-dependent viral entry (Baldick *et al*. 2010), or amiloride, a known inhibitor of membrane ruffling and macropinocytosis (West *et al*. 1989). Either treatment inhibited both lymphocyte-mediated and cell-free trans-infection very efficiently, with no significant differences between any of the conditions (**Figure 9**). As treatments inhibited cell-free virus entry, we could not deduce the role of internalisation of dead cells in trans-infection.

Recent unpublished data from our lab suggested that tumour necrosis factor alpha (TNFα) and secretory leukocyte protease inhibitor (SLPI), when given together, potentiated phagocytosis of lymphocytes by Huh-7 cells (Weight *et al.*, manuscript in preparation). We therefore treated the hepatomas with this combination treatment to examine whether it had an impact on lymphocyte-mediated HCVcc trans-infection. In parallel, we used confocal microscopy to confirm phagocytosis of dead Jurkat T-lymphocytes by Huh-7 cells after combined treatment with TNFα and SLPI.

In our trans-infection assay, we observed no significant potentiation of infection in any of the lymphocyte cell lines, whether live or dead (**Figure 10**). In fact, treatment with TNFα and SLPI in the presence of live Jurkat or Raji resulted in a slight decrease in the number of infected foci compared to untreated Huh-7, although this was not significant. Similarly, the treatment had no effect on cell-free infection. In the parallel lymphocyte entry assay, we were not able to see an increase or decrease in phagocytosis of dead T-cells by TNFα/SLPI-treated compared to untreated hepatomas (data not shown). We were therefore unable to draw meaningful conclusions from the result of this first experiment. More work is needed with matching phagocytosis and trans-infection experiments run in parallel in order to establish any effects of TNFα and SLPI on trans-infection.

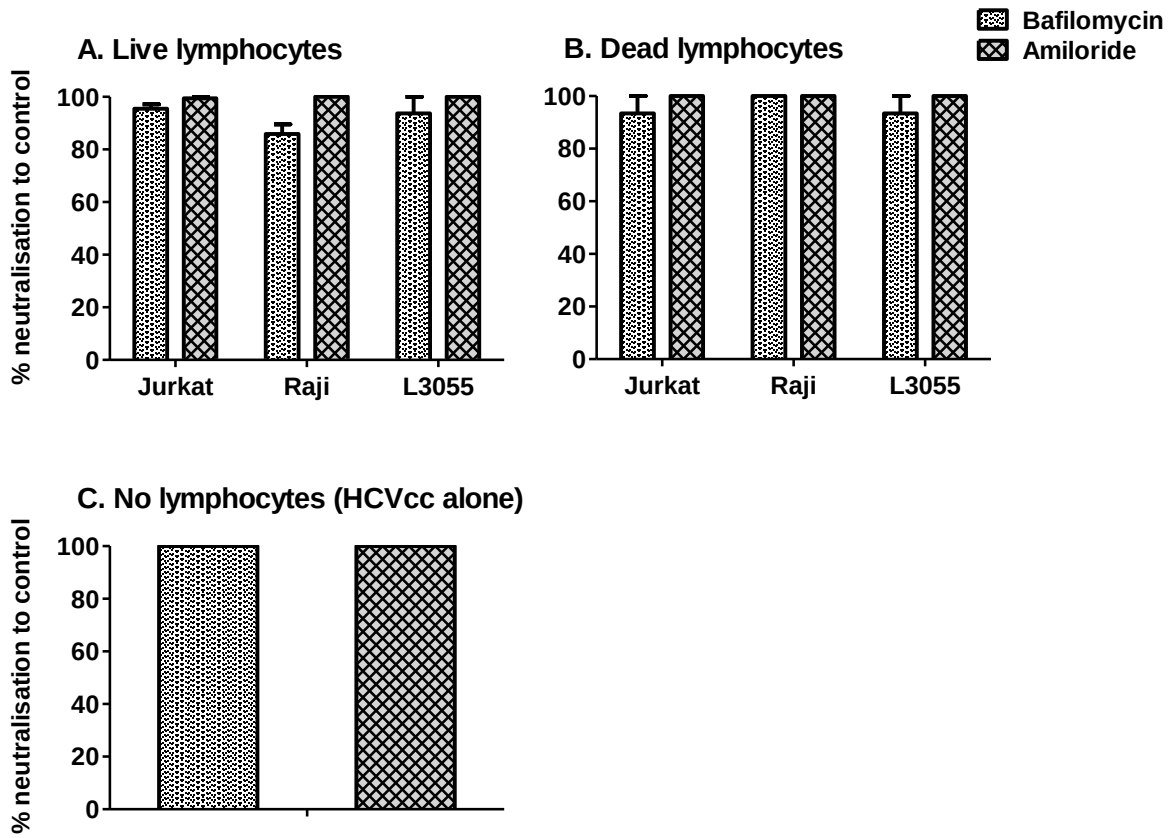

Figure 9 – Effect of inhibition of pH-dependent entry or macropinocytosis on HCVcc trans-infection in Huh-7 in the presence or absence of live or dead lymphocytes.
Huh-7 cells were left untreated or pre-treated with bafilomycin A1 or amiloride before HCVcc-carrying lymphocytes (live or dead) or virus alone were added to them. Infection was allowed to occur for 48h and was measured by NS5A staining. The average numbers of FFU/well were compared between each treatment and untreated controls and plotted as % FFU that were neutralised relative to untreated Huh-7 for **(A)** live lymphocytes, **(B)** dead lymphocytes and **(C)** no lymphocytes (HCVcc alone). **(A)**, two-way ANOVA showed a significant effect of the type of treatment ($P<0.01$), but not lymphocyte type, on trans-infection. Data are mean ± SEM from three replicates, n=1.

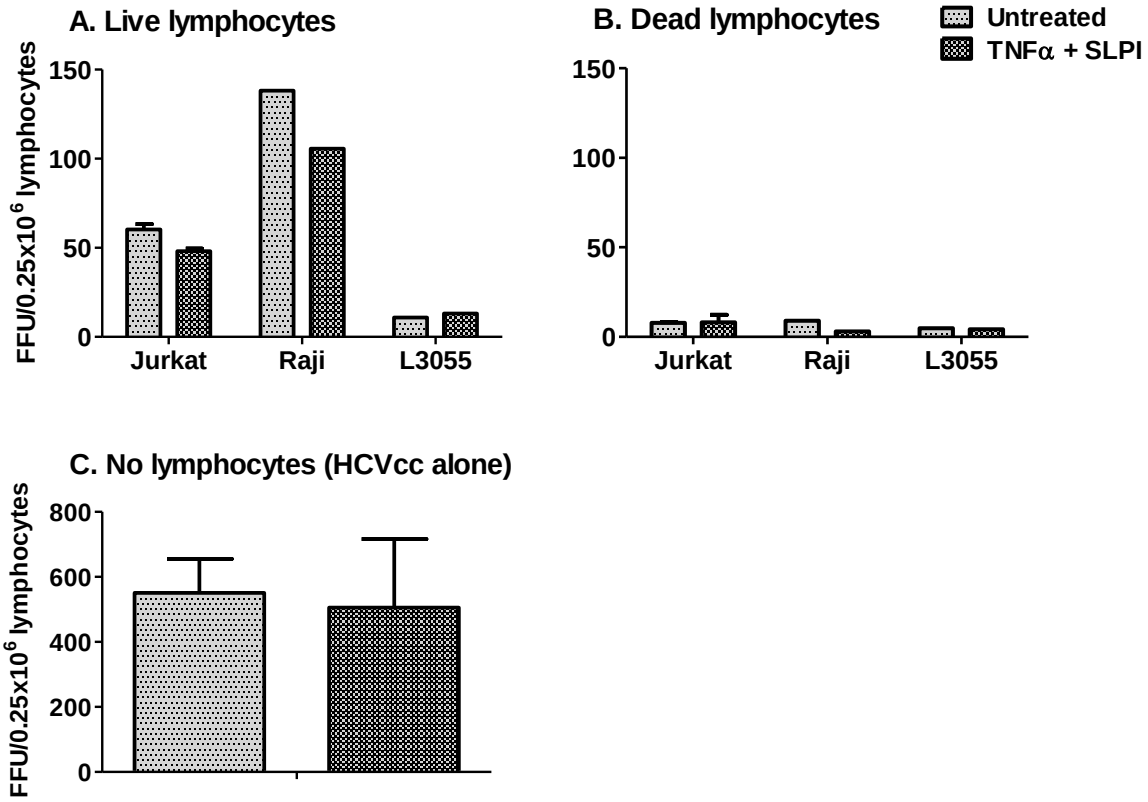

Figure 10 – Effect of combined treatment of TNFα and SLPI on HCVcc trans-infection in Huh-7 in the presence or absence of live or dead lymphocytes.

Huh-7 cells were left untreated or pre-treated with a combination of tumour necrosis factor alpha (TNFα) and secretory leukocyte protease inhibitor (SLPI) before HCVcc-carrying lymphocytes (live or dead) or virus alone were added to them. Infection was allowed to occur for 48h and was measured by NS5A staining. The average numbers of FFU/well were compared between the treatment and untreated controls in the presence of **(A)** live lymphocytes, **(B)** dead lymphocytes and **(C)** no lymphocytes (HCVcc alone). **(A)**, two-way ANOVA showed a significant effect of both treatment ($P<0.05$) and lymphocyte type ($P<0.01$) on trans-infection. Data are mean ± SEM. n=2 for Jurkat T-lymphocytes and cell-free infection (HCVcc alone). n=1 for Raji and L3055 B-lymphocytes.

3.5 The actin cytoskeleton of Huh-7 is important for HCVcc trans-infection by live and dead lymphocytes

We wished to examine the role of the actin cytoskeleton in hepatomas on HCVcc trans-infection, and whether the extent of infection correlated with the ability of Huh-7 to take up dead lymphocytes by phagocytosis. We therefore treated the hepatoma cells with actin polymerisation inhibitors latrunculin-A (lat-A) or cytochalasin-D (cyt-D), both of which would prevent phagocytosis, before adding live or dead Jurkat T-lymphocytes or virus alone. As before, we used confocal microscopy in parallel to look at lymphocyte entry into cells after the above treatments were applied.

Both inhibitors showed very similar levels of neutralisation of infection (close to 40%) under all the examined conditions (**Figure 11**), although more variability in neutralisation was seen in the presence of dead T-cells. Studying the confocal images revealed a significant impact on the actin cytoskeleton of Huh-7 by both lat-A and cyt-D compared to untreated controls, although lat-A appeared to have a more potent effect (**Figure 12**). When Jurkat T-cells were present they were taken up by Huh-7 in the absence of inhibitors, but clustered on the outside of the hepatoma cells when the actin microfilaments were disrupted. This held true for both live (**Figure 13**) and dead lymphocytes (**Figure 14**), although uptake of live lymphocytes by Huh-7 was rarely seen in untreated controls in the first place. We concluded that the actin cytoskeleton is important for HCVcc infection of hepatomas, either by cell-free virus or by trans-infection via lymphocyte vectors. However, we were not able to find a role for phagocytosis of dead lymphocytes in this process.

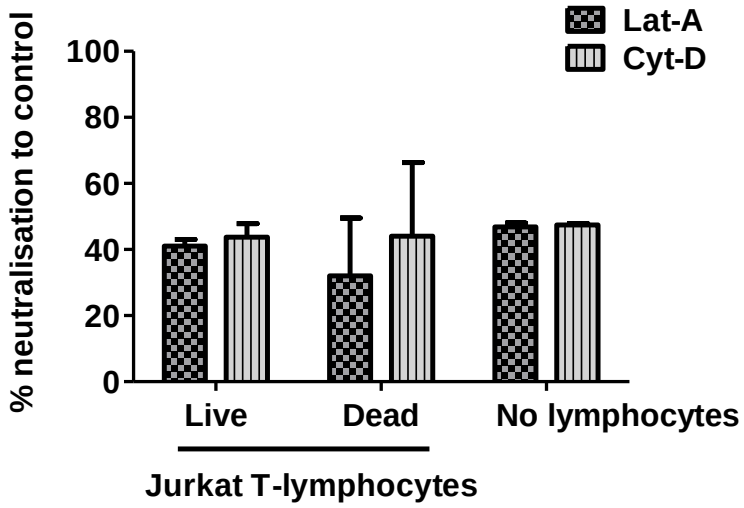

Figure 11 – Effect of inhibition of actin polymerisation on HCVcc trans-infection in Huh-7 in the presence or absence of live or dead lymphocytes.
Huh-7 cells were left untreated or pre-treated with actin polymerisation inhibitors latrunculin-A (lat-A) or cytochalasin-D (cyt-D) before live or dead HCVcc-carrying Jurkat T-lymphocytes, or virus alone, were added to them. Infection was allowed to occur for 48h and was measured by NS5A staining. The average numbers of FFU/well were compared between each treatment and untreated control and plotted as % FFU that were neutralised relative to untreated Huh-7. Data are mean ± SEM from three replicates, n=1.

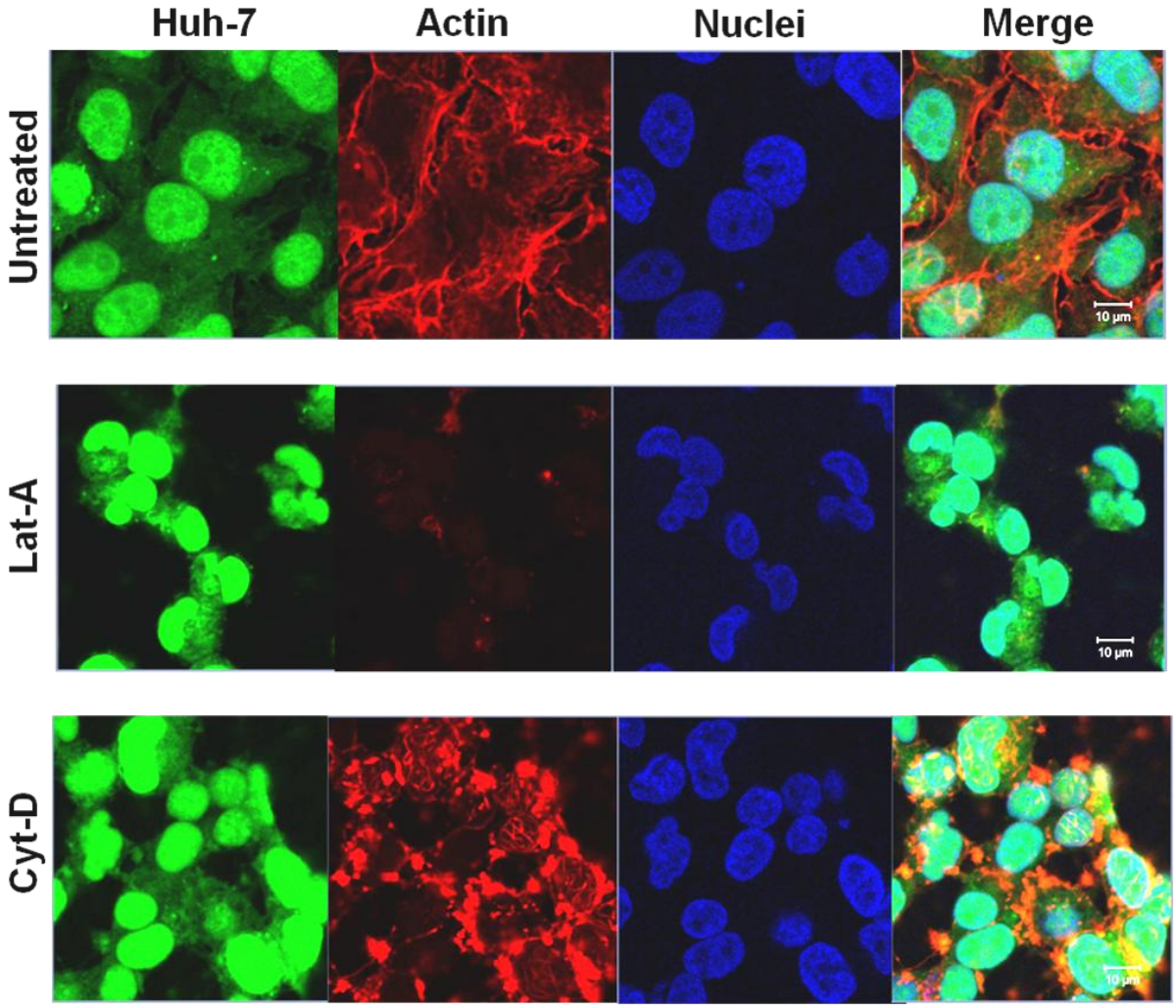

Figure 12 – Representative confocal images of actin polymerisation disruption in Huh-7.

Huh-7 were stained using CellTracker™ Green CMFDA before being treated with lat-A or cyt-D. The actin cytoskeleton and the nuclei of Huh-7 cells were visualised with red Alexa Fluor Phalloidin 568 and blue DAPI dye, respectively. Each row, from left to right: Huh-7 cytoplasm (green), actin cytoskeleton (red), nuclei (blue), and merged image with scale bar. Actin microfilament disruption is visible with both lat-A and cyt-D.

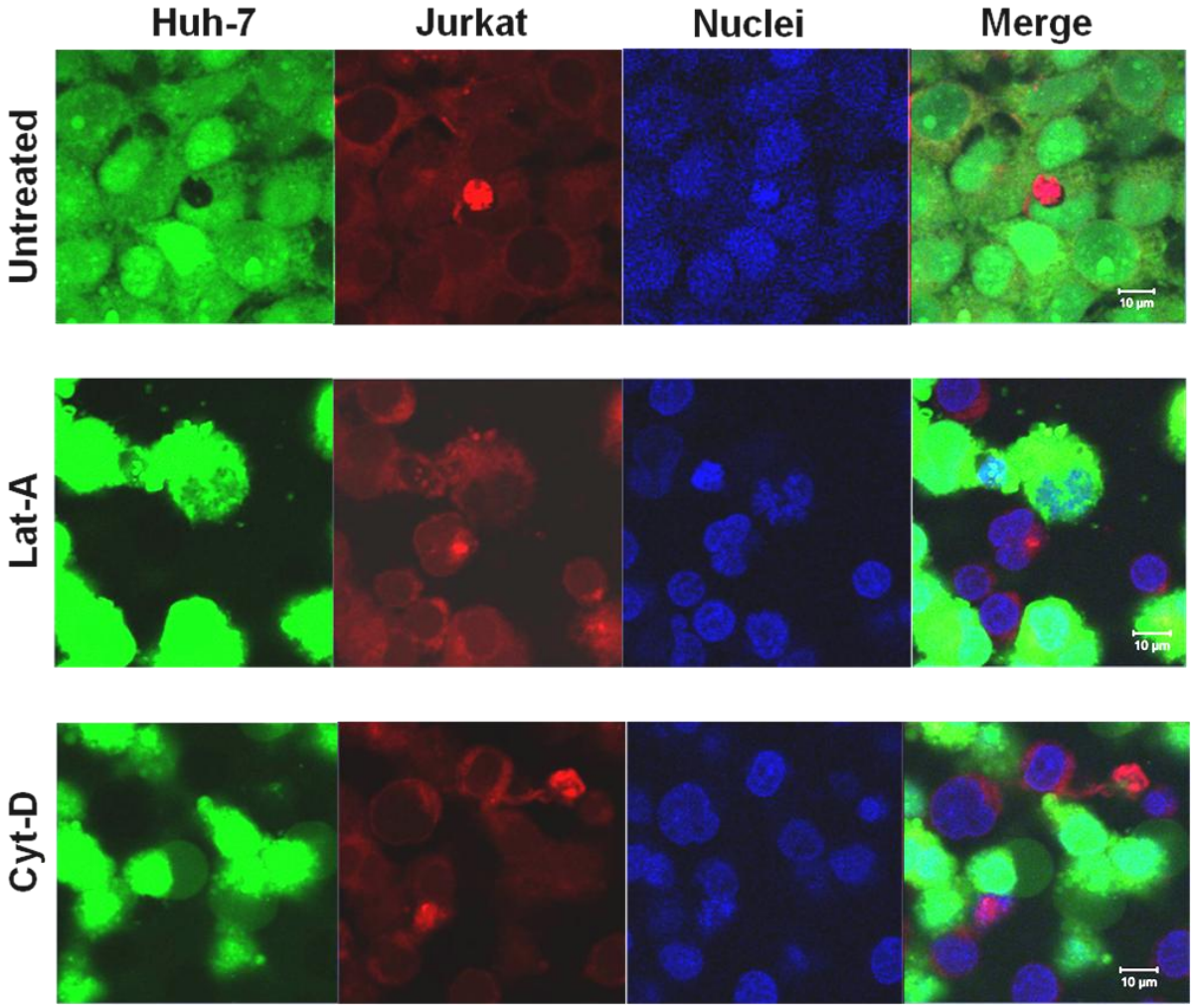

Figure 13 – Chemical disruption of the actin cytoskeleton prevents internalisation of live T cells by hepatomas.

Huh-7 and Jurkat T-lymphocytes were stained using CellTracker™ Green CMFDA and CellTracker™ Red CMTPX respectively before being incubated together to allow the lymphocytes to enter the hepatoma cells. The nuclei of all cells were visualised with blue DAPI dye. Each row, from left to right: Huh-7 cytoplasm (green), live Jurkat T-lymphocytes (red, with some background staining of Huh-7), nuclei (blue), and merged image with scale bar.

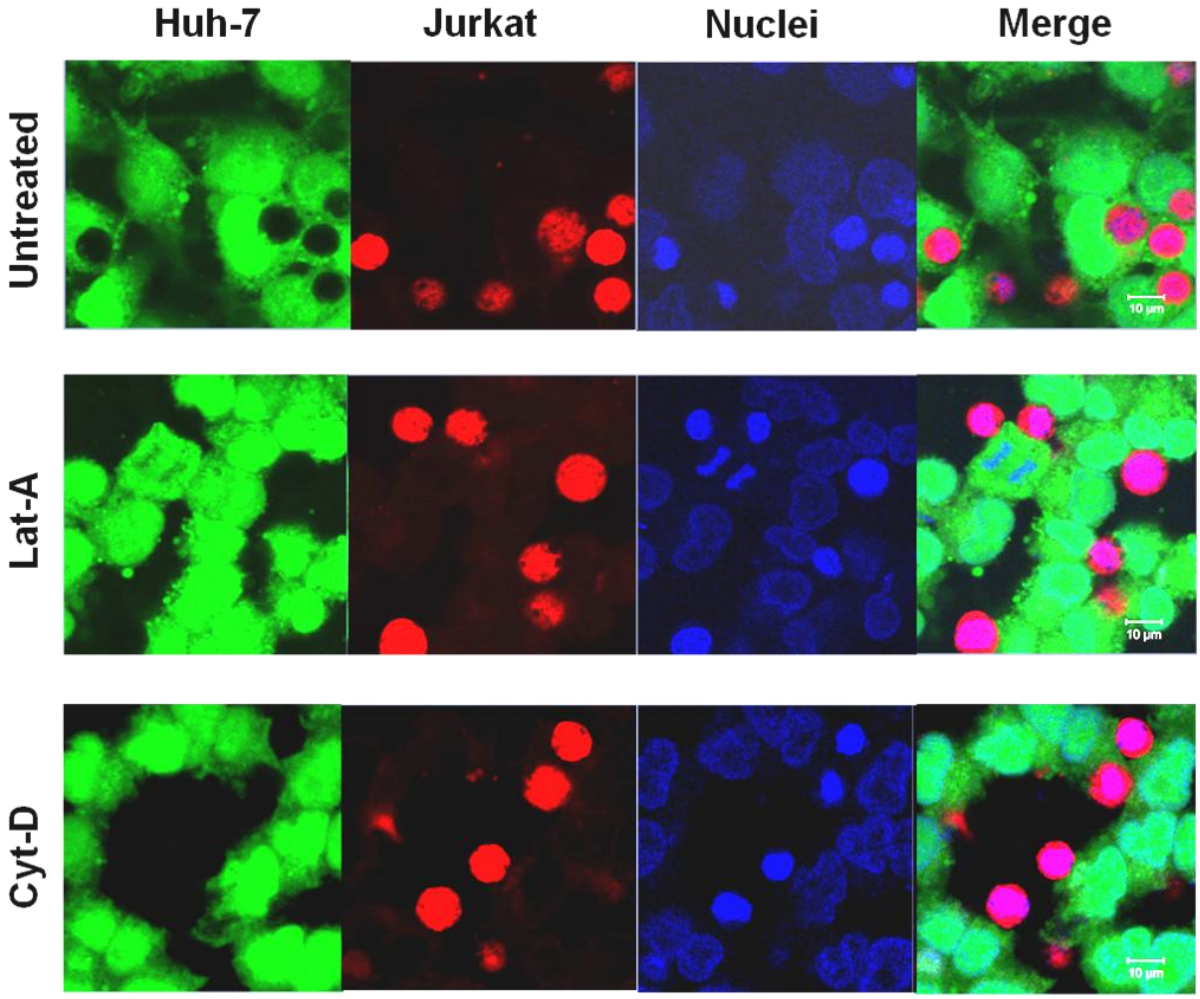

Figure 14 – Chemical disruption of the actin cytoskeleton prevents phagocytosis of heat-killed T cells by hepatomas.
Huh-7 and Jurkat T-lymphocytes were stained using CellTracker™ Green CMFDA and CellTracker™ Red CMTPX respectively before being incubated together to allow phagocytosis. The nuclei of all cells were visualised with blue DAPI dye. Each row, from left to right: Huh-7 cytoplasm (green), dead Jurkat T-lymphocytes (red), nuclei (blue), and merged image with scale bar.

4. DISCUSSION

In this project we used the fully replicating and infective HCV in cell culture (HCVcc) (Lindenbach *et al.* 2005; Jensen *et al.* 2008) to study the recently highlighted phenomenon of lymphocyte-mediated trans-infection of hepatomas in more detail. To model hepatocytes we utilised the 'gold-standard' permissive Huh-7 cells, a monolayer-forming, non-polarised tumour cell line which provides an excellent platform for studying HCV infection. We were able to demonstrate for the first time that HCV trans-infection of Huh-7 cells by both live and dead lymphocytes is sensitive to entry receptor inhibition and antibody neutralisation. We also examined alternative treatments with possible impact on this process and concluded that the actin cytoskeleton plays a significant role in trans-infection as well as cell-free infection. Further studies are needed to fully characterise HCV transmission to and between hepatocytes by lymphocyte vectors, potentially leading to novel therapeutic approaches in the treatment of this virus.

4.1 Live and dead B-lymphocytes exhibit different HCVcc trans-infection potentials but similar transmission kinetics

We examined whether incubation of Huh-7 with HCVcc-carrying live or dead B-lymphocyte cell lines resulted in productive infection in the hepatomas. Consistent with previous findings (Stamataki *et al.* 2009), B-lymphocytes led to successful Huh-7 trans-infection with HCVcc, but only when Raji or, to a much lesser extent, DG75 cells were used as virus carriers. This points to heterogeneities in the ability to mediate HCV trans-infection between B-cell subsets. The fact that heat-killing the B-lymphocyte cell lines nearly abolished the difference in trans-infection seen between

them when they were viable is interesting. It could mean that there were distinct lymphocyte-mediated trans-infection mechanisms depending on lymphocyte viability. B-cells are professional antigen-presenting cells (APCs), and live B-cells from different sources may have different antigen processing ability. For example, it is possible the KEM line was incapable of capturing virus particles, as it did not trans-infect when alive or dead. Conversely, the L3055 B-cells, Raji B-cells and Jurkat T-cells may capture the same amount of virus since they transmit equally well when dead. However, while alive, it is possible that L3055 degrade more virus through antigen processing or shed less virus than Raji and Jurkat, hence failing to transmit as well when alive. Quantitative polymerase chain reaction (qPCR) measurements of viral RNA captured by these cell lines while alive and when dead would shed light on these hypotheses.

We also wanted to establish whether the kinetics of virus transmission to hepatomas differed between live and dead B-lymphocytes by looking at the size of focus-forming units after 72h. The fact that all B-cell lines apart from KEM resulted in almost equal FFU size, whether live or dead, could suggest that transmission by live and dead B-lymphocytes occurred at similar times, allowing virus to spread from infected hepatomas and generate comparable foci at 72h. This would be in conflict with distinct mechanisms of trans-infection existing for live and dead lymphocytes suggested above. Alternatively, phagocytosis may allow hepatocyte infection at similar times as cell-free virus entry. HCVcc has been reported to enter Huh-7 cells as early as 20-60 minutes post-attachment (Farquhar *et al.* 2012), while unpublished

work from our lab indicates that Huh-7 cells can phagocytose dead lymphocytes as early as 30 minutes of co-culture.

4.2 B- and T-lymphocytes may cause HCVcc trans-infection of hepatomas by virus internalisation

Next we compared the trans-infection potential of T-lymphocytes with that of B-lymphocytes. Jurkat T-lymphocytes caused almost identical levels of infection in Huh-7 as Raji B-lymphocytes, suggesting that these two activated cell types may share the same trans-infection mechanism. Stamataki *et al.* have previously shown that, despite its inability to establish a productive infection in lymphocytes *in vitro*, HCVcc is internalised into B-cells (Stamataki *et al.* 2009; Stamataki *et al.* 2011). Another study (Sarhan *et al.* 2012) found that patient-derived HCV can also gain entry into T-cells, and seemed to suggest that the virus is in fact capable of propagating in this cell compartment. Therefore, HCV may be internalised into live B- and T-lymphocytes both, and subsequently transmitted to Huh-7. Our observation that, upon heat-killing, the levels of trans-infection with Jurkat T- and Raji B-cells were very similar to those observed in the poorly transmitting L3055 B-cell line, suggests that this particular mechanism of transmission may be an active process that was lost on cell death.

4.3 Lymphocyte-mediated HCVcc trans-infection is more dependent on CD81 than SR-BI

We found that lymphocyte-mediated trans-infection depended on both CD81 and SR-BI. SR-BI had previously been found to be crucial for HCV entry into hepatocytes (Scarselli *et al.* 2002; Dao Thi *et al.* 2012), which we confirmed by showing high

levels of neutralisation of cell-free HCVcc infection when SR-BI was inhibited. However, this neutralisation – although still present – was markedly reduced in lymphocyte-mediated trans-infection, especially when the lymphocytes were viable. It could be that careful titration of SR-BI inhibitor ITX5061 may reveal additional differences in its potential to inhibit cell-free and lymphocyte-mediated HCVcc entry. In addition, previous work showed that SR-BI inhibition preferentially reduced cell-to-cell HCV transmission otherwise resistant to neutralising antibodies (nAbs) (Brimacombe *et al.* 2011). The fact that this inhibition was not as effective in trans-infection suggests a mechanism other than cell-to-cell HCV transmission is taking place. Conversely, anti-CD81 antibody proved effective in both cell-free infection and lymphocyte-mediated trans-infection. The role of this receptor in HCV entry is well-established (Pileri *et al.* 1998; Harris *et al.* 2010), but its impact on cell-to-cell transmission is more controversial. While some studies found it necessary for this process (Russell *et al.* 2008; Brimacombe *et al.* 2011), others showed that it may be partially or completely dispensable (Timpe *et al.* 2008; Witteveldt *et al.* 2009). This conflicting evidence may be due to differing viral strains, nAbs and origins of cells used for the different studies. Nevertheless, none of the studies above looked at heterologous HCV transmission from lymphocytes to hepatoma cells, where we found that CD81 inhibition does play a role almost independently of lymphocyte viability. Further work is, however, necessary to elucidate the exact involvement of CD81 and SR-BI in trans-infection.

4.4 Lymphocyte-mediated HCVcc trans-infection is susceptible to antibody neutralisation

Our model showed high susceptibility to neutralising antibodies, both a HCV-specific polyclonal antibody derived from pooled patient IgG (BT003) and a recently discovered broadly neutralising heavy-chain alpaca antibody (nanobody). The nanobody had previously shown potent inhibition of both cell-free HCV entry and cell-to-cell transmission by interfering with the CD81 binding site on the virus (Tarr *et al*. 2013). Consistent with this, the reduction in HCV cell-free infection and trans-infection with both CD81 inhibition and nanobody-mediated neutralisation was reflected in our results. The reduced effectiveness of BT003 in live lymphocyte-mediated trans-infection could show some resistance of the virus to this nAb, therefore suggesting cell-to-cell HCV transmission may be taking place as previously described (Brimacombe *et al.* 2011). Once again, however, this study did not examine heterologous lymphocyte–Huh-7 viral transfer, which may possess a distinct mechanism of transmission to that exhibited by neighbouring hepatomas, and therefore possibly be more sensitive to nAb neutralisation. It would be useful to directly compare neutralisation titres (IC_{50} measurements) between cell-free infection and trans-infection for BT003 and for the alpaca nanobody. This would help determine which mode of transmission is least susceptible to neutralisation using specific antibodies, which would in turn be useful for the design of B-cell vaccines.

4.5 Defining the mechanism of lymphocyte-mediated HCVcc trans-infection

The inhibitory concentrations of amiloride and bafilomycin A1 used in this study had been previously determined in titration experiments by other members of the lab for the purpose of measuring cell-free HCVcc infection. It is therefore possible that the same concentrations were toxic to lymphocytes carrying the virus, resulting in cell death which manifested as apparent reduction in hepatoma infection. These compounds were, however, not toxic to hepatomas at the concentrations tested. Dose titration of both chemicals is needed before meaningful conclusions can be drawn from their trans-infection inhibition.

On the other hand, there is growing evidence that pro-inflammatory cytokines such as TNFα and interferon-gamma (IFNγ) work either individually or together to induce tight junction remodelling and change CLDN1 and OCLN expression in several epithelial and endothelial cell types (e.g. reviewed in Walsh *et al.* 2000 and Capaldo & Nusrat 2009). However, little is known about their impact on hepatocytes. Our group recently observed that both TNFα/IFNγ and TNFα/SLPI combinations may increase phagocytosis of dead lymphocytes by Huh-7 cells (Weight *et al.*, manuscript in preparation). In addition to cytokine effects on actin cytoskeleton, it was previously shown that cortical actin modification is a necessary step for HCV internalisation *via* its interaction with CD81 and TJ proteins CLDN1 and OCLN (Brazzoli *et al.* 2008; Farquhar *et al.* 2012) (Figure 1). Drawing on all of the above evidence, we examined whether changes in actin cytoskeleton impacted on lymphocyte uptake by Huh-7, and whether this played a role in lymphocyte-mediated HCVcc trans-infection.

Because the antiviral action of IFNγ would make it difficult to interpret our results, we focused on treatment with TNFα/SLPI, as well as direct inhibition of actin polymerisation by lat-A and cyt-D.

In contrast to previous findings, we were not able to see an effect of TNFα/SLPI on phagocytosis of dead lymphocytes, or a significant impact on either cell-free HCV infection or lymphocyte-mediated trans-infection. As SLPI is a very unstable enzyme, this could be due to reagent degradation. More studies of phagocytosis and trans-infection performed in parallel, and incorporating dose titrations of this combination treatment, would be needed before conclusions can be made on its effect. However, lat-A and cyt-D disrupted actin microfilaments as expected, resulting in moderate inhibition of trans-infection mediated by both live and dead Jurkat T-lymphocytes. This, along with the same level of inhibition exhibited for cell-free HCV infection, suggests that phagocytosis of dead lymphocytes may not play a role in HCVcc trans-infection of hepatomas. Very little is known about hepatocyte phagocytosis of dead cells, however, and identifying specific pathways that perturb this process in order to examine whether they play a role in viral entry could provide us with further insight into HCV infection of liver cells.

4.6 Future studies

A lot still remains to be elucidated about HCV entry into hepatocytes *via* the trans-infection route. We showed that B- and T-lymphocytes are capable of transmitting HCVcc infection to hepatomas, but the way in which they do this remains poorly defined. For example, the so-called ‘virological synapses’ have been found to have a

role in virus entry into lymphocytes (Dustin & Cooper 2000; Piguet & Sattentau 2004), and the more recently discovered membrane nanotubules permitted the sequential spread of HIV-1 through T-cells (Sowinski *et al.* 2008). It would be interesting to examine the potential role of these in HCV-lymphocyte interactions, even if they do not result in productive infection within the lymphocytes themselves. This, in turn, could provide us with clues as to what may happen at the point of HCV transmission from lymphocytes to hepatocytes.

As mentioned previously, dose titration experiments with the reagents used in this study, in particular the SR-BI inhibitor ITX5061, bafilomycin A1, amiloride and TNFα/SLPI would increase our understanding of how these chemicals impact on the trans-infection potential of lymphocytes compared to cell-free HCV infection. In addition, we looked at the role of CD81 and SR-BI but not at that of CLDN1 and OCLN in the trans-infection process. Inhibiting these and observing the effect on lymphocyte-mediated HCV infection would be the logical next step. We also identified that the actin cytoskeleton plays a role in trans-infection, but have not yet elucidated the extent of this involvement. RHO GTPases are known to mediate actin remodelling during HCV entry (Brazzoli *et al.* 2008; Farquhar *et al.* 2012; Lindenbach & Rice 2013), so inhibiting the action of these could be an interesting avenue of further trans-infection research. Finally, polarisation of hepatocytes is crucial for normal functioning of the liver *in vivo*, and limits HCV entry *in vitro*; this suggests that polarity perturbation in the liver may increase its propensity towards HCV infection (Meredith *et al.* 2012). Comparing the results from this study to a similar one done on

polarised HepG2 cells in the future could give us important insights into how altering hepatocyte polarisation may influence HCV trans-infection.

4.7 Conclusion

We confirmed that both B- and T-lymphocytes can mediate HCVcc trans-infection of Huh-7 hepatoma cells, and showed for the first time that this process can be markedly reduced by entry receptor inhibition and antibody neutralisation. Moreover, heat-killed lymphocytes were still able to transmit infection to hepatomas albeit at a reduced efficiency, revealing that there are passive and active elements of trans-infection in operation. The actin cytoskeleton also plays a significant, but incompletely defined role in trans-infection. We have found no evidence for lymphocyte uptake by hepatoma cells having an effect on trans-infection, although further studies are necessary in order to provide new insights into this potentially significant mode of HCV transmission.

5. REFERENCES

Acton, S. *et al*., 1996. Identification of scavenger receptor SR-BI as a high density lipoprotein receptor. *Science*, 271(5248), pp.518–20.

Baldick, C.J. *et al*., 2010. A novel small molecule inhibitor of hepatitis C virus entry M. S. Diamond, ed. *PLoS Pathogens*, 6(9), p.e1001086.

Bartosch, B., Dubuisson, J. & Cosset, F.-L., 2003. Infectious hepatitis C virus pseudo-particles containing functional E1-E2 envelope protein complexes. *The Journal of Experimental Medicine*, 197(5), pp.633–42.

Bertaux, C. & Dragic, T., 2006. Different domains of CD81 mediate distinct stages of hepatitis C virus pseudoparticle entry. *Journal of Virology*, 80(10), pp.4940–8.

Blanchard, E. *et al*., 2006. Hepatitis C virus entry depends on clathrin-mediated endocytosis. *Journal of Virology*, 80, pp.6964–72.

Blight, K.J., McKeating, J.A. & Rice, C.M., 2002. Highly permissive cell lines for subgenomic and genomic hepatitis C virus RNA replication. *Journal of Virology*, 76(24), pp.13001–14.

Brazzoli, M. *et al*., 2008. CD81 is a central regulator of cellular events required for hepatitis C virus infection of human hepatocytes. *Journal of Virology*, 82(17), pp.8316–29.

Brimacombe, C.L. *et al*., 2011. Neutralizing antibody-resistant hepatitis C virus cell-to-cell transmission. *Journal of Virology*, 85(1), pp.596–605.

Capaldo, C.T. & Nusrat, A., 2009. Cytokine regulation of tight junctions. *Biochimica et Biophysica Acta*, 1788(4), pp.864–71.

Carloni, G. *et al*., 2012. HCV infection by cell-to-cell transmission: choice or necessity? *Current Molecular Medicine*, 12(1), pp.83–95.

Ciesek, S. & Wedemeyer, H., 2012. Immunosuppression, liver injury and post-transplant HCV recurrence. *Journal of Viral Hepatitis*, 19(1), pp.1–8.

Dao Thi, V.L. *et al*., 2012. Characterization of hepatitis C virus particle subpopulations reveals multiple usage of the scavenger receptor BI for entry steps. *The Journal of Bological Chemistry*, 287(37), pp.31242–57.

Dorner, M. *et al*., 2013. Completion of the entire hepatitis C virus life cycle in genetically humanized mice. *Nature*, 501(7466), pp.237–41.

Dustin, M.L. & Cooper, J.A., 2000. The immunological synapse and the actin cytoskeleton: molecular hardware for T cell signaling. *Nature Immunology*, 1(1), pp.23–9.

Farquhar, M.J. *et al*., 2012. Hepatitis C virus induces CD81 and claudin-1 endocytosis. *Journal of Virology*, 86(8), pp.4305–16.

Germi, R. *et al*., 2002. Cellular glycosaminoglycans and low density lipoprotein receptor are involved in hepatitis C virus adsorption. *Journal of Medical Virology*, 68(2), pp.206–15.

Harris, H.J. *et al*., 2010. Claudin association with CD81 defines hepatitis C virus entry. *The Journal of Biological Chemistry*, 285(27), pp.21092–102.

Jensen, T.B. *et al*., 2008. Highly efficient JFH1-based cell-culture system for hepatitis C virus genotype 5a: failure of homologous neutralizing-antibody treatment to control infection. *The Journal of Infectious Diseases*, 198(12), pp.1756–65.

Kato, T. *et al*., 2003. Efficient replication of the genotype 2a hepatitis C virus subgenomic replicon. *Gastroenterology*, 125(6), pp.1808–17.

Kolykhalov, A.A. *et al*., 1997. Transmission of hepatitis C by intrahepatic inoculation with transcribed RNA. *Science*, 277(5325), pp.570–4.

Lindenbach, B.D. *et al*., 2006. Cell culture-grown hepatitis C virus is infectious in vivo and can be recultured in vitro. *Proceedings of the National Academy of Sciences of the United States of America*, 103(10), pp.3805–9.

Lindenbach, B.D. *et al*., 2005. Complete replication of hepatitis C virus in cell culture. *Science*, 309, pp.623–6.

Lindenbach, B.D. & Rice, C.M., 2013. The ins and outs of hepatitis C virus entry and assembly. *Nature Reviews. Microbiology*, 11(10), pp.688–700.

Lohmann, V., 2009. HCV replicons: overview and basic protocols. *Methods in Molecular Biology*, 510, pp.145–63.

Marukian, S. *et al*., 2008. Cell culture-produced hepatitis C virus does not infect peripheral blood mononuclear cells. *Hepatology*, 48(6), pp.1843–50.

Mee, C.J. *et al*., 2008. Effect of cell polarization on hepatitis C virus entry. *Journal of Virology*, 82(1), pp.461–70.

Meredith, L.W. *et al*., 2012. Hepatitis C virus entry: beyond receptors. *Reviews in Medical Virology*, 22, pp.182–93.

Mittapalli, G.K. *et al*., 2011. Discovery of highly potent small molecule Hepatitis C Virus entry inhibitors. *Bioorganic & Medicinal Chemistry Letters*, 21, pp.6852–5.

Piguet, V. & Sattentau, Q., 2004. Dangerous liaisons at the virological synapse. *The Journal of Clinical Investigation*, 114(5), pp.605–10.

Pileri, P. *et al*., 1998. Binding of Hepatitis C Virus to CD81. *Science*, 282(5390), pp.938–41.

Ploss, A. *et al*., 2010. Persistent hepatitis C virus infection in microscale primary human hepatocyte cultures. *Proceedings of the National Academy of Sciences of the United States of America*, 107(7), pp.3141–5.

Rappocciolo, G. *et al*., 2006. DC-SIGN on B lymphocytes is required for transmission of HIV-1 to T lymphocytes. *PLoS Pathogens*, 2(7), p.e70.

Rappocciolo, G. *et al*., 2008. Human herpesvirus 8 infects and replicates in primary cultures of activated B lymphocytes through DC-SIGN. *Journal of Virology*, 82(10), pp.4793–806.

Rupp, D. & Bartenschlager, R., 2014. Targets for antiviral therapy of hepatitis C. *Seminars in Liver Disease*, 34(1), pp.9–21.

Russell, R.S. *et al*., 2008. Advantages of a single-cycle production assay to study cell culture-adaptive mutations of hepatitis C virus. *Proceedings of the National Academy of Sciences of the United States of America*, 105(11), pp.4370–5.

Sarhan, M.A. *et al*., 2012. Hepatitis C virus infection of human T lymphocytes is mediated by CD5. *Journal of Virology*, 86(7), pp.3723–35.

Scarselli, E. *et al*., 2002. The human scavenger receptor class B type I is a novel candidate receptor for the hepatitis C virus. *The EMBO Journal*, 21(19), pp.5017–25.

Sharma, N.R. *et al*., 2011. Hepatitis C virus is primed by CD81 protein for low pH-dependent fusion. *The Journal of Biological Chemistry*, 286(35), pp.30361–76.

Sowinski, S. *et al*., 2008. Membrane nanotubes physically connect T cells over long distances presenting a novel route for HIV-1 transmission. *Nature Cell Biology*, 10(2), pp.211–9.

Stamataki, Z. *et al*., 2009. Hepatitis C virus association with peripheral blood B lymphocytes potentiates viral infection of liver-derived hepatoma cells. *Blood*, 113(3), pp.585–93.

Stamataki, Z. *et al*., 2011. Rituximab treatment in hepatitis C infection: an in vitro model to study the impact of B cell depletion on virus infectivity. *PloS One*, 6(9), p.e25789.

Stamataki, Z. *et al*., 2013. T Cells Facilitate Hepatitis C Virus Transmission To Polarised Liver and Brain Cell Lines, Revealing a New Role for Viral Quasispecies. *Journal of Hepatology*, 58, p.S4.

Tarr, A.W. *et al*., 2013. An alpaca nanobody inhibits hepatitis C virus entry and cell-to-cell transmission. *Hepatology*, 58(3), pp.932–9.

Timpe, J.M. *et al*., 2008. Hepatitis C virus cell-cell transmission in hepatoma cells in the presence of neutralizing antibodies. *Hepatology*, 47(1), pp.17–24.

Tscherne, D.M. *et al*., 2006. Time- and temperature-dependent activation of hepatitis C virus for low-pH-triggered entry. *Journal of Virology*, 80(4), pp.1734–41.

Valli, M.B. *et al*., 2006. Transmission in vitro of hepatitis C virus from persistently infected human B-cells to hepatoma cells by cell-to-cell contact. *Journal of Medical Virology*, 78(2), pp.192–201.

Wakita, T. *et al*., 2005. Production of infectious hepatitis C virus in tissue culture from a cloned viral genome. *Nature Medicine*, 11(7), pp.791–6.

Walsh, S. V, Hopkins, A.M. & Nusrat, A., 2000. Modulation of tight junction structure and function by cytokines. *Advanced Drug Delivery Reviews*, 41(3), pp.303–13.

West, M.A., Bretscher, M.S. & Watts, C., 1989. Distinct endocytotic pathways in epidermal growth factor-stimulated human carcinoma A431 cells. *The Journal of Cell Biology*, 109(6 Pt 1), pp.2731–9.

Wilson, G.K. & Stamataki, Z., 2012. In vitro systems for the study of hepatitis C virus infection. *International Journal of Hepatology*, 2012, pp.292591, 1–8.

Witteveldt, J. *et al*., 2009. CD81 is dispensable for hepatitis C virus cell-to-cell transmission in hepatoma cells. *The Journal of General Virology*, 90, pp.48–58.

Yanagi, M. *et al*., 1997. Transcripts from a single full-length cDNA clone of hepatitis C virus are infectious when directly transfected into the liver of a chimpanzee. *Proceedings of the National Academy of Sciences of the United States of America*, 94(16), pp.8738–43.

UNIVERSITY OF BIRMINGHAM

NEUTROPHIL RECRUITMENT TO MICROVASCULAR ENDOTHELIUM: THE IMPACT OF MESENCHYMAL STEM CELLS

by Kristina Petrovic

This project is submitted in partial fulfilment of the requirements for the award of the MRes

wellcome trust

School of Immunity and Infection
College of Medical and Dental Sciences
University of Birmingham
May 2014

ABSTRACT

Neutrophil recruitment to inflamed tissue is a crucial process in the immune system's defense against infection and inflammation. Mesenchymal stem cells (MSC) found in the surrounding tissue stroma are normally immunosuppressive, and have recently been shown to reduce neutrophil adhesion to inflamed macrovascular endothelium. However, there is evidence to suggest that MSC may become immunostimulatory in chronically inflamed tissue, such as that found in autoimmune disease. This project aimed to (i) characterise neutrophil recruitment to the more physiologically relevant microvascular endothelium, (ii) examine whether MSC could suppress this process, and (iii) find out how MSC phenotype may change on prolonged exposure to pro-inflammatory cytokines. We found that micro- and macrovascular endothelium supported neutrophil adhesion equally well *in vitro*, but we did not observe suppression of neutrophil recruitment in the presence of MSC. Upon prolonged stimulation with transforming growth factor β (TGFβ) under low-serum conditions, MSC surface marker expression was altered, which could indicate a phenotypic shift or differentiation. Further studies of MSC phenotype changes in inflammatory conditions, and how they may affect neutrophil recruitment to vascular endothelium, may help shed light on the complex cellular interactions within chronically inflamed tissue.

ACKNOWLEDGEMENTS

I would like to thank my supervisors, Dr Helen McGettrick and Professor Gerard Nash, for their invaluable support, knowledge, guidance and continued reassurance for the duration of this project. I also wish to extend my gratitude to Hafsa Munir and all the other students and staff in the Leukocyte Trafficking Group who helped and encouraged me during my time in the lab.

Table of Contents

List of figures and tables

FIGURES

TABLES

1. INTRODUCTION

White blood cells (leukocytes) need to undergo successful extravasation from the blood into target tissue in order to defend the host from infection and inflammation. Neutrophils are among the first to get recruited; their abundance and crucial role in phagocytosing invading pathogens makes them a key component of the innate immune system (Johnson-Léger *et al.* 2000). The recruitment of neutrophils to the vascular endothelium consists of a series of tightly regulated steps collectively known as the leukocyte adhesion cascade (Ley *et al.* 2007). This process, and the fate of neutrophils once inside the target tissue, is influenced by the state of the recruiting endothelium as much as by its stromal microenvironment. Crosstalk between vascular endothelial cells (EC) and stromal cells (such as fibroblasts and mesenchymal stem cells) influences EC phenotype and, as a result, modulates their ability to support neutrophil recruitment (e.g. reviewed by McGettrick *et al.* 2012). In particular, mesenchymal stem cells (MSC) have recently been shown to down-regulate the adhesion of neutrophils to inflamed endothelium *in vitro* (Luu *et al*. 2013). However, exposure to a chronic inflammatory milieu, such as the one found in inflammatory and autoimmune diseases, can cause the MSC phenotype to shift towards immune stimulation rather than suppression (El-Jawhari *et al.* 2014). While the immunosuppressive and anti-inflammatory properties of MSC have been the focus of much research, little is known about how their phenotype may change in response to the conditions in the surrounding stroma, or the impact this may have on neutrophil recruitment to the endothelium. This project will therefore aim to be one of the first to address these important questions.

1.1 Neutrophil recruitment to vascular endothelium

Neutrophils are generated in the bone marrow, and circulate in the bloodstream for several hours before being recruited to sites of infection, inflammation or injury. They are the first leukocytes to appear in inflamed tissue, their primary role being elimination of microbes and ingestion of cell debris by phagocytosis (Springer 1995; Zarbock & Ley 2008). Their importance is perhaps most strikingly demonstrated by individuals suffering from leukocyte adhesion deficiency (LAD), a disorder in which neutrophils fail to accumulate at sites of inflammation. People with LAD suffer from recurrent bacterial infections that, if left untreated, often prove fatal (Anderson & Springer 1987; Johnson-Léger *et al.* 2000; Zarbock & Ley 2008).

The first prerequisite for neutrophil recruitment is the presence of pro-inflammatory signals in the target tissue that activate the local vascular endothelium, rendering it capable of attracting circulating leukocytes (Springer 1995). Depending on shear stress and interactions with other blood cells, leukocytes will eventually flow closer to endothelial surface rather than in the centre of the blood vessel – a process referred to as margination. The bulk of neutrophil adhesion to the endothelium happens in postcapillary venules, where margination is enhanced due to shear stress being low enough to support attachment (Springer 1995; Langer & Chavakis 2009). The recruitment process continues in a sequence of well-documented steps known as the adhesion cascade, of which neutrophil rolling, activation, arrest and transendothelial migration are the major stages (Ley *et al.* 2007). Recently it was found that the basement membrane deposited by the endothelium represents an additional barrier

that neutrophils need to overcome before being able to gain access to tissue interstitium (Burton *et al.* 2011).

1.1.1 Adhesion cascade and the signalling molecules involved

Activation of the vascular endothelium by thrombin, histamine or pro-inflammatory cytokines such as TNFα and IL-1β results in endothelial expression of E- and P-selectin (Springer 1995; Sanz & Kubes 2012). These glycoproteins facilitate the initial tethering and rolling of neutrophils by binding to their counter-receptors on the neutrophil surface, namely P-selectin glycoprotein ligand-1 (PSGL-1), E-selectin ligand-1 (ESL-1) and CD44. Another molecule with a role in neutrophil capture and rolling is L-selectin, also expressed on the surface of neutrophils (Springer 1995; Williams *et al*. 2011). The importance of selectins in the adhesion cascade has been well-established in both *in vitro* and *in vivo* studies. For example, concurrent antibody blockade of E- and P-selectin significantly decreased capture of neutrophils on TNFα-treated human umbilical vein endothelial cells (HUVEC), although this decrease was not observed in IL-1β-treated endothelium (Sheikh *et al.* 2005). *In vivo,* P-selectin$^{-/-}$ mice exhibited increased numbers of circulating neutrophils and delayed neutrophil recruitment to inflamed tissue (Mayadas *et al.* 1993). In another study which employed antibody blockade of P- and L-selectin in wild-type or P- and L-selectin$^{-/-}$ mice, it was concluded that P-selectin was necessary for the initial stages of rolling, while L-selectin mediated most of it at later time-points. Interestingly, and in contrast to the *in vitro* studies on human tissue referred to above, evidence could not be found for E-selectin involvement in leukocyte rolling in mice (Ley *et al.* 1995).

While rolling, neutrophils come into contact with chemokines presented by glycosaminoglycans (GAGs) on the endothelial luminal membrane. The chemokines which selectively interact with neutrophils include CXCL1, CXCL2, and CXCL5; all of them bind to their common G-protein coupled receptor (GPCR) on the neutrophil surface, CXCR2 (Sanz & Kubes 2012). Functional blockade of any of these through the use of neutralising antibodies has effectively reduced neutrophil adhesion to inflamed microvasculature *in vivo (*Nabah *et al.* 2004; Duchene *et al.* 2007; Coelho *et al.* 2008). Chemokine engagement of their neutrophil GPCRs leads to “inside-out” signalling, resulting in the activation of β_2 integrins expressed on neutrophil surface. Activated integrins cluster together and undergo a conformational change from bent, inactive to fully extended, active form with high binding affinity (Luo *et al.* 2007). This enables them to bind to their corresponding ligands on the endothelium which, for β_2 integrins, is the intercellular adhesion molecule-1 (ICAM-1). This in turn causes stable adhesion and arrest of neutrophils on the vascular endothelium (Luo *et al.* 2007).

Integrins are also responsible for transferring signals from extracellular space into the neutrophils themselves (“outside-in” signalling). Adhesion is strengthened further as a consequence, leading to leukocyte flattening and crawling across the endothelial surface in search of a preferred site to migrate across (Ley *et al*. 2007; Sanz & Kubes 2012). While initial neutrophil adhesion is mediated by the $\alpha_L\beta_2$ integrin, intraluminal crawling is instead mediated by the $\alpha_M\beta_2$ integrin via its interaction with ICAM-1 (Ley *et al.* 2007). This was elucidated through intravital and confocal microscopy of inflamed microvessels in wild-type as well as $\alpha_L\beta_2^{-/-}$ and $\alpha_M\beta_2^{-/-}$ mice, where $\alpha_L\beta_2^{-/-}$

neutrophils showed very little adhesion and $\alpha_M\beta_2^{-/-}$ neutrophils crawled much less once adhered (Phillipson *et al.* 2006).

In a recent *in vitro* study, neutrophils were shown to need an additional stimulus before they can migrate across the endothelium (Tull *et al.* 2009). This is supplied in the form of a lipid signal, prostaglandin-D_2 (PGD_2), generated from metabolism of arachidonic acid by cyclooxygenase (COX) enzymes. When an alternative dietary fatty acid was metabolised by COX to PGD_3 instead, this was found to antagonise the PGD_2 receptor and lead to inhibition of neutrophil migration across TNFα-stimulated endothelial cells (Tull *et al.* 2009). Once activation by chemokines and PGD_2 signalling, in that order, have taken place, neutrophils can cross the endothelium by interacting with molecules including ICAM-1, platelet-endothelial cell adhesion molecule-1 (PECAM-1), junctional adhesion molecule-A (JAM-A) and CD99 (Ley *et al.* 2007; Sanz & Kubes 2012). Reduced neutrophil infiltration into tissue has been observed in both PECAM-$1^{-/-}$ (Schenkel *et al.* 2004) and JAM-$A^{-/-}$ mice (Corada *et al.* 2005; Khandoga *et al.* 2005), providing evidence for their role in transmigration. Neutrophils transmigrate either through endothelial cell junctions (paracellular route) or, less commonly, through the body of the EC (transcellular route) (Ley *et al.* 2007). Several *in vitro* studies on both primary EC and endothelial cell lines have concluded that leukocytes overwhelmingly cross the endothelium via the paracellular route (Engelhardt & Wolburg 2004). A recent *in vivo* study supported this by using intravital microscopy to show that leukocytes transmigrated at tricellular junctional regions of the endothelium, of which a significant proportion were ICAM-1 enriched (Sumagin & Sarelius 2010). However, *in vivo* migration across the blood-brain barrier (BBB) has

been shown to happen invariably via the transcellular route (Engelhardt & Wolburg 2004). Imaging evidence has also been produced of neutrophils crossing the skin endothelium in a transcellular manner, i.e. through the body of the EC, when they have been stimulated with a chemoattractant (Feng *et al.* 1998). The data on which route neutrophils normally take in the body in order to transmigrate is therefore likely to be context-dependent.

The final stage of neutrophil migration into tissue is the migration across the EC basement membrane (BM) – a process found to be β_3 integrin-dependent (Burton *et al.* 2011) – and through the pericyte sheath (Ley *et al.* 2007) in order to gain access to tissue stroma. Crosstalk between EC and tissue stromal cells can modulate the state of the endothelium, thus changing the extent to and the way in which neutrophils are recruited in the first place (McGettrick *et al.* 2012). This modulation becomes even more important in disease states characterised by chronic inflammation, where stromal cells may undergo phenotypic alterations that support excessive neutrophil infiltration and thus contribute towards inflammatory disease pathology.

1.2 The influence of the stromal microenvironment on neutrophil adhesion

Neutrophil (and, more generally, leukocyte) recruitment to the endothelium is a crucial part of physiological inflammation, which is necessary in order to clear infection and repair damaged tissue. The process requires controlled leukocyte entry into and clearance from the target tissue to be successful. Dysregulated, persistent

infiltration of leukocytes leads to tissue damage and chronic inflammation, which form the pathological basis of many autoimmune and inflammatory diseases such as rheumatoid arthritis (RA) (McGettrick *et al.* 2012).

In the past decade, a hypothesis has emerged that leukocyte recruitment patterns to different tissues are strongly influenced by the local EC microenvironment. EC exist in close proximity to various cells of the tissue stroma, such as smooth muscle cells (SMC), pericytes and fibroblasts, all of which are capable of conditioning endothelial responses and therefore leukocyte adhesion to EC (Nash *et al.* 2004) (**Figure 1**). The evidence that eventually confirmed this hypothesis can be neatly traced using the example of fibroblasts. These stromal cells normally provide tissue structural support (Nash *et al.* 2004). However, an early *in vitro* study found that soluble factors secreted by human skin fibroblasts were able to change the shape and organisation of animal-derived EC when the two were co-cultured in collagen gels (Kuzuya & Kinsella 1994). It was later shown that fibroblasts originating from different tissues – namely skin, inflamed synovium and lymphoid tissue – showed markedly different gene expression in response to pro-inflammatory stimuli such as TNFα (Parsonage *et al.* 2003). Skin and synovial fibroblasts also differed in the patterns and amounts of cytokines they secreted in response, indicating that inflammatory reactions, in which they seem to play an active part, were tissue-specific (Parsonage *et al.* 2003). The studies that followed established a difference between fibroblasts originating from healthy and those coming from diseased tissue in their effect on the endothelium. “Healthy” fibroblasts were able to maintain the vascular endothelium in a resting state and prevent excessive leukocyte infiltration. Conversely, those found in diseased

tissues, such as the rheumatoid joint, were imprinted with a pro-inflammatory phenotype which further stimulated inappropriate leukocyte recruitment (McGettrick *et al.* 2009; McGettrick *et al.* 2012). Neutrophil recruitment was mediated by P- and E-selectin, β_2 integrins, CXCR2 and its ligand CXCL5, as evidenced by antibody neutralisation of these molecules which reduced or abolished neutrophil adhesion (Lally *et al.* 2005; Smith *et al.* 2008). CXCL5 was fibroblast-derived and transported to the endothelial surface in order to activate neutrophils (Smith *et al.* 2008). This finding provided an example of how EC-stromal crosstalk can promote inflammation; in this case, the pro-inflammatory fibroblast phenotype translated to the endothelium in the form of chemokine expression.

Naturally, other components of the stroma, such as the BM and the SMC, can also modulate endothelial phenotype and consequently neutrophil recruitment in both health and disease (McGettrick *et al.* 2012), although these will not be discussed here. On the whole, it is clear that in conditions such as RA – the most common autoimmune joint disease – the stroma takes an active role in mediating dysregulated leukocyte adhesion. Understanding the mechanisms by which this happens is crucial to finding a way to switch off excessive inflammation and help treat this debilitating condition. A recent review highlighted the possibility that mesenchymal stem cells (MSC) resident in the synovium may be capable of suppressing exaggerated immune responses mediated by other stromal cells including fibroblasts (El-Jawhari *et al.* 2014). This provides an exciting avenue for further research into the ability of MSC to modulate leukocyte, and more specifically neutrophil, recruitment to the endothelium.

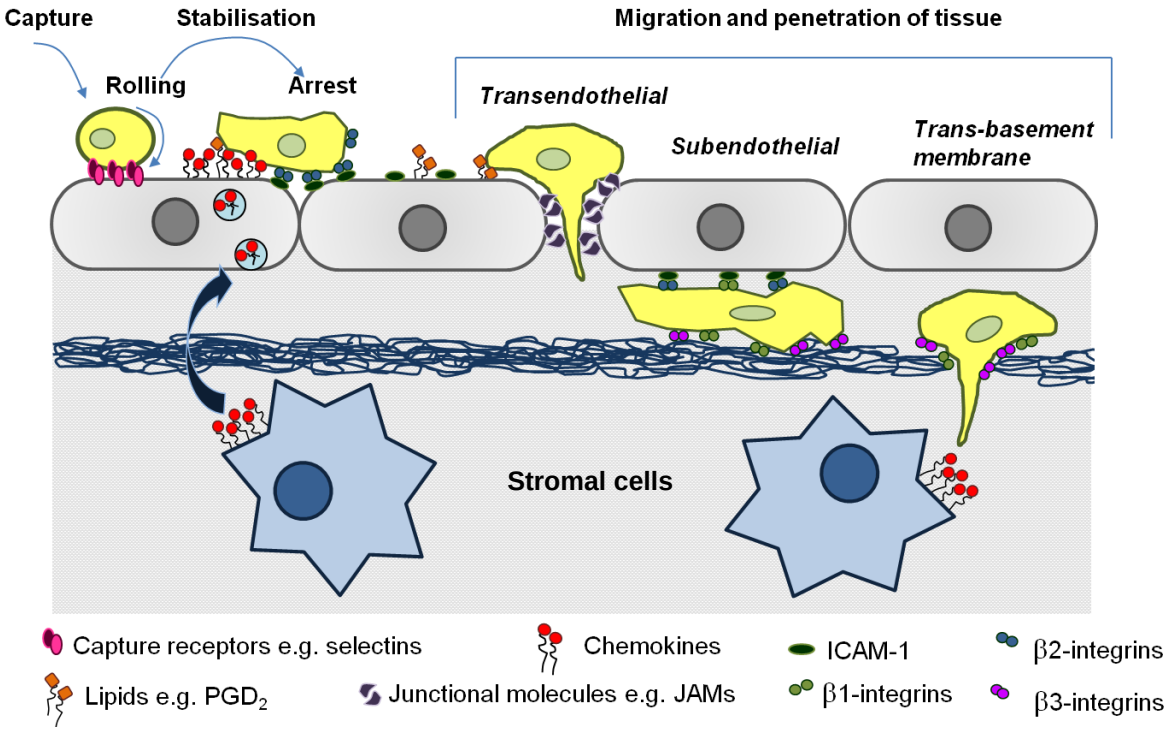

Figure 1 – Neutrophil adhesion cascade and its interactions with tissue stromal cells. Activated vascular endothelium expresses selectins, which mediate neutrophil capture from flow and their rolling across endothelial surface. Subsequent expression of endothelial-derived chemokines, or transcellular transportation of stromal cell-derived chemokines to the endothelial surface, stabilises neutrophil adhesion. This activates β_2 integrins on neutrophil surface, which interact with endothelial ICAM-1 to mediate arrest of the leukocytes. Once neutrophils receive the PGD_2 signal, they can cross the endothelium by binding to junctional molecules such as JAMs. Subendothelial crawling is mediated by a combination of β_1 and β_2 integrins, while crossing of the basement membrane is β_3 integrin-dependent. Once inside the tissue, neutrophils may be directed to the site of inflammation by chemotactic gradients generated by stromal cells.
Adapted from McGettrick *et al.* 2012.

1.3 Mesenchymal stem cells as modulators of neutrophil recruitment

MSC are multipotent, fibroblastic-like stromal progenitor cells capable of self-renewal and differentiation into multiple cell types of the mesodermal lineage (Krampera 2011; Tyndall 2014) (**Figure 2**). These characteristics mean that MSC have persistently generated great interest among researchers, but different investigators have reported using vastly different approaches to their isolation, expansion and characterisation. In an attempt to standardise the use of these cells and thus render varied study outcomes comparable, the International Society for Cellular Therapy has proposed three minimal criteria for the definition of human MSC (Dominici *et al.* 2006). They must: (i) adhere to plastic in standard cell culture; (ii) express CD73, CD90 and CD105 while lacking expression of haematopoietic markers (including CD14, CD34 and CD45) and major histocompatibility complex (MHC) class II surface molecules; and (iii) be capable of differentiating into osteoblasts, chondroblasts and adipocytes *in vitro* (Dominici *et al.* 2006).

Numerous studies carried out over the years, both in animal models and as part of human clinical trials, have demonstrated that infused MSC homed to injured tissue and induced its repair. However, it became increasingly apparent that they were able to bring about functional improvement without actual target tissue engraftment or even differentiation (Prockop 2009; Waterman *et al.* 2010). For example, when human bone marrow-derived MSC were injected into immunodeficient mice with acute myocardial infarction, cardiac function and fibrosis significantly improved without apparent MSC engraftment into cardiac tissue (Iso *et al*. 2007). This and other studies pointed to the possibility that, in fact, immunomodulation by MSC *via*

paracrine signals and cell-to-cell contacts was taking place in the target tissue. Not only that, but it was proposed that MSC were activated by crosstalk with their microenvironment to secrete cytokines, chemokines and other factors that were specifically adapted to the tissue in question (Prockop 2009).

The immunomodulatory capacity of MSC has since been extensively studied in relation to cells of both adaptive and innate immune system, including T- and B-lymphocytes, natural killer (NK) cells and dendritic cells. MSC exerted anti-proliferative effects on B-cells and NK-cells through the secretion of, among other factors, prostaglandin E_2 (PGE_2) and transforming growth factor β (TGFβ). They were also able to induce apoptosis of activated T-cells *via* the action of indoleamine 2,3-dioxygenase (IDO) (Koh & Kang 2012). Comparatively fewer studies looked at MSC effects on neutrophils. One of them found that, when MSC from healthy donors were cultured with freshly isolated neutrophils *in vitro*, they significantly inhibited apoptosis of both resting and activated neutrophils *via* the secretion of soluble factors. Antibody blockade determined that the relevant anti-apoptotic factor was interleukin-6 (IL-6) (Raffaghello *et al.* 2008). This study, however, focused on replicating the bone marrow niche and consequently did not look at the effects of MSC in inflamed tissue. In fact, our group was the first to show that MSC, like other stromal cells, are capable of modulating leukocyte recruitment to inflamed endothelium *via* actions on the EC themselves (Luu *et al*. 2013). When brought together in co-culture *in vitro*, MSC and HUVEC supported markedly lower levels of neutrophil adhesion compared to HUVEC monoculture when both were stimulated with either TNFα or IL-1β. Furthermore, MSC-derived IL-6 was detected as the soluble factor responsible for

this decrease in recruitment, contrary to its more established role as a pro-inflammatory cytokine; when IL-6 was neutralised using an antibody, the anti-inflammatory effects of co-culture were lost (Luu *et al*. 2013) (**Figure 3**).

The immunomodulation capabilities of MSC quickly led to them being explored for therapeutic potential in RA, where apart from excessive leukocyte infiltration, dysregulated fibroblast activation contributed to joint destruction (Bottini & Firestein 2013). MSC were found to be modulated by pro-inflammatory cytokines such as TNFα or IL-1β which were present in the inflamed microenvironment, a process referred to as 'licensing' (Krampera 2011). This in turn caused them to increase the production of chemokines and inducible nitric oxide synthase (iNOS) which drove immunosuppression, as evidenced by their immunosuppressive effect being abolished *in vitro* by chemokine receptor blockade or in MSC derived from $iNOS^{-/-}$ mice (Ren *et al*. 2008). However, this finding was in conflict with the results from an earlier *in vivo* study, where MSC injected into mice with collagen-induced arthritis (a murine model of RA) conferred no therapeutic benefit. In fact, their immunosuppressive capability was reversed by subsequently adding TNFα to them *in vitro* (Djouad *et al.* 2005). While both studies looked at MSC effects on T-cell proliferation rather than neutrophil recruitment, it became clear that the local environment could influence MSC phenotype and consequently their anti-inflammatory properties. In particular, the activation of Toll-like receptors (TLRs) on the surface of MSC was recently found to differentially polarise them towards a pro- (MSC1) or anti-inflammatory (MSC2) phenotype. TLR4 stimulation caused pro-inflammatory cytokines such as IL-6, IL-8 or TGFβ to be produced, while TLR3

activation induced the secretion of IDO and therefore rendered the cells immunosuppressive (Waterman *et al.* 2010). All of the above provided evidence that, while they may normally be able to suppress immune responses, MSC function is likely to shift towards immune stimulation in a chronically inflamed milieu such as that found in RA (El-Jawhari *et al.* 2014).

Taking the available evidence into account, we propose to lead the study of the immunomodulatory properties of MSC in a new direction. Recent findings using a mouse model of cartilage destruction (Croft *et al.* n.d., unpublished data) suggested that, in the inflamed synovium of RA, fibroblasts were able to differentiate into two distinct subsets. Those found in the lining expressed GP38, displayed a more aggressive, migratory phenotype and mediated cartilage degradation. Conversely, fibroblasts in the sub-lining (and therefore further away from the cartilage) expressed CD248 and were not migratory, suggesting they had a role in regulation rather than invasion. GP38 expression could be induced in cell culture by stimulating RA synovial fibroblasts (RASF) with TNFα, which in turn mediated cartilage destruction. Stimulating them with TGFβ1, on the other hand, induced expression of CD248 and reduced *in vitro* degradation of cartilage (Croft *et al.* n.d., unpublished data). Considering MSC share a lot of their characteristics with fibroblasts (Haniffa *et al.* 2009), and in view of their immunomodulatory capacity, it would be interesting to see whether stimulation of MSC with the above cytokines resulted in similar changes in surface expression and phenotype. Furthermore, the study of the effect this would have on MSC:EC co-culture and subsequent neutrophil recruitment to the

endothelium would provide very useful additional insights into the regulation of the immune response by MSC in chronic inflammation.

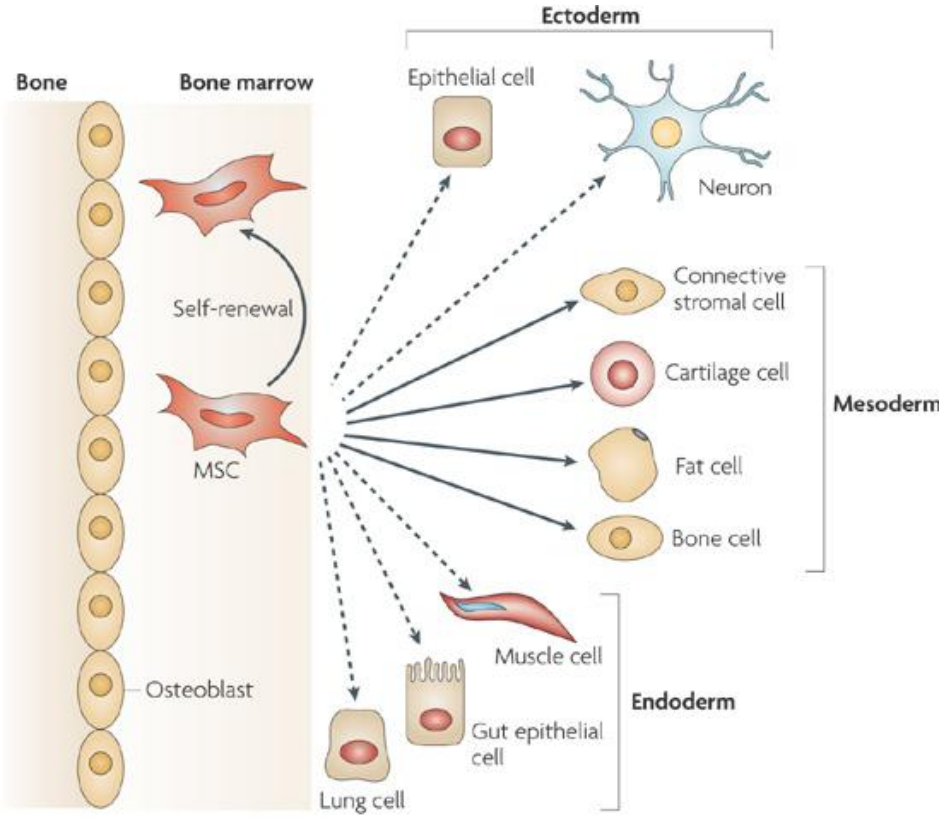

Figure 2 – The multipotentiality of MSC.
MSC are capable of self-renewal in the bone-marrow cavity, as well as differentiation towards cells of the mesodermal lineage. Their reported ability to transdifferentiate into cells of other lineages (ecto- and endoderm) is controversial *in vivo*.
Reprinted by permission from Macmillan Publishers Ltd: Nature Reviews Immunology (Uccelli *et al.* 2008), copyright © Macmillan Publishers Limited (2008)

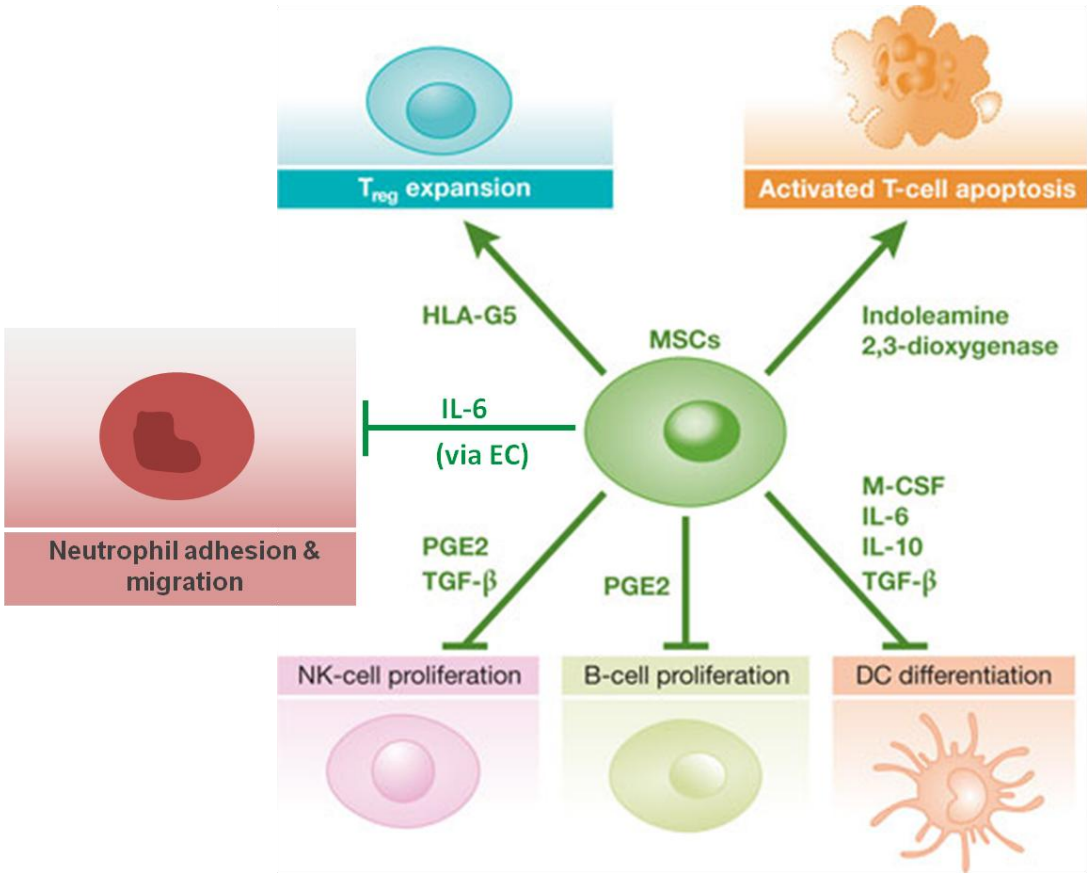

Figure 3 – The immunomodulatory capabilities of MSC.
MSC can exert their immunosuppressive effects on cells of both innate and adaptive immune system *via* the secretion of different chemokines and soluble factors. They can induce expansion of immunosuppressive T_{reg} cells as well as apoptosis of activated T-cells by secreting human leukocyte antigen-G5 (HLA-G5) and IDO respectively. They are also capable of inhibiting NK-cell and B-cell proliferation through the actions of PGE_2 and TGFβ, and can suppress DC differentiation *via* the action of, among other factors, IL-6 and IL-10. Most recently, MSC have been shown to suppress neutrophil adhesion and transendothelial migration by acting on the vascular endothelium, which in turn supported less neutrophil recruitment; this effect was also found to be mediated by IL-6.
Adapted from: The pro-metastatic role of bone marrow-derived cells: a focus on MSCs and regulatory T cells. Koh, B.I. & Kang, Y. *EMBO Reports*, 13(5). Copyright © 2012 European Molecular Biology Organization

1.4 Hypothesis and aims

We hypothesise that MSC exposed to pro-inflammatory cytokines, such as TNFα, for several days prior to co-culture with EC acquire an immunostimulatory phenotype, thus causing significantly greater neutrophil adhesion levels to those seen in normal co-culture conditions.

The main aims of the project are:

- To characterise neutrophil recruitment to cytokine-stimulated dermal microvascular endothelial cells (DMEC), which may be a more representative model of *in vivo* neutrophil recruitment than HUVEC;
- To compare the effects of MSC on neutrophil adhesion to cytokine-stimulated HUVEC and DMEC;
- To assess the effects of prolonged cytokine treatment (TNFα and TGFβ) on MSC phenotype, specifically focusing on surface expression of GP38, CD248 and MSC surface markers CD73 and CD90.

2. MATERIALS AND METHODS

2.1 Isolation and culture of EC and MSC

HUVEC were isolated as described previously (Cooke *et al.* 1993) from umbilical cords obtained from the Human Biomaterials Resource Centre (University of Birmingham, UK) following informed consent. The cells were cultured in Medium 199 (M199; Gibco Invitrogen Compounds, Paisley, Scotland, UK) supplemented with 20% foetal calf serum (FCS), 35µg/ml gentamycin sulphate, 10ng/ml epidermal growth factor (EGF), 1µg/ml hydrocortisone (all Sigma-Aldrich, Poole, UK) and 2.5µg/ml amphotericin B (Gibco Invitrogen Compounds). HUVEC were used at passage 1.

DMEC were obtained from PromoCell and cultured in endothelial cell growth medium MV supplemented with 5% FCS, 0.4% endothelial cell growth supplement (ECGS, bovine hypothalamic extract), 10ng/ml EGF, 90µg/ml heparin and 1µg/ml hydrocortisone (all PromoCell GmbH, Heidelberg, Germany). DMEC were used at passage 4.

Human bone marrow-derived MSC (BMMSC), purchased from Lonza, were cultured in MSCGM™ Mesenchymal Stem Cell Growth Medium BulletKit as recommended by the manufacturer (Lonza Ltd, Basel, Switzerland). BMMSC were expanded by three-way splits and used between 3rd and 5th passages.

2.2 Isolation of neutrophils

Following informed consent, blood was obtained by venepuncture from healthy volunteers and collected into ethylenediaminetetraacetic acid (EDTA)-coated tubes (Sarstedt Ltd, Leicester, UK). Neutrophils were isolated by overlaying whole blood on density gradients of Histopaque 1077 above Histopaque 1119 (both Sigma-Aldrich) and centrifuging at 800g for 30 minutes (**Figure 4**). The neutrophil fraction was harvested and washed twice by spinning at 250g for 5 minutes and re-suspending in phosphate-buffered saline (PBS; Sigma-Aldrich) containing 1mM Ca^{2+}, 0.5mM Mg^{2+} and 0.15% bovine serum albumin (BSA; Gibco; PBS/BSA). Neutrophils were counted using a Z2 Coulter® Particle Count & Size Analyzer (Beckman Coulter Ltd, High Wycombe, UK) and diluted with PBS/BSA to a final concentration of $1x10^6$ cells/ml.

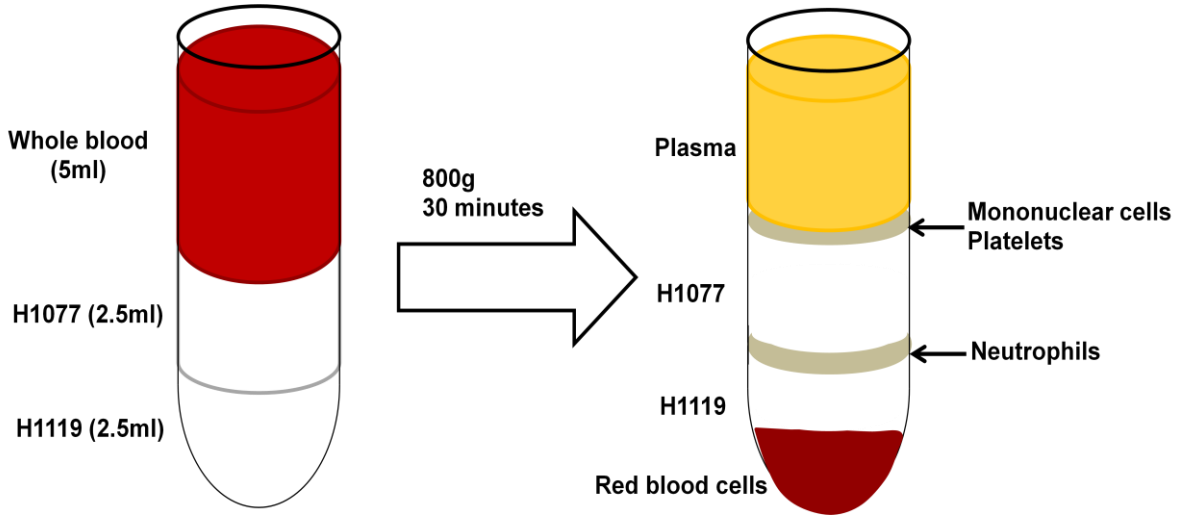

Figure 4 – Neutrophil isolation using the Histopaque density gradient.
Whole blood was overlayed on the density gradient of Histopaque 1077 (H1077) over Histopaque 1119 (H1119) and centrifuged at 800g for 30 minutes to give the separation of blood components as shown above. Plasma and the upper cell band containing mononuclear cells and platelets were removed before harvesting neutrophils from the lower band. Neutrophils were washed twice and re-suspended in the correct volume of PBS/BSA to give $1x10^6$ cells/ml.

2.3 Seeding of EC monoculture and MSC:EC co-culture

Confluent flasks of HUVEC and DMEC were rinsed with 0.02% EDTA for 2 minutes before dislodging the cells using 0.25% trypsin (both Sigma-Aldrich) in a 2:1 ratio with EDTA. Serum-containing neutralising medium was added before centrifuging at 250g for 5 minutes. HUVEC were re-suspended in MSCGM (BMMSC culture medium containing 10% FCS), and DMEC in DMEC culture medium with or without hydrocortisone. Endothelial cells were then seeded into µ-slide VI channel slides (ibidi GmbH, Martinsried, Germany) at a seeding density designed to give confluent monocultures in 24h (Luu *et al.* 2013).

For MSC:EC co-culture, flasks of BMMSC were treated with EDTA and trypsin as above and MSC were resuspended in serum-free rather than complete (10%) MSCGM. MSC were labelled with 5 µM Cell Tracker Green (Life Technologies Ltd, Paisley, UK) for one hour, with serum-free medium being replaced by complete medium halfway through to avoid cell starvation. MSC were then counted using a Cellometer® (Nexcelom Bioscience, Lawrence, Massachusetts, USA) and adjusted to a final concentration of $1.5x10^5$ cells/ml before being added to the ibidi channel slides containing confluent EC monolayers (Luu *et al.* 2013). After 60-90 minutes, non-adherent MSC were washed off and the rest were allowed to incorporate into the monolayer for 24h.

After 24h, mono- and co-cultures were treated with TNF-α (0, 1, 10 or 100 U/ml) or IL-1β ($5x10^{-9}$ g/ml) (both Sigma-Aldrich) for 4h before being attached to the flow-based adhesion assay system (**section 2.4**).

2.4 Flow-based adhesion assay

The flow system was assembled as described previously (McGettrick *et al*. 2007) (**Figure 5**). Plastic tubing was used to attach ibidi channel slides to the flow apparatus which was enclosed in a temperature-controlled chamber at 37°C and linked to a fluorescent video-microscope. PBS/BSA was used to wash the system for 2 minutes. Neutrophils were then perfused over EC or MSC:EC monolayers at a wall shear stress of 0.05Pa and flow rate of 0.4ml/min for 4 minutes. This was followed by a second washout period, during which digitised recordings were taken of ten random fields along the centre of the flow channel at 2 and 9 minutes relative to end of neutrophil bolus. A 5-minute recording of a separate single microscope field was also made to analyse the migration of neutrophils under the endothelium. In addition, matched phase-contrast and fluorescent images were taken of channels containing MSC in order to visualise MSC integration into the EC monolayer and calculate the MSC:EC ratio (**Figure 6**). Images were analysed offline using ImagePro analysis software (DataCell Limited, Finchampstead, UK).

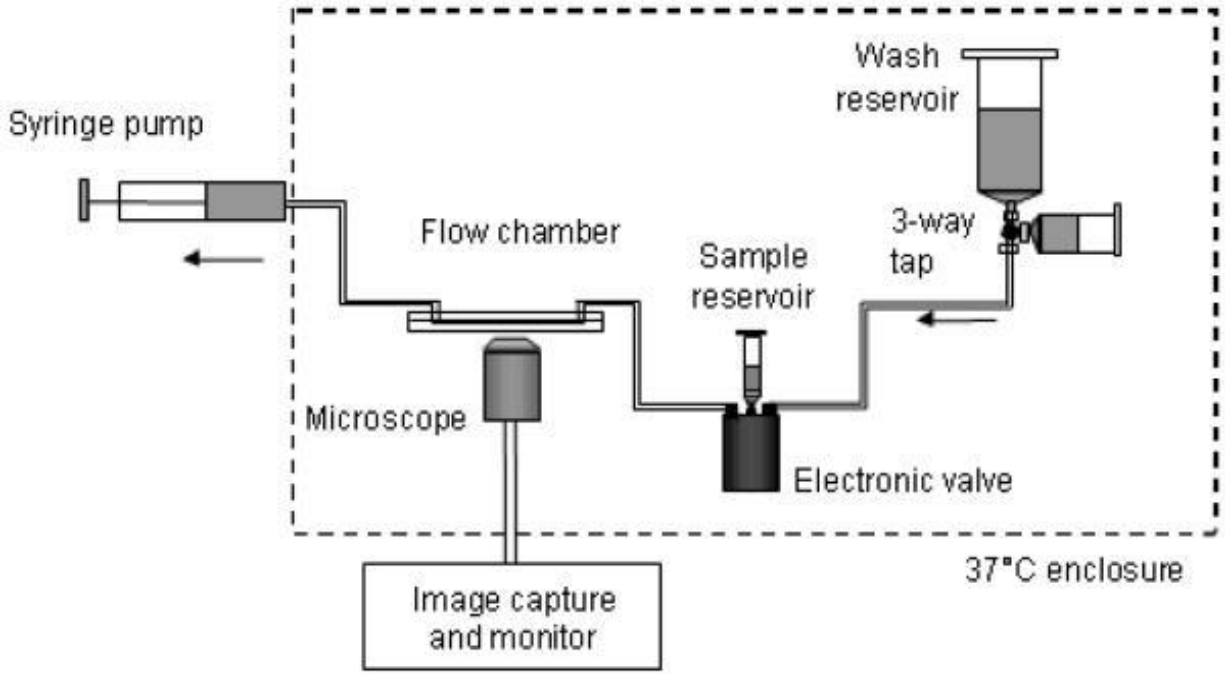

Figure 5 – Schematic of the flow-based adhesion assay system.
Ibidi channel slides were placed within an enclosed flow chamber set at a constant temperature of 37°C. A syringe pump was used to pull the neutrophils from the sample reservoir and allow them to flow over the cell monolayers within the channels at a flow rate of 0.4ml/min. A cell-free wash buffer (PBS/BSA) contained within the wash reservoir was run before and after the 4-minute neutrophil bolus. Images and recordings were captured live and visualised on the monitor using ImagePro software.

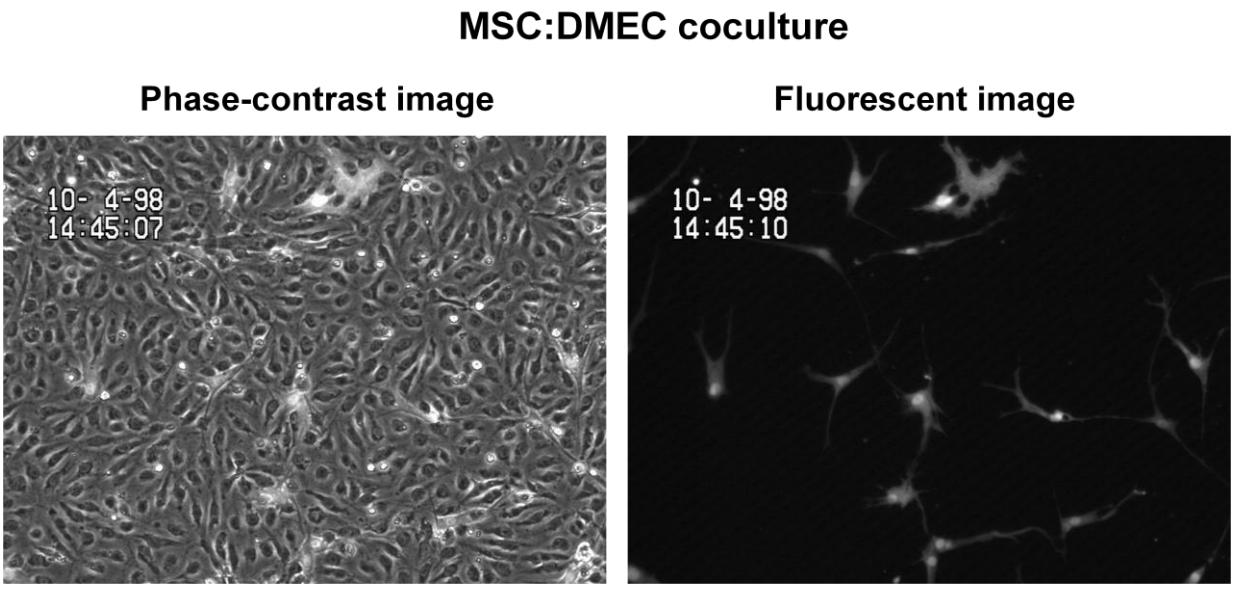

Figure 6 – Representative video-microscope image of MSC:EC co-culture.
DMEC were seeded into ibidi channel slides such that they would yield a confluent monolayer within 24h. MSC labelled with Cell Tracker Green were then added to the same channel slides and allowed to incorporate for a further 24h. The co-cultures were treated with TNFα for 4h before being exposed to neutrophil flow. Following the flow-based adhesion assay, four matched phase-contrast and fluorescent images were taken down the centre of each channel using x10 magnification. EC were counted from phase-contrast, and labelled MSC from fluorescent images to determine MSC:EC ratio.

2.5 Image analysis

Adherent neutrophils were classified as:

a) Rolling – spherical cells moving fast across the endothelium, but more slowly than free-flowing neutrophils;
b) Stationary – spherical or cells of distorted shape firmly adhering to the endothelium or oscillating slightly around their position;
c) Migrated – phase-dark cells of various shapes that have crossed the endothelium and typically migrate away from their point of entry once underneath.

The number of neutrophils in each classification and the total number of adherent neutrophils were averaged from the ten microscope fields per channel and converted to number/mm^2/10^6 perfused. Rolling and migration velocities were also obtained by tracking the movement of rolling and transmigrated cells and finding the average distance travelled from ten cells in each category. The velocities were then expressed in μm/s (rolling) and μm/min (migration). In co-cultures, the calculated number of EC and MSC per channel was used to determine the MSC:EC ratio.

2.6 Preparation and labelling of MSC for flow cytometry

BMMSC were dissociated from the flask using EDTA and trypsin as described in section 2.3 and seeded into 12-well plates at the seeding density of 7-10,000 cells/well for 24h. Some wells were incubated in low-serum (2%) BMMSC medium for 6h, after which MSC in both complete and low-serum media were treated with 100U/ml TNF-α or 10ng/ml TGF-β1 (PeproTech, Rocky Hill, New Jersey, USA) for 4-6 days. MSC were then lifted from the wells using accutase (Gibco) in order to

preserve surface marker expression, centrifuged at 250g for 5 minutes and resuspended in PBS/BSA. The cells were subsequently labelled with antibodies listed in **Table 1**, washed with PBS/BSA and fixed with 2% paraformaldehyde (Sigma-Aldrich). Samples were analysed in a FACS Analyser (CyAn ADP, DakoCytomation, Glostrup, Denmark) and the fluorescence data obtained using Summit 4.3 software. Data were expressed as mean fluorescence intensities (MFI) and percentages of positive fluorescing cells of each sample.

2.7 Statistical analysis

All data were analysed using GraphPad Prism 5 and expressed as mean ± standard error of the mean (SEM). Analysis of variance (ANOVA) was used to assess variation between multiple conditions, while Bonferroni post-tests compared individual treatments, as appropriate. Statistical significance was assumed if $P < 0.05$. Where ANOVA did not show statistical significance for any of the parameters, no mention of it was made in the figure legends.

Table 1 – List of antibodies used to label MSC for surface expression of GP38, CD248 and MSC positive surface markers CD73 and CD90

Antibody	Clone	Conjugated dye	Manufacturer
Anti-Human Podoplanin (GP38)	NZ-1.3	PE	eBioscience Inc, San Diego, California, USA
Rat IgG2a Isotype Control for Anti-Human Podoplanin (GP38)	eBR2a	PE	"
Mouse Anti-Human CD248	B135.1, 10x	Unconjugated (requires 2° antibody)	In-house antibody
Goat Anti-Mouse IgG (2° antibody to Mouse Anti-Human CD248)	1010-02	FITC	SouthernBiotech, Birmingham, Alabama, USA
Mouse Anti-Human CD73	AD2	FITC	BD Biosciences – Pharmingen, San Diego, California, USA
Mouse Anti-Human CD90	5E10	Brilliant Violet™ 421	"

3. RESULTS

3.1 Neutrophil recruitment to TNF-α treated DMEC is dose-dependent

The studies of neutrophil recruitment have overwhelmingly been performed on HUVEC, with very little known about how DMEC support this process. Being of micro- rather than macrovascular origin, DMEC are potentially more representative of the endothelium neutrophils encounter *in vivo*, where the vast majority of adhesion happens in microvessels. To address this, we investigated the ability of TNFα-stimulated DMEC to support neutrophil recruitment. DMEC monocultures were either left untreated or were treated with 1, 10 or 100U/ml TNFα for 4h before being exposed to a flow of neutrophils. We observed a dose-dependent increase in neutrophil recruitment (**Figure 7**), with adhesion remaining reasonably stable over the course of the assay. Transendothelial migration was significantly higher at 100U/ml compared to 10U/ml TNFα, where most of the neutrophils were firmly adherent on the DMEC surface. Behaviour was not determined for 1U/ml TNFα as neutrophil adhesion was too low (**Figure 8**).

From the results above we concluded that DMEC were able to support neutrophil recruitment in a TNFα dose-dependent manner, supporting the observations made in HUVEC in previous studies (e.g. Luu *et al.* 2013).

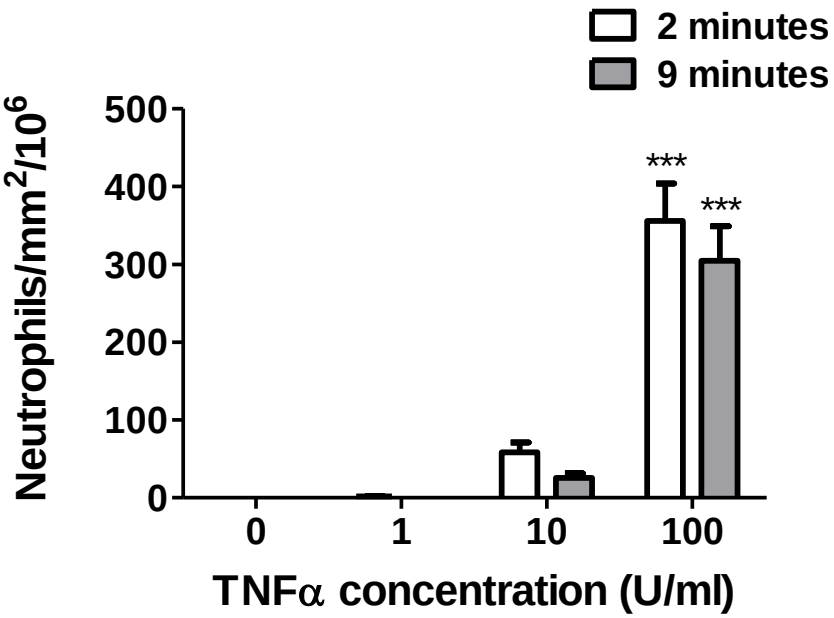

Figure 7 – Effect of TNFα concentration on neutrophil recruitment to DMEC from flow. DMEC monocultures were stimulated with TNFα for 4h before being exposed to a flow of neutrophils ($1x10^6$/ml) at a rate of 0.4ml/min for 4 minutes. The total number of adhering neutrophils was expressed as neutrophils/$mm^2/10^6$ cells perfused and determined at 2 and 9 minutes after neutrophil flow stopped. Two-way ANOVA showed a significant effect of TNFα concentration ($P<0.0001$), but not time, on neutrophil adhesion. *** = $P<0.001$ for comparison of 100U/ml TNFα to each of the other TNFα concentrations by Bonferroni post-tests. Data are mean ± SEM, n=4.

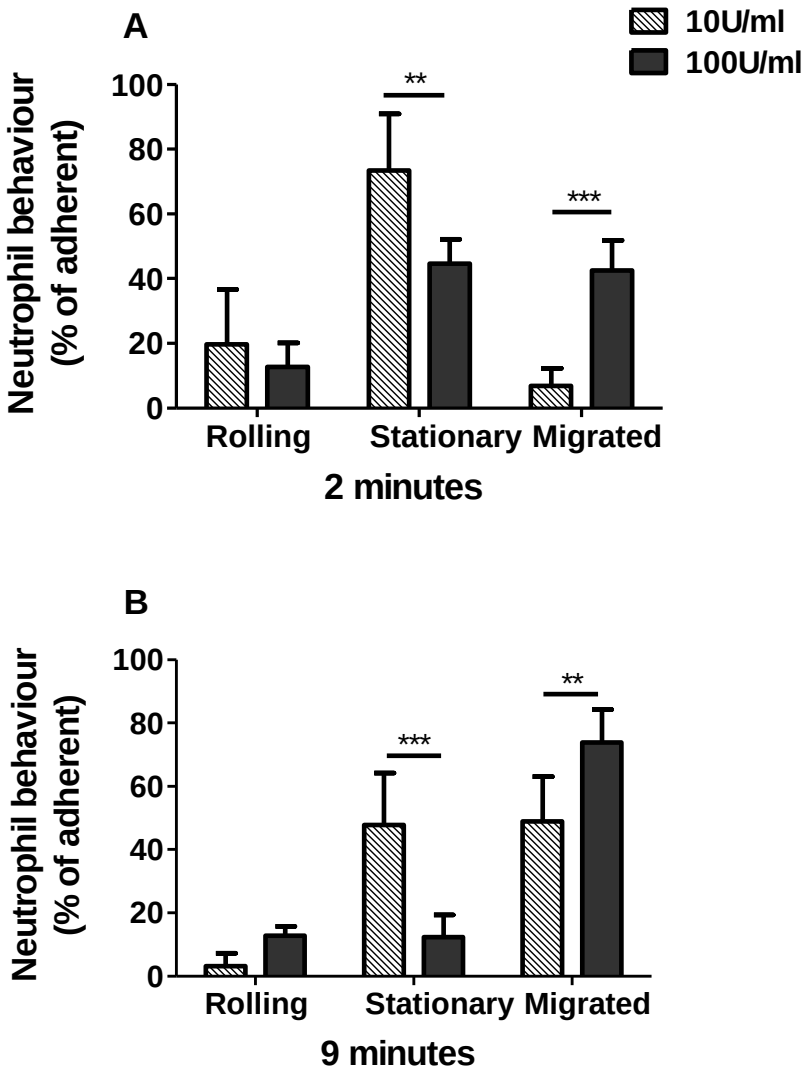

Figure 8 – Effect of TNFα concentration on the behaviour of neutrophils recruited to DMEC from flow.

DMEC monocultures were stimulated with TNFα for 4h before being exposed to a flow of neutrophils ($1x10^6$/ml) at a rate of 0.4ml/min for 4 minutes. Rolling, stationary and migrated neutrophils were analysed at **(A)** 2 and **(B)** 9 minutes after neutrophil flow stopped, and each expressed as a percentage of total adherent cells. Two-way ANOVA showed a significant effect of neutrophil behaviour ($P<0.001$), but not TNFα concentration, on % adherent neutrophils. ** = $P<0.01$ and *** = $P<0.001$ for comparison of 10U/ml to 100U/ml TNFα by Bonferroni post-tests. Data are mean ± SEM, n=4.

3.2 TNFα and IL-1β stimulation of DMEC result in similar neutrophil adhesion and behaviour

In previous studies using HUVEC, comparable neutrophil recruitment and behaviour were observed for endothelial stimulation with TNFα or IL-1β (Sheikh *et al.* 2005). We wished to examine whether the same held true for DMEC. We therefore stimulated DMEC monocultures with high-dose TNFα (100U/ml) or IL-1β ($5x10^{-9}$ g/ml) for 4h before perfusing neutrophils over them. Total neutrophil adhesion levels were very similar with both cytokines (**Figure 9**). Neutrophil behaviour was also analogous, with stationary neutrophil numbers decreasing in favour of migrated neutrophils over time (**Figure 10**). Rolling and migration velocities were compared as well (**Figure 11**). From two separate experiments, we noticed a tendency for neutrophils to roll more quickly and migrate more slowly on TNFα-stimulated compared to IL-1β-treated DMEC. However, further experiments are required to determine whether this is statistically significant.

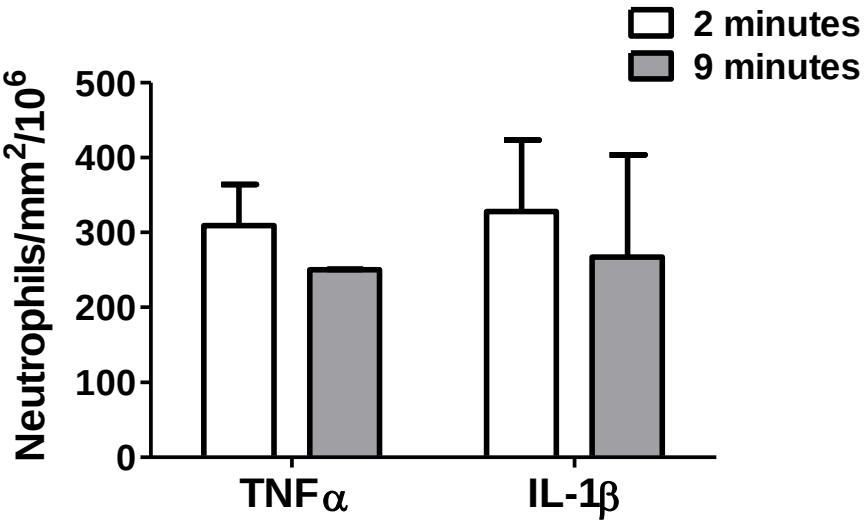

Figure 9 – Comparison of the effect of TNFα and IL-1β on neutrophil recruitment to DMEC from flow.

DMEC monocultures were stimulated with 100U/ml TNFα or $5x10^{-9}$g/ml IL-1β for 4h before being exposed to a flow of neutrophils ($1x10^6$/ml) at a rate of 0.4ml/min for 4 minutes. The total number of adhering neutrophils was expressed as neutrophils/$mm^2/10^6$ cells perfused and determined at 2 and 9 minutes after neutrophil flow stopped. Data are mean ± SEM, n=2.

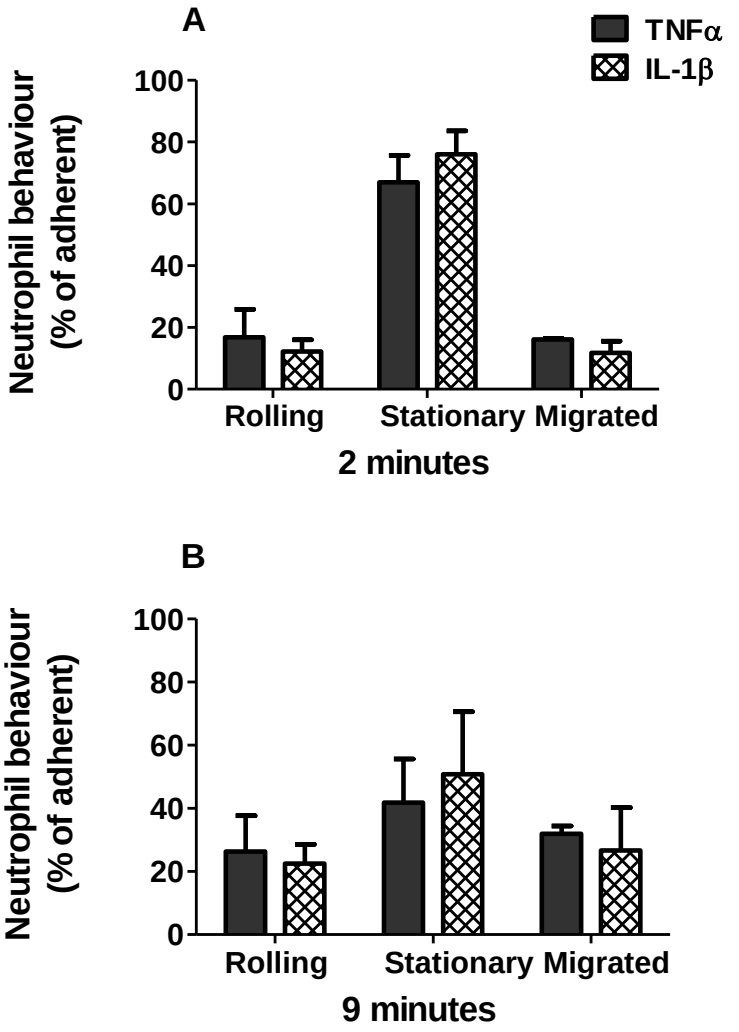

Figure 10 – Comparison of the effect of TNFα and IL-1β on the behaviour of neutrophils recruited to DMEC from flow.

DMEC monocultures were stimulated with 100U/ml TNFα or $5x10^{-9}$ g/ml IL-1β for 4h before being exposed to a flow of neutrophils ($1x10^{6}$/ml) at a rate of 0.4ml/min for 4 minutes. Rolling, stationary and migrated neutrophils were counted at **(A)** 2 and **(B)** 9 minutes after neutrophil flow stopped, and each expressed as a percentage of total adherent cells. Data are mean ± SEM, n=2.

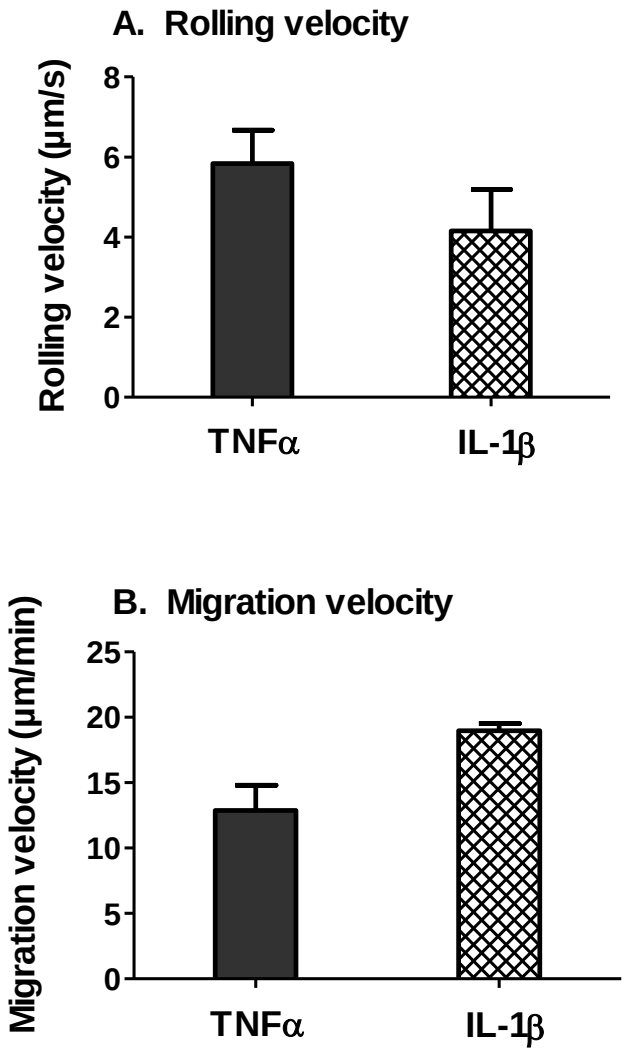

Figure 11 – Comparison of the effect of TNFα and IL-1β on the rolling and migration velocities of neutrophils recruited to DMEC from flow.

DMEC monocultures were stimulated with 100U/ml TNFα or $5x10^{-9}$ g/ml IL-1β for 4h before being exposed to a flow of neutrophils ($1x10^{6}$/ml) at a rate of 0.4ml/min for 4 minutes. **(A)** Rolling and **(B)** migration velocities were calculated as average values from ten rolling or transmigrated cells respectively, and expressed in µm/s (rolling) and µm/min (migration). Data are mean ± SEM, n=2.

3.3 The presence of hydrocortisone affects neutrophil recruitment to DMEC at low doses of TNFα

Neutrophil adhesion to DMEC at 1U/ml and 10U/ml TNFα was lower than expected from historical data obtained with HUVEC. We subsequently identified hydrocortisone (HC) in the DMEC medium and hypothesised that its presence was responsible for our observations. To test this, we cultured DMEC in the presence or absence of HC and, as before, stimulated them with increasing doses of TNFα (0, 1, 10 and 100U/ml) for 4h before the perfusion of neutrophils. Dose-dependent neutrophil recruitment was apparent once again (**Figure 12**), however much higher levels of adhesion were observed when DMEC were stimulated with 1 and 10U/ml TNFα in the absence of HC compared to those cultured in HC-containing medium (**Figure 13**). In contrast to adhesion, HC presence had little effect on neutrophil behaviour. Low dose TNFα (1U/ml) supported more rolling and stationary neutrophils compared to 10 and 100U/ml, while significantly more migration was observed at 100U/ml compared to lower TNFα concentrations (**Figure 14**). Rolling velocity was also highest at 1U/ml (**Figure 15**).

Taken together, the above results confirmed our hypothesis that hydrocortisone reduced neutrophil recruitment to DMEC at low TNFα doses. In view of this, all subsequent experiments were conducted in hydrocortisone-free media.

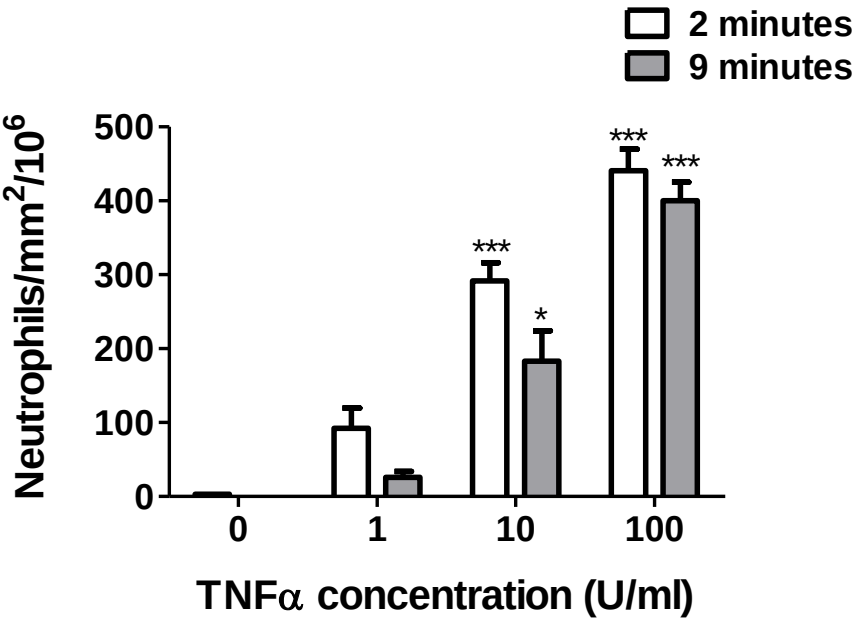

Figure 12 – Effect of TNFα concentration on neutrophil recruitment to DMEC from flow in hydrocortisone-free DMEC medium.

DMEC monocultures in hydrocortisone-free DMEC medium were stimulated with TNFα for 4h before being exposed to a flow of neutrophils ($1x10^6$/ml) at a rate of 0.4ml/min for 4 minutes. The total number of adhering neutrophils was expressed as neutrophils/$mm^2/10^6$ cells perfused and determined at 2 and 9 minutes after neutrophil flow stopped. Two-way ANOVA showed a significant effect of both TNFα concentration ($P<0.0001$) and time ($P<0.05$) on neutrophil adhesion. * = $P<0.05$ and *** = $P<0.001$ for comparison of 10U/ml and 100U/ml TNFα to unstimulated control (0U/ml TNFα) by Bonferroni post-tests. Data are mean ± SEM, n=3.

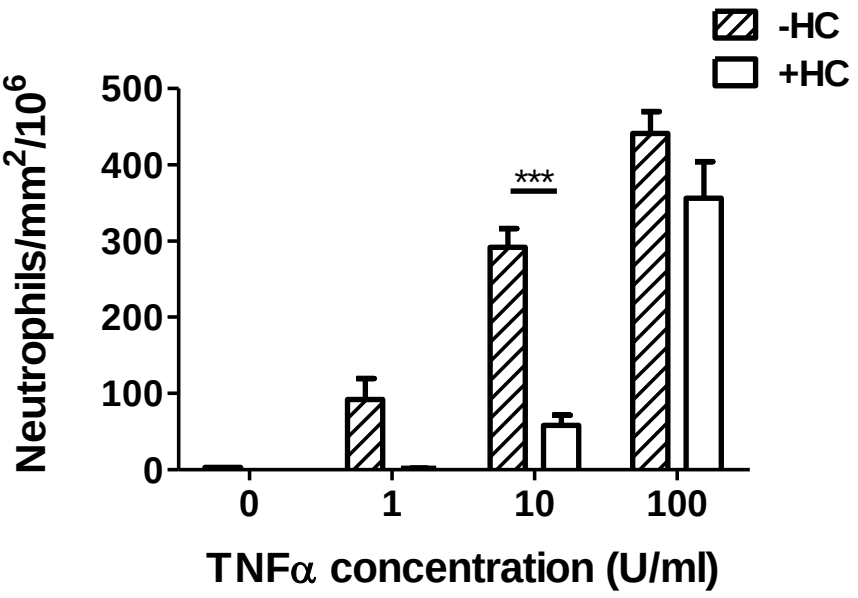

Figure 13 – Effect of hydrocortisone (HC) on neutrophil recruitment to TNFα-stimulated DMEC from flow.

DMEC monocultures in hydrocortisone-free or complete DMEC medium were stimulated with TNFα for 4h before being exposed to a flow of neutrophils ($1x10^6$/ml) at a rate of 0.4ml/min for 4 minutes. The total number of adhering neutrophils was expressed as neutrophils/$mm^2/10^6$ cells perfused and determined at 2 minutes after neutrophil flow stopped. Two-way ANOVA showed a significant effect of both TNFα concentration and HC on neutrophil adhesion ($P \leq 0.0001$). *** = $P<0.001$ for the effect of HC at 10U/ml TNFα by Bonferroni post-test. Data are mean ± SEM, n=3.

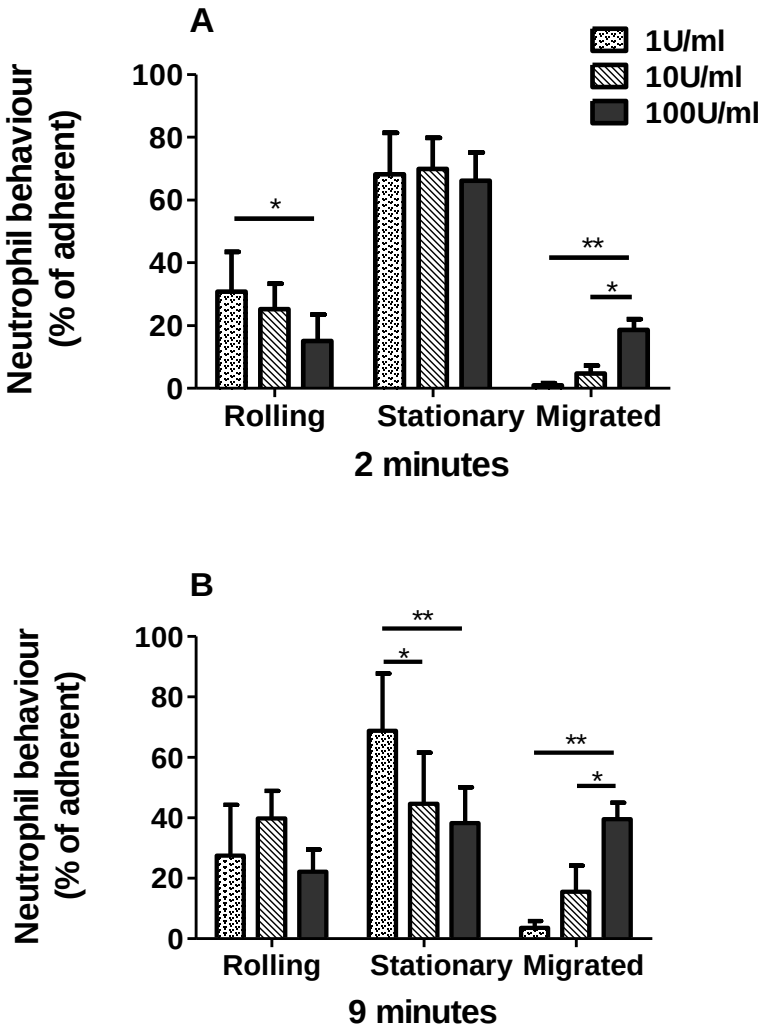

Figure 14 – Effect of TNFα concentration on the behaviour of neutrophils recruited to DMEC from flow in hydrocortisone-free DMEC medium.

DMEC monocultures in hydrocortisone-free DMEC medium were stimulated with TNFα for 4h before being exposed to a flow of neutrophils ($1x10^6$/ml) at a rate of 0.4ml/min for 4 minutes. Rolling, stationary and migrated neutrophils were counted at **(A)** 2 and **(B)** 9 minutes after neutrophil flow stopped, and each expressed as a percentage of total adherent cells. In A, two-way ANOVA showed a significant effect of neutrophil behaviour (P = 0.05), but not TNFα concentration, on % adherent neutrophils. * = P<0.05 and ** = P<0.01 by Bonferroni post-tests. Data are mean ± SEM, n=3.

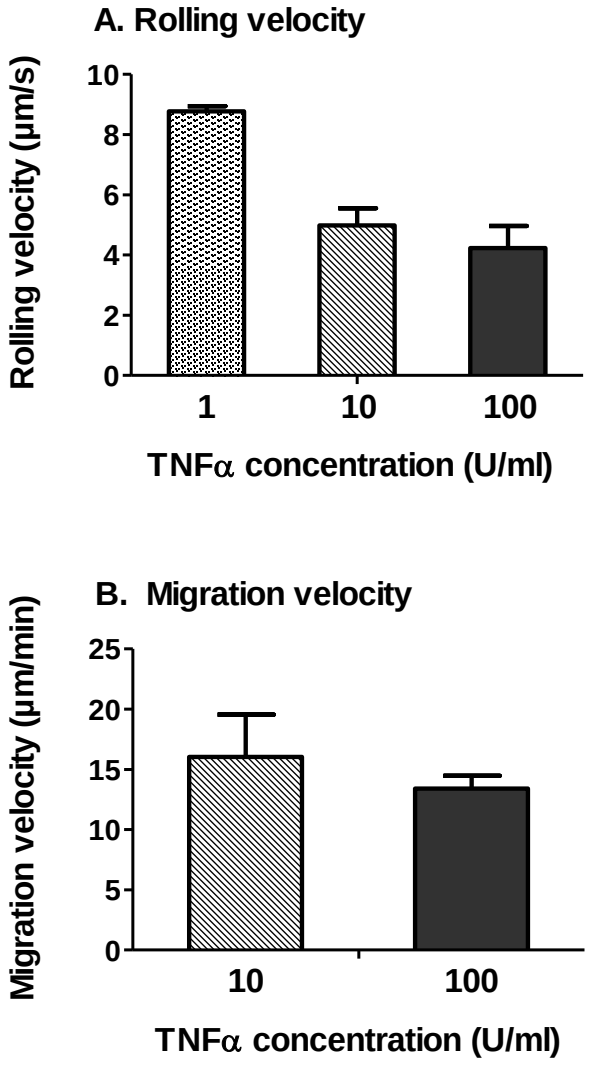

Figure 15 – Effect of TNFα concentration on the rolling and migration velocities of neutrophils recruited to DMEC from flow in hydrocortisone-free DMEC medium.
DMEC monocultures in hydrocortisone-free DMEC medium were stimulated with TNFα for 4h before being exposed to a flow of neutrophils ($1x10^6$/ml) at a rate of 0.4ml/min for 4 minutes. **(A)** Rolling and **(B)** migration velocities were calculated as average values from ten rolling or transmigrated cells respectively, and expressed in µm/s (rolling) and µm/min (migration). Two-way ANOVA showed a significant effect of both TNFα concentration and neutrophil rolling and migration velocity ($P < 0.05$). Data are mean ± SEM, n=3.

3.4 MSC in co-culture with DMEC or HUVEC do not significantly reduce neutrophil adhesion

Previously it has been shown that BMMSC in co-culture with HUVEC significantly reduced cytokine-induced neutrophil adhesion and transmigration compared to HUVEC monoculture (Luu *et al*. 2013). The effect on neutrophil adhesion was apparent at MSC:HUVEC ratio of 1:25, while reduction in transmigration was already seen at ratios of 1:500 and below (Luu *et al.* 2013). We wished to examine if the same happened with DMEC by directly comparing neutrophil recruitment to MSC:DMEC and MSC:HUVEC co-cultures. The two co-cultures, and their respective monocultures, were incubated with 100U/ml TNFα for 4h before neutrophils were perfused as before. In contrast to findings by Luu *et al*, DMEC and HUVEC co-cultures with BMMSC did not have a significant impact on neutrophil adhesion levels compared to monocultures (**Figure 16**). Similarly, we did not observe an effect on neutrophil behaviour (**Figure 17**) or on the velocity of rolling or migrating cells (**Figure 18**). Of note, the calculated MSC:EC ratios were very variable between individual experiments, providing a possible explanation for lack of co-culture effect (**Table 2**). We also observed that the presence of BMMSC appeared to cause DMEC to retract or detach over the duration of the flow assay, leaving large gaps in the monolayer which were not evident in DMEC monoculture (**Figure 19A**). The same was not true for MSC:HUVEC co-cultures, which remained intact (**Figure 19B**).

Overall, we concluded that the presence of BMMSC did not suppress neutrophil recruitment to DMEC or HUVEC, but that DMEC may not be suitable for MSC co-culture studies due to their tendency to retract under flow.

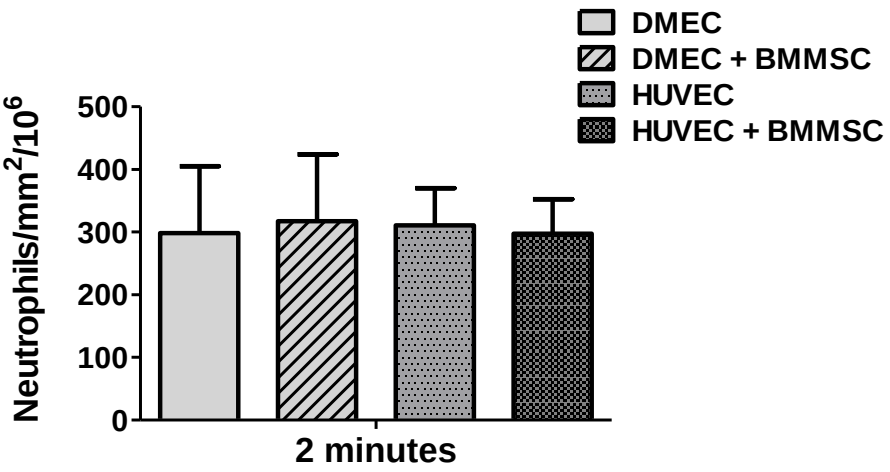

Figure 16 – Effect of MSC:EC co-culture on neutrophil recruitment to TNFα-stimulated endothelium from flow.

DMEC or HUVEC monocultures and their respective co-cultures with BMMSC were stimulated with 100U/ml TNFα for 4h before being exposed to a flow of neutrophils ($1x10^6$/ml) at a rate of 0.4ml/min for 4 minutes. The total number of adhering neutrophils was expressed as neutrophils/mm^2/10^6 cells perfused and determined at 2 minutes after neutrophil flow stopped. Data are mean ± SEM, n=4.

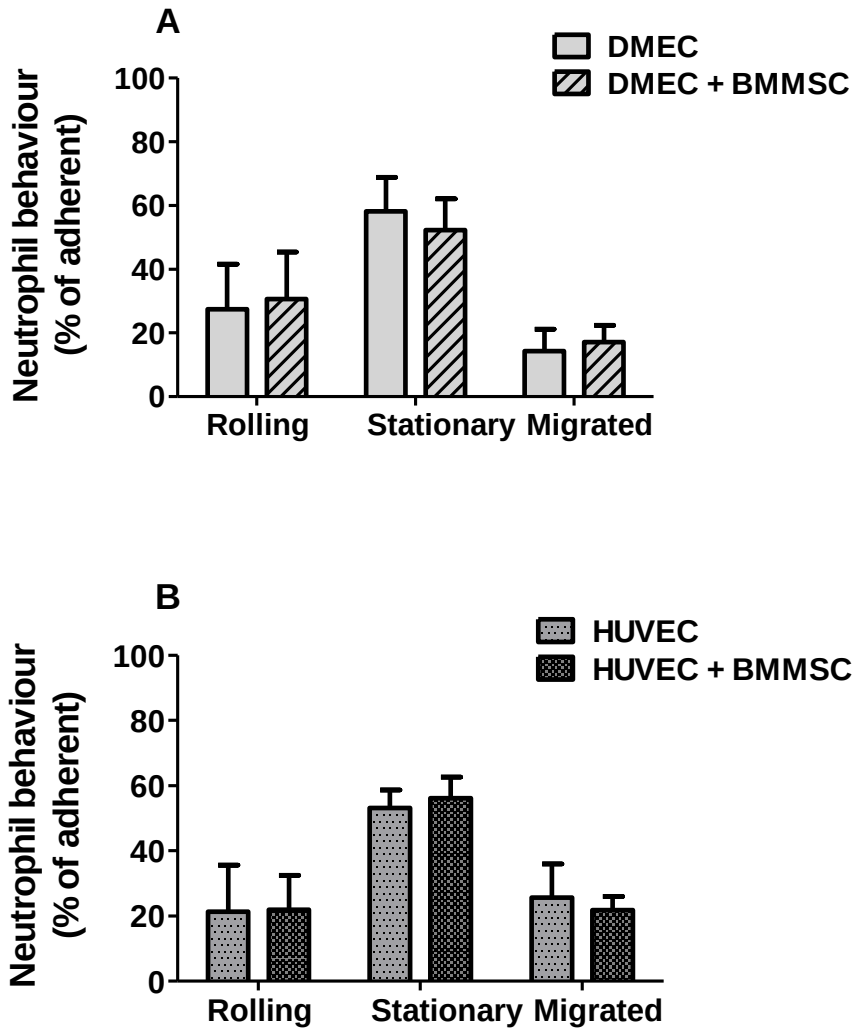

Figure 17 – Effect of MSC:EC co-culture on the behaviour of neutrophils recruited to TNFα-stimulated endothelium from flow.

(A) DMEC or **(B)** HUVEC monocultures and their respective co-cultures with BMMSC were stimulated with 100U/ml TNFα for 4h before being exposed to a flow of neutrophils ($1x10^6$/ml) at a rate of 0.4ml/min for 4 minutes. Rolling, stationary and migrated neutrophils were counted at 2 minutes after neutrophil flow stopped, and each expressed as a percentage of total adherent cells. Data are mean ± SEM, n=4.

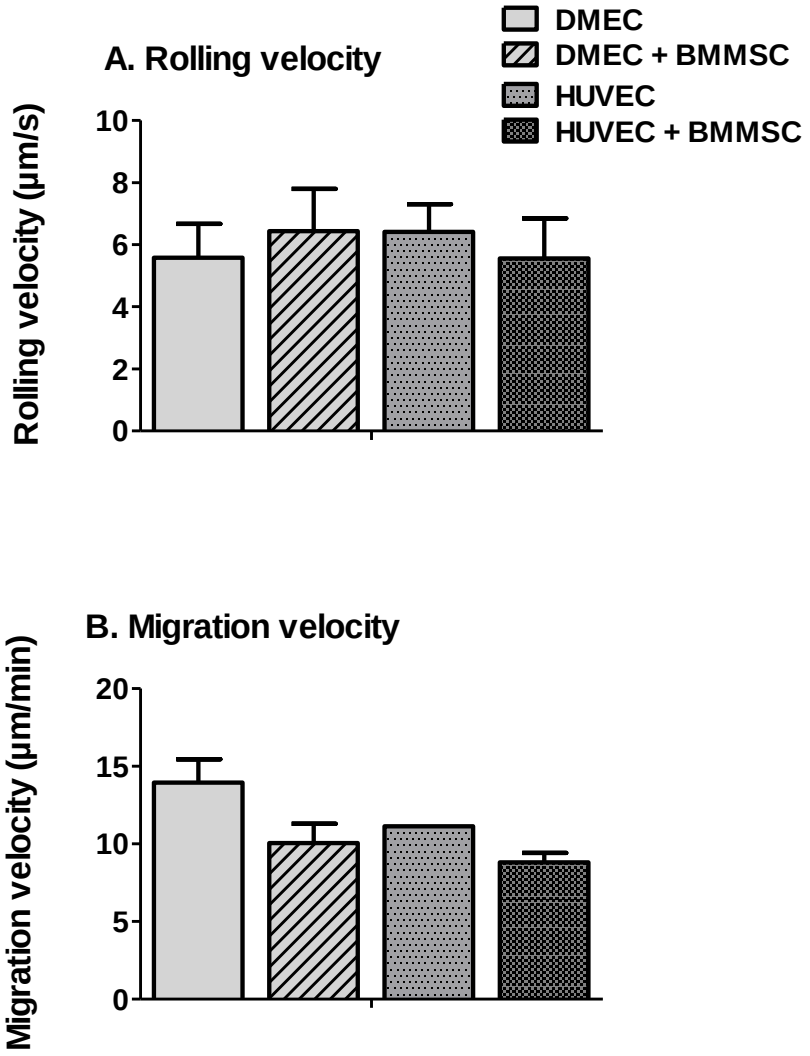

Figure 18 – Effect of MSC:EC co-culture on the rolling and migration velocities of neutrophils recruited to TNFα-stimulated endothelium from flow.
DMEC or HUVEC monocultures and their respective co-cultures with BMMSC were stimulated with 100U/ml TNFα for 4h before being exposed to a flow of neutrophils ($1x10^6$/ml) at a rate of 0.4ml/min for 4 minutes. **(A)** Rolling and **(B)** migration velocities were calculated as average values from ten rolling or transmigrated cells respectively, and expressed in µm/s (rolling) and µm/min (migration). Data are mean ± SEM, n=4.

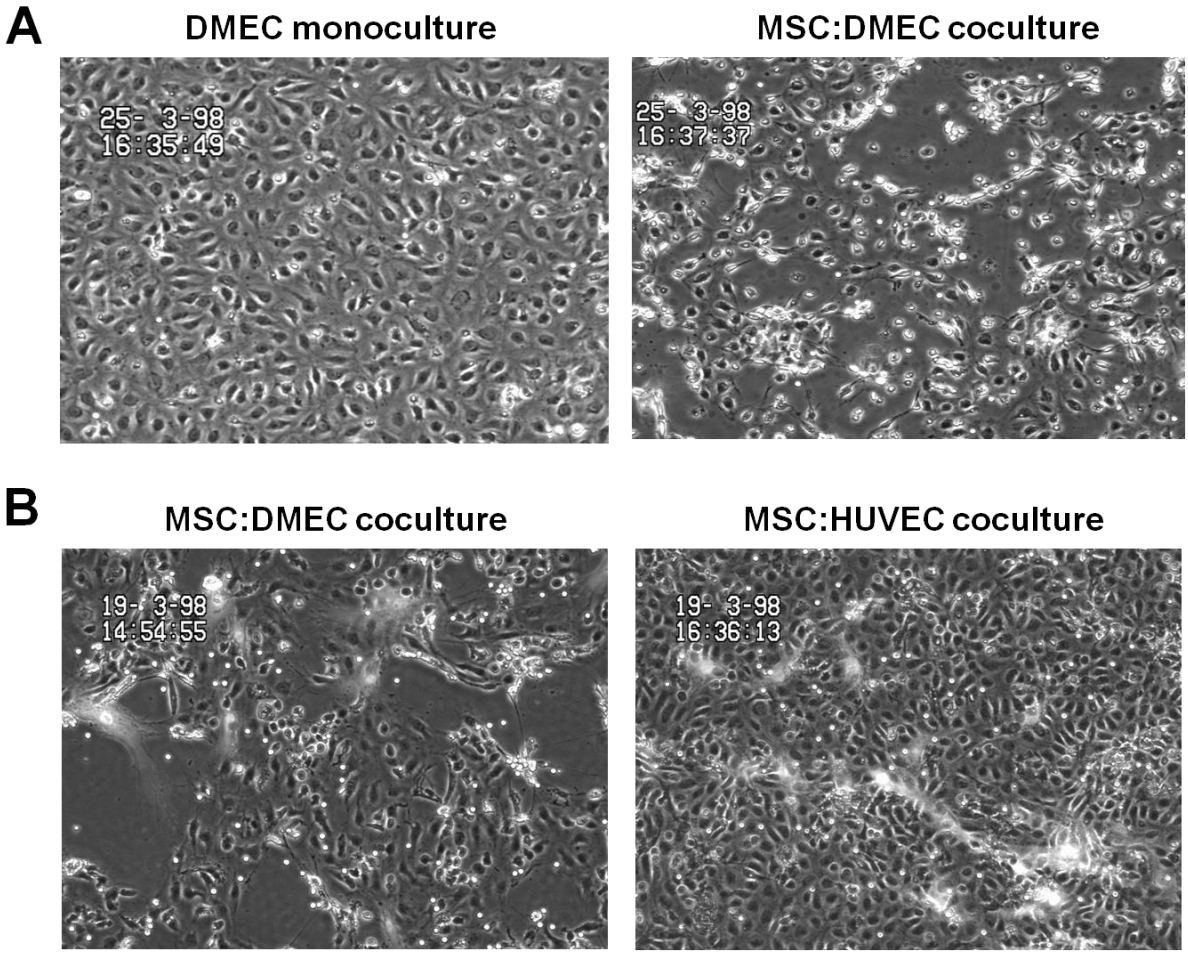

Figure 19 – Effect of MSC incorporation into the endothelium on the EC monolayer.
DMEC or HUVEC were seeded into ibidi channel slides such that they would yield a confluent monolayer within 24h. BMMSC labelled with Cell Tracker Green were then added to the same channel slides and allowed to incorporate for a further 24h. The co-cultures were treated with TNFα for 4h before being exposed to neutrophil flow. Following the flow-based adhesion assay, phase-contrast and fluorescent images were taken down the centre of each channel using x10 magnification. **(A)** Comparison of DMEC monoculture and MSC:DMEC co-culture during the same experiment, where BMMSC (fluorescent cells) caused DMEC to retract or detach over the course of the flow assay. **(B)** Comparison of MSC:DMEC and MSC:HUVEC co-culture during the same experiment, where BMMSC caused DMEC but not HUVEC to retract or detach over the course of the flow assay. Images representative of 4 independent experiments, where DMEC were observed to retract in three out of the four experiments.

Table 2 - MSC:EC ratios obtained during co-culture of BMMSC with DMEC or HUVEC

Experiment no.	MSC:DMEC ratio	MSC:HUVEC ratio
1	1:25	1:40
2	1:80	1:40
3	1:14	1:8
4	1:40	1:16

3.5 MSC phenotype may be affected by prolonged cytokine treatment

Our collaborators have observed that synovial fibroblasts (SF) cultured in low-serum media upregulate their expression of GP38 upon prolonged stimulation with TNFα, and that of CD248 when exposed to TGFβ (Croft *et al.* n.d., unpublished data). Here we address two distinct questions. We examine whether there is an effect of low-serum media on MSC surface marker expression. We also inspect whether similar changes occur in the phenotype of MSC when treated with cytokines for prolonged periods. We therefore stimulated BMMSC with TNFα or TGFβ for 4-6 days before analysing the expression of GP38, CD248 and MSC surface markers CD73 and CD90. This was done in both complete and low-serum media for comparison.

BMMSC expressed both CD73 and CD90 in complete media, and this was unchanged in low-serum conditions. Prolonged cytokine treatment made a substantial difference to the expression of these markers only in the case of TGFβ stimulation in low-serum media. In this instance CD73 and CD90 expression was, though still positive, markedly reduced (**Figure 20**). The effect was especially pronounced for CD73. Therefore, while low-serum media alone did not impact on MSC marker expression, it did produce a notable change when coupled to TGFβ treatment, suggesting a role for this cytokine in altering the MSC phenotype.

For assessment of GP38 expression we used lymphatic endothelial cells (LEC), which are known to express high levels of this protein, as positive control. Compared to LEC, none of the BMMSC under investigation expressed GP38 (**Figure 21**). The mean fluorescence intensities (MFI) were similarly low for all BMMSC treatment

groups, with no significant effect of serum deprivation or cytokine stimulation. To confirm this, the fluorescence emission spectra of serum-deprived cytokine-treated BMMSC were compared to those of untreated BMMSC (**Figure 22**). All of them overlapped and were in the negative fluorescence region. It was concluded, therefore, that BMMSC did not express GP38, and this remained unchanged with serum deprivation or cytokine treatment.

Based on evidence suggesting that a subset of $CD8^+$ T lymphocytes expresses CD248 (Watkins *et al.* 2009), we used freshly isolated peripheral blood lymphocytes (PBL) as our positive control for BMMSC CD248 expression. Labelling PBL with a FITC-conjugated anti-human CD8 antibody (BD Biosciences – Pharmingen, San Diego, California, USA) yielded a substantial $CD8^+$ population, but CD248 expression could not be detected (**Figure 23**). This meant we had no positive control for our assay, rendering the interpretation of the results difficult. The only sample to show any shift in the direction of positive fluorescence compared to CD248-negative isotype control were the untreated BMMSC cultured in complete media (**Figure 24**). This suggests these cells could be expressing some CD248, although it is impossible to say for certain without a positive control. The MFI of all the other BMMSC subsets and PBL were comparatively lower (Figure 24). To confirm this difference in fluorescence, the emission spectra of serum-deprived cytokine-treated BMMSC were once again compared to those of untreated cells. They showed that any CD248 expression that might have been present in untreated BMMSC was lost upon serum deprivation and cytokine treatment (**Figure 25**).

Overall, the effects of low-serum conditions and cytokine stimulation, or lack thereof, on BMMSC expression of CD73, CD90 and GP38 were clear. On the other hand, we were unable to draw any definite conclusions regarding CD248 expression by BMMSC due to lack of a positive control for this assay.

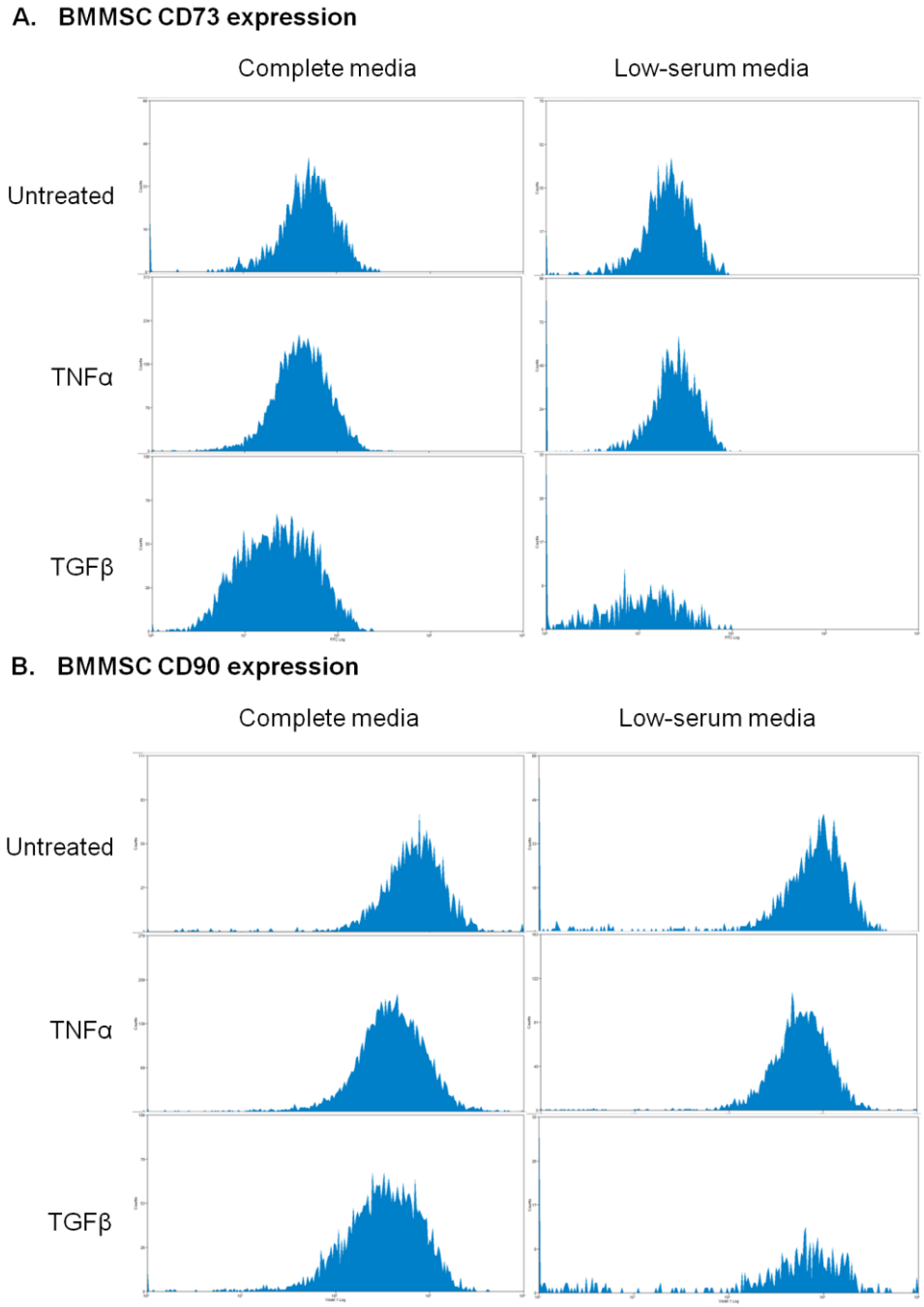

Figure 20 – CD73 and CD90 expression by BMMSC.
BMMSC cultured in complete or low-serum media were either left untreated or treated with TNFα or TGFβ for 4-6 days. Upon completion of treatment, BMMSC were labelled with anti-human CD73-FITC or anti-human CD90-Brilliant Violet™ 421 antibodies, and their fluorescence emission spectra for **(A)** CD73 and **(B)** CD90 examined by flow cytometry. Low cell numbers in the sample prevented use of negative isotype controls; however, the MSC flow cytometry protocol had been extensively employed before and was deemed reliable. Representative histograms from n=2.

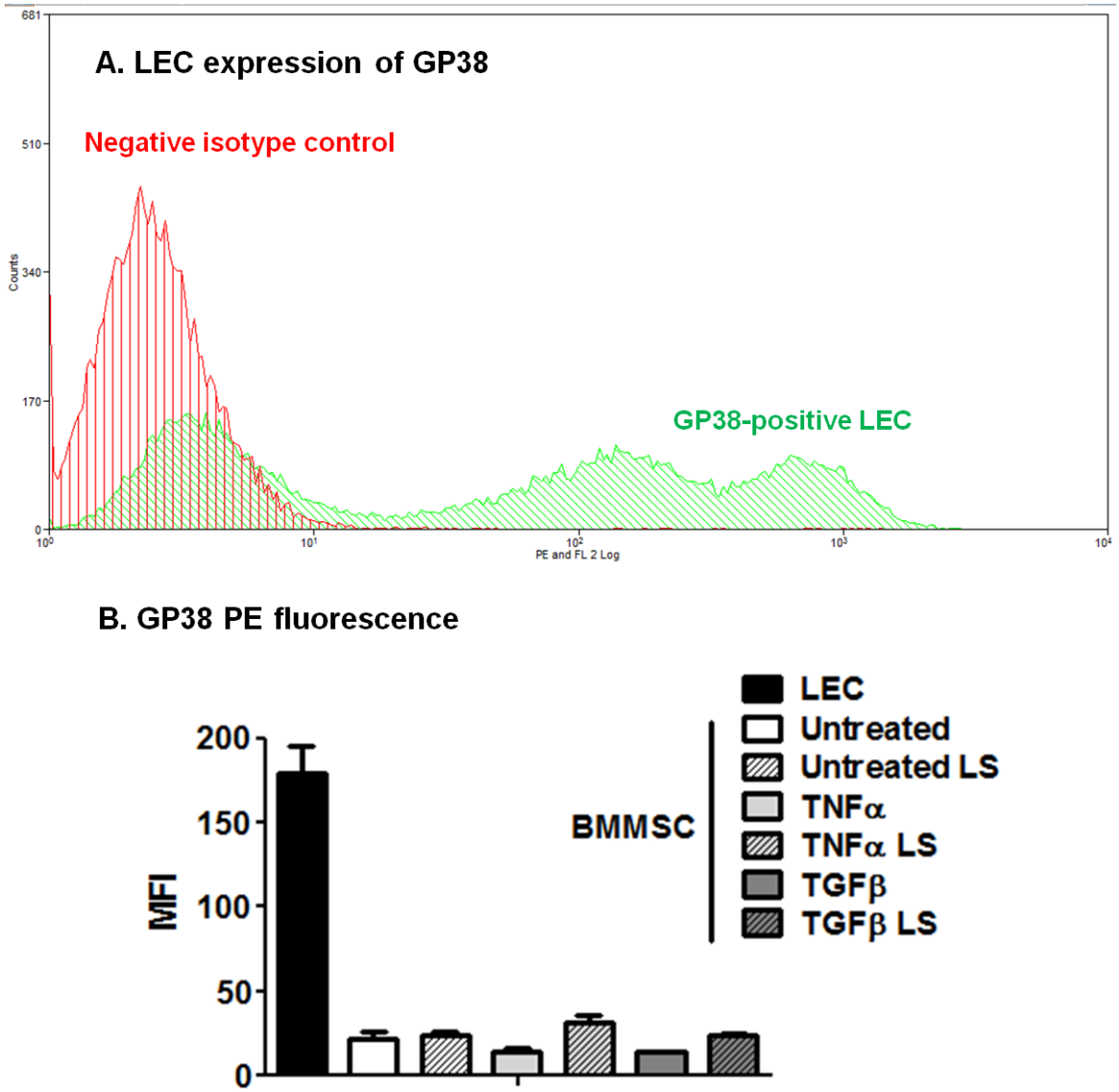

Figure 21 – GP38 expression by BMMSC compared to lymphatic endothelial cells (LEC).

BMMSC cultured in complete or low-serum (LS) media were either left untreated or treated with TNFα or TGFβ for 4-6 days. Upon completion of MSC treatment, LEC and BMMSC were labelled with anti-human GP38 antibody conjugated to PE dye and their fluorescence emission compared to that of negative isotype control. **(A)** Representative histogram of LEC showing positive fluorescence. **(B)** Mean fluorescence intensities (MFI) of BMMSC in complete or LS media compared to LEC. Data are mean ± SEM, n=3.

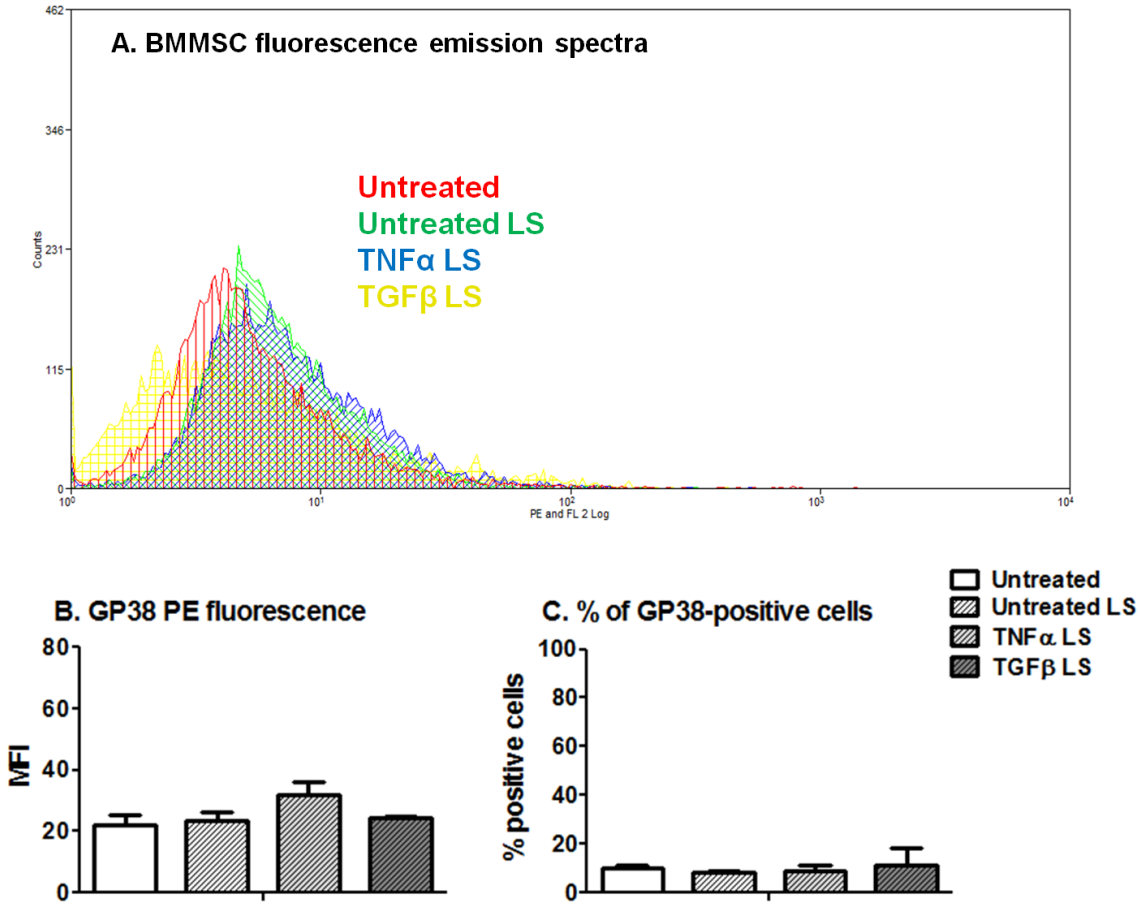

Figure 22 – GP38 expression by serum-deprived cytokine-treated BMMSC compared to untreated controls.

BMMSC cultured in complete or LS media were either left untreated or treated with TNFα or TGFβ for 4-6 days. Upon completion of treatment, BMMSC were labelled with anti-human GP38 antibody conjugated to PE dye. Fluorescence emission for TNFα- and TGFβ-treated BMMSC in LS media was compared to those of untreated controls in both complete and LS media to obtain their **(A)** representative histograms showing negative fluorescence, **(B)** MFI and **(C)** % positive-fluorescing cells. Data are mean ± SEM, n=3.

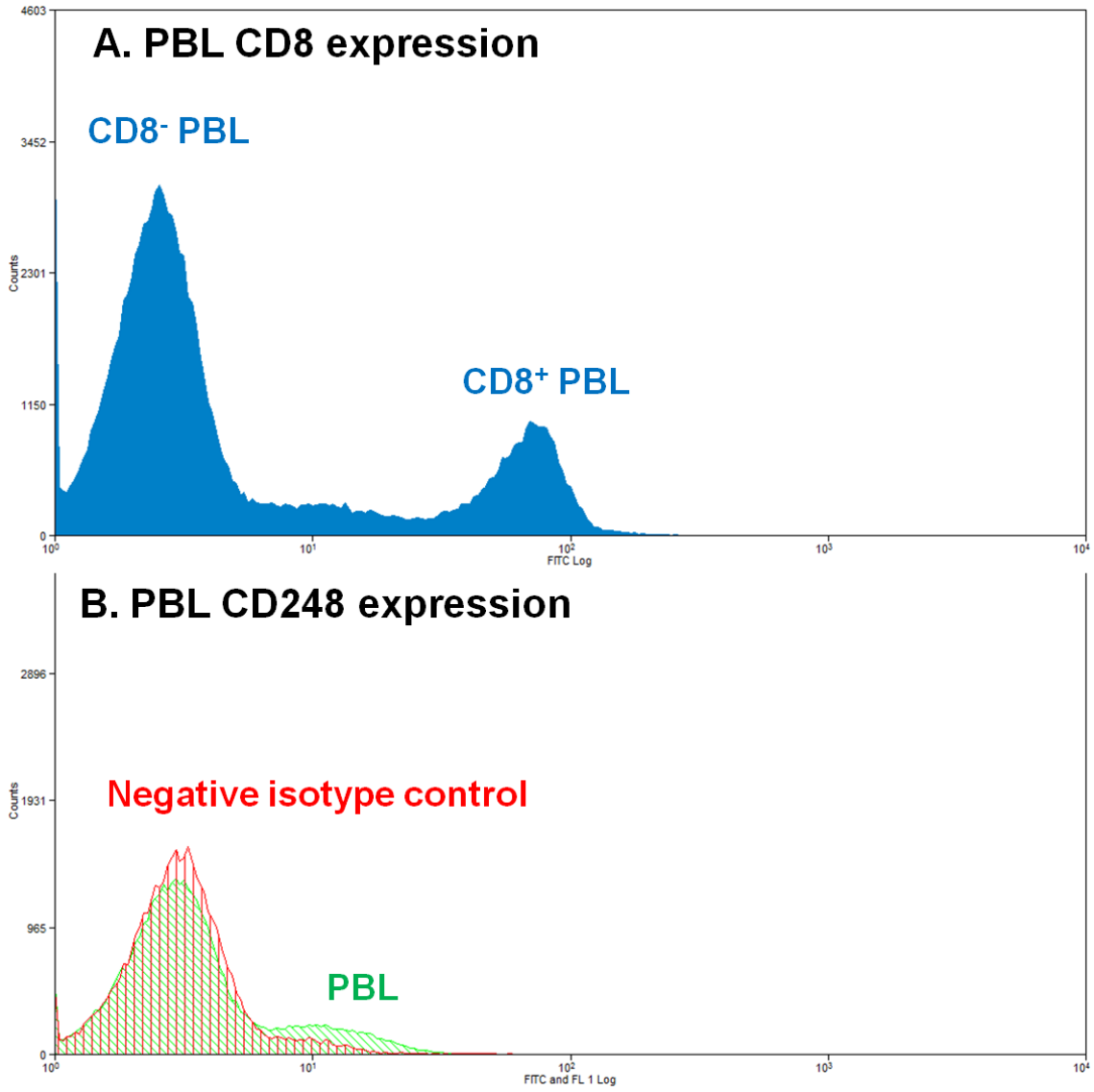

Figure 23 – CD8 and CD248 expression by peripheral blood lymphocytes (PBL).
PBL were labelled with anti-human CD8-FITC or anti-human CD248-FITC antibody. Fluorescence emission spectra were compared for PBL expression of **(A)** CD8 and **(B)** CD248, showing there was no overlap between $CD8^+$ PBL and CD248 expression. Representative histograms from n=2.

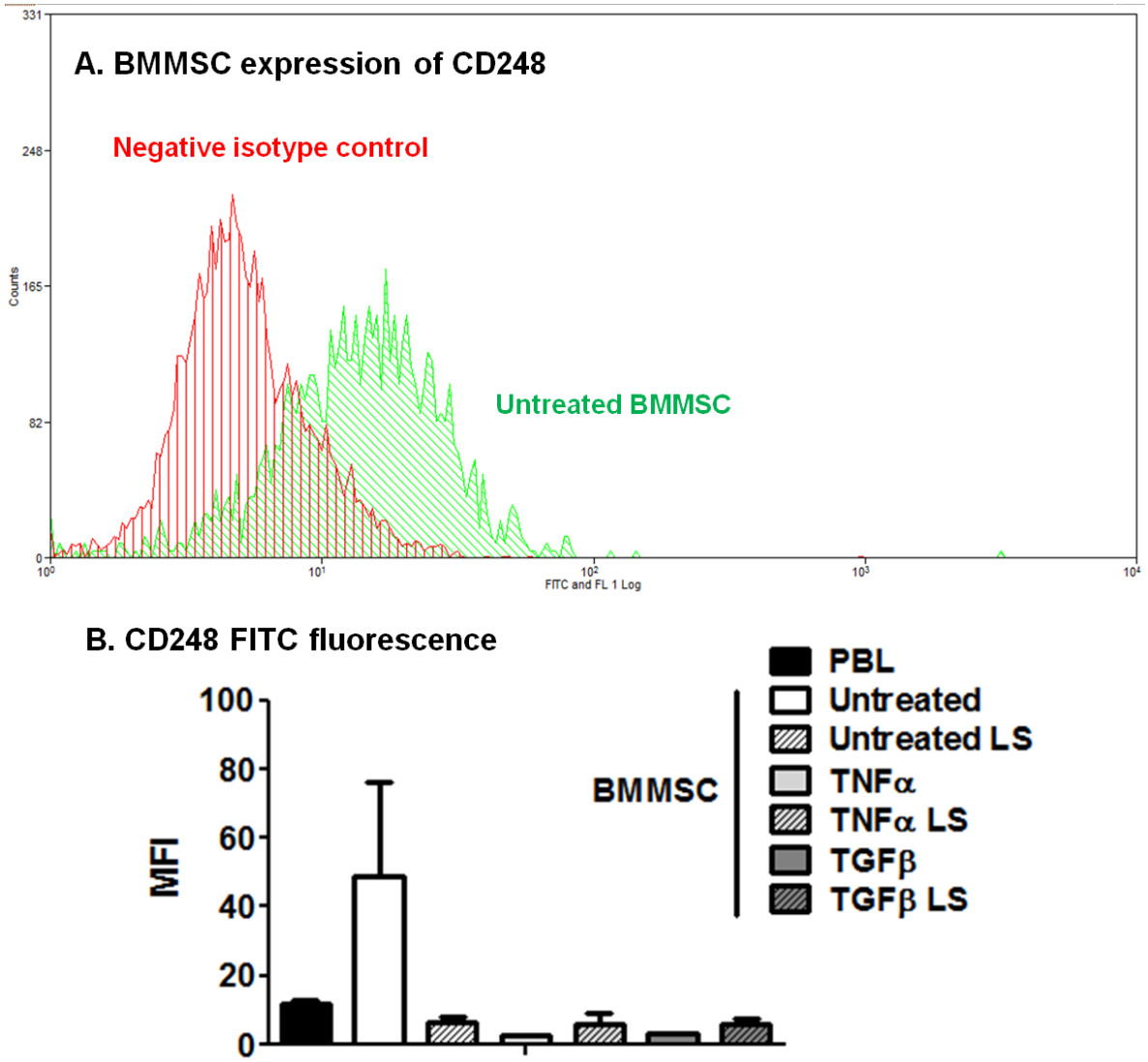

Figure 24 – CD248 expression by BMMSC compared to PBL.
BMMSC cultured in complete or LS media were either left untreated or treated with TNFα or TGFβ for 4-6 days. Upon completion of MSC treatment, PBL and BMMSC were labelled with anti-human CD248 antibody conjugated to FITC dye and their fluorescence emission compared to that of negative isotype control. **(A)** Representative histogram of untreated BMMSC in complete media. **(B)** MFI of BMMSC in complete or LS media compared to PBL. Data are mean ± SEM, n=3.

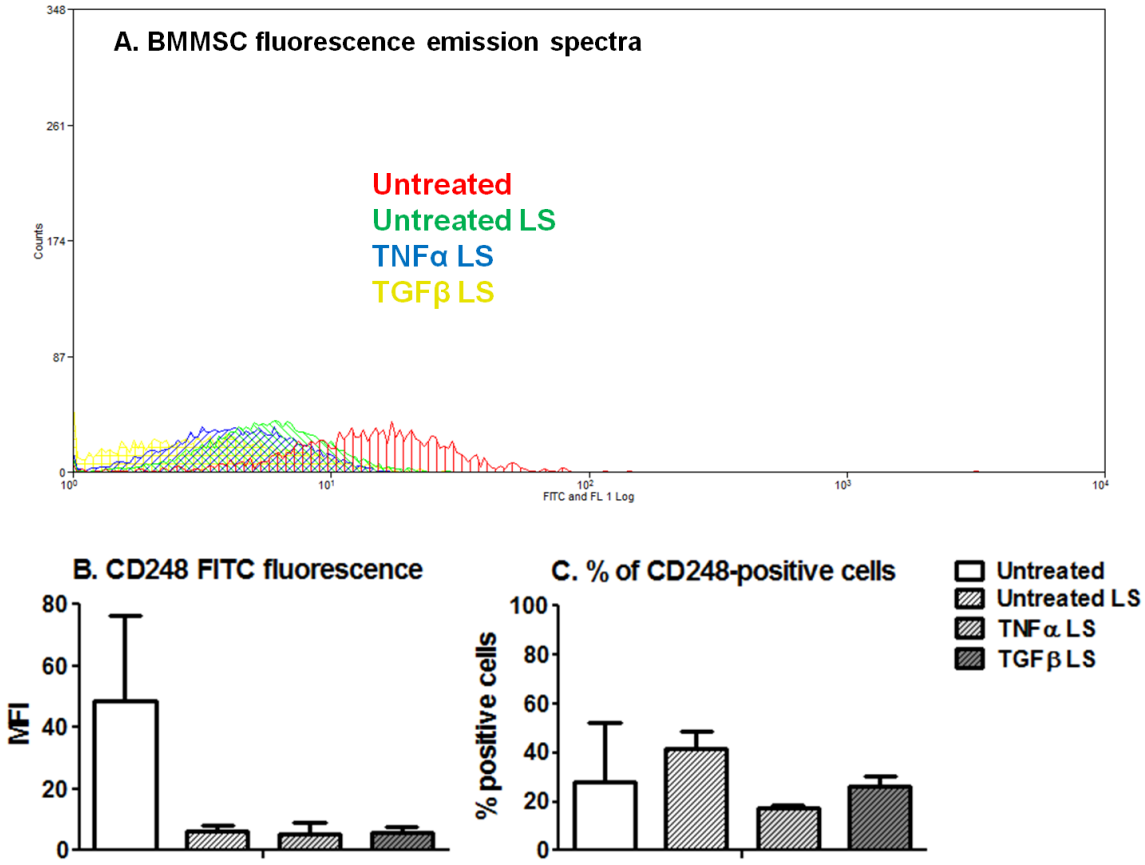

Figure 25 – CD248 expression by serum-deprived cytokine-treated BMMSC compared to untreated controls.

BMMSC cultured in complete or LS media were either left untreated or treated with TNFα or TGFβ for 4-6 days. Upon completion of treatment, BMMSC were labelled with anti-human CD248 antibody conjugated to FITC dye. Fluorescence emission for TNFα- and TGFβ-treated BMMSC in LS media was compared to those of untreated controls in both complete and LS media to obtain their **(A)** representative histograms, **(B)** MFI and **(C)** % positive-fluorescing cells. Data are mean ± SEM, n=3.

4. DISCUSSION

The immunomodulatory properties of MSC have been the subject of much research, but their ability to suppress neutrophil adhesion to inflamed endothelium has only been demonstrated recently (Luu *et al.* 2013) using macrovascular EC. In this project we sought to characterise neutrophil adhesion to the more physiologically relevant microvascular endothelium and examine whether it can be suppressed by MSC. We also studied how MSC phenotype may change in response to prolonged cytokine treatment, with a view to incorporating these altered cells into neutrophil adhesion assays in the future. We found that DMEC supported TNFα dose-dependent neutrophil recruitment, which was reduced in the presence of hydrocortisone at low doses of the cytokine. TNFα and IL-1β stimulation of DMEC resulted in comparable levels of neutrophil adhesion. We did not observe suppression of endothelial neutrophil recruitment in MSC:EC co-cultures, but we were able to show that MSC phenotype may change with cytokine treatment under low-serum conditions. Characterising these changes further, and how they may modulate neutrophil recruitment to vascular endothelium, could significantly expand our knowledge on MSC-EC crosstalk within a chronically inflamed environment.

4.1 DMEC support neutrophil adhesion in the same way as HUVEC

While neutrophil recruitment to cytokine-stimulated HUVEC has been extensively studied in the past (e.g. Bahra *et al.* 1998; Luu *et al.* 2003; Sheikh *et al.* 2005; Burton *et al.* 2011), only a handful of studies examined interactions between neutrophils and DMEC. They looked at either static adhesion of neutrophils to inflamed endothelium (Saalbach *et al.* 2000; Schmitz *et al.* 2011) or at routes of neutrophil transendothelial

migration (Marmon, Hinchey, *et al.* 2009; Marmon, Cammer, *et al.* 2009). None have examined neutrophil recruitment from flow. In addition, no studies have looked at MSC:DMEC co-culture or its impact on neutrophil adhesion before, making this project the first to address this gap in knowledge.

We first examined and characterised neutrophil adhesion to DMEC monoculture from flow. The TNFα dose-dependence of neutrophil recruitment and the maximum adhesion levels were consistent with previous findings in HUVEC (e.g. Bahra *et al.* 1998; Sheikh *et al.* 2005; Luu *et al.* 2013). However, the levels of adhesion at lower TNFα concentrations (1 and 10U/ml) were unexpectedly low at first, which was subsequently found to be due to the presence of hydrocortisone (HC) in DMEC medium. HC naturally exerted its anti-inflammatory effect and overwhelmed the effect of TNFα when the concentration of the latter was low enough. Once hydrocortisone was left out of the monoculture preparation, the levels of adhesion at low TNFα concentrations rose significantly to match those previously seen in HUVEC (e.g. Sheikh *et al.* 2005). We concluded that DMEC and HUVEC supported dose-dependent neutrophil recruitment equally well. This similarity is supported by a study which found comparable levels of E-selectin expressed on both HUVEC and DMEC when they were exposed to inflammatory stimuli (Vora *et al.* 1996).

Stimulation of the DMEC monolayer with high-dose IL-1β compared to high-dose TNFα did not show any significant differences in neutrophil adhesion levels, suggesting these two pro-inflammatory cytokines had much the same effect on microvascular endothelium. This was once again in keeping with previous findings in HUVEC, where both cytokines induced similar levels of neutrophil capture (Sheikh *et*

al. 2005). However, increases in shear stress have been shown to lead to a decrease in endothelial response to TNFα but not IL-1β (Sheikh *et al.* 2005; Luu *et al.* 2010); this would be worth investigating in DMEC in the future.

Neutrophil behaviour upon adhering to DMEC monoculture was comparable to previous observations in HUVEC, where increases in TNFα concentration led to decreases in rolling and firm adhesion and increases in transendothelial migration of neutrophils (Bahra *et al.* 1998; Luu *et al.* 1999; Luu *et al.* 2000). The kinetics of migration, however, were not significantly affected by increasing TNFα concentration, once again making DMEC comparable with HUVEC (Luu *et al.* 1999). Even the migration velocities supported by the two endothelia were both found to be in the region of 14μm/min (Luu *et al.* 2003). Consistent with the above observations that TNFα and IL-1β induced much the same neutrophil adhesion levels, the behaviour seen for the two cytokines was largely similar as well.

The above findings suggested that DMEC were a suitable EC model to take forward in our studies, supporting largely the same neutrophil adhesion and behaviour as HUVEC. In view of the fact that hydrocortisone was clearly able to reduce the effect of low-dose TNFα on neutrophil adhesion to DMEC, it was decided to move onto MSC:EC studies using hydrocortisone-free media. Our interest in the potential of MSC to suppress endothelial neutrophil recruitment meant that any presence of hydrocortisone could ‘mask’ the immunosuppressive effect of MSC.

4.2 MSC:EC co-culture does not show immunosuppressive effects

The only study to have examined MSC modulation of neutrophil recruitment to HUVEC (Luu *et al.* 2013) found that MSC:HUVEC co-culture was capable of down-regulating neutrophil adhesion and transmigration compared to HUVEC monoculture. We applied the same methods used by Luu *et al*. to study neutrophil adhesion to MSC:DMEC and MSC:HUVEC co-cultures in parallel, comparing them to their respective monocultures and to each other. In contrast to findings from the study above, we did not observe any effects of MSC co-culture with DMEC or HUVEC on neutrophil adhesion, behaviour or migration kinetics. Since this was the first study of its kind to be performed, and there is a general lack of relevant literature on MSC:EC co-cultures – particularly in the case of DMEC – it is difficult to interpret the lack of immunosuppression in this instance. MSC have previously shown a tendency towards differentiation when in co-culture with DMEC (Laranjeira *et al.* 2012), although this is unlikely to have happened in such a short time span. It is possible that using a different batch of BMMSC to that utilised in the study by Luu *et al*. decreased the suppressive effect on neutrophil adhesion and transmigration, such that it would not be seen in n=4. Consequently, increasing the number of experiment repeats may highlight a difference in neutrophil recruitment between DMEC and HUVEC mono- and co-cultures.

It is important to note that MSC:EC ratios were very variable between experiments, unlike those obtained by Luu *et al*. This was most likely due to the large gaps apparent in DMEC:MSC co-culture where DMEC had either retracted or detached, thus rendering the calculation of ratios difficult. The gaps were mostly around the

areas of MSC integration into the monolayer, and it is likely this happened during or just after the flow assays, when the cells coming off could have been carried away by the flow. The fact that such gaps were not seen in DMEC monocultures or in HUVEC mono- or co-cultures would suggest that DMEC are not suitable for supporting integration of MSC *in vitro*. HUVEC did not detach or retract like DMEC did, although here too the variable ratios were apparent. This may be explained by the varying confluence of the monolayers at the point of the assay. It was not always easy to evaluate how confluent the HUVEC culture flasks were before the cells were resuspended and seeded, therefore possibly resulting in channels where the EC population was too dense.

4.3 MSC surface marker expression changes with cytokine treatment

MSC and fibroblasts have been shown to be closely related, both exhibiting differentiation potential and expression of MSC surface markers such as CD73 and CD90 (Haniffa *et al.* 2009; Alt *et al.* 2011). Our collaborators recently demonstrated that synovial fibroblasts cultured in low-serum conditions were able to adopt a pro-inflammatory ($GP38^+$) or regulatory ($CD248^+$) phenotype, depending on their stimulation with TNFα or TGFβ respectively (Croft *et al.* n.d., unpublished data). We therefore wished to characterise potential changes in MSC phenotype under serum deprivation and after prolonged cytokine stimulation.

Our results clearly showed that BMMSC, unlike fibroblasts, did not express GP38 under any of the conditions tested, suggesting they had not adopted a more pro-inflammatory phenotype. This seemed consistent with previous findings that the

presence of pro-inflammatory cytokines such as TNFα 'primed' the MSC towards immunosuppression and tissue regeneration rather than immune stimulation (e.g. Ren *et al.* 2008; Prasanna *et al.* 2010; Kemp *et al.* 2010; Hemeda *et al.* 2010). These studies, however, examined the effects of MSC on lymphocyte proliferation rather than neutrophil recruitment, and in almost all cases required the additional presence of interferon-gamma (IFNγ) to lead to correct MSC priming (Prasanna *et al.* 2010; Hemeda *et al.* 2010; Ren *et al.* 2008; Krampera *et al.* 2006). We have not yet looked at the potential of serum-deprived, cytokine-stimulated MSC to modulate neutrophil recruitment, but future studies of this kind may reveal interesting immunomodulatory effects.

We were not able to draw definite conclusions about MSC expression of CD248, but the obvious decrease in CD73 and CD90 expression after treatment with TGFβ in low-serum conditions is interesting. A previous study reported that *in vitro* angiogenic stimuli combined with low-serum conditions led to the appearance of a CD90-negative MSC subset, which had high proliferative potential and increased propensity towards osteogenic and adipogenic differentiation (Campioni *et al.* 2008). It is entirely possible that TGFβ with low-serum media started inducing MSC differentiation in our study. Interestingly, a direct involvement of CD90 in neutrophil binding to activated DMEC and fibroblasts has been previously reported (Saalbach *et al.* 2000). Exploring what happens to CD73 and CD90 expression after longer periods of MSC cytokine stimulation (7-14 days), and whether this may lead to suppression of neutrophil recruitment to DMEC, could therefore be of interest.

4.4 Future studies

In light of the observed changes in CD73 and CD90 expression, further studies of how expression of these and other MSC surface markers (e.g. CD44, CD105) may change under serum deprivation and prolonged cytokine treatment would be interesting. Assaying supernatants from long-term cultures of MSC under the above conditions would reveal if they secrete any immunomodulatory soluble factors, such as IL-6, IDO or iNOS (Waterman *et al.* 2010). Subsequent incorporation of these MSC into co-culture with DMEC and HUVEC could give us valuable insights into their capability to modulate endothelial neutrophil recruitment from flow depending on changes in MSC phenotype. Obtaining consistent MSC:EC ratios across experiments would be crucial for successful data interpretation. Finally, in order to mimic the *in vivo* stromal microenvironment more faithfully, examining the immunosuppressive effects of co-culture when MSC and EC are seeded on opposite sides of a Transwell filter (McGettrick *et al.* 2009) or in 3D culture constructs (Jeffery *et al.* 2013) rather than incorporated into endothelial monolayers would be of value.

4.5 Conclusion

We used a well-established flow-based adhesion assay model to show that neutrophil recruitment is equally well supported by DMEC as it is by HUVEC. We were not able to replicate the neutrophil recruitment suppression previously seen in MSC:HUVEC co-culture, which could have been due to technical difficulties encountered during the experiment. However, we showed that MSC phenotype may change during prolonged cytokine stimulation. Further studies of this phenomenon, as well as how it may impact neutrophil adhesion in MSC:EC co-culture, are needed

to better understand the interactions that may take place between these cells in inflammatory environments.

5. REFERENCES

Alt, E. *et al*., 2011. Fibroblasts share mesenchymal phenotypes with stem cells, but lack their differentiation and colony-forming potential. *Biology of the Cell*, 103(4), pp.197–208.

Anderson, D.C. & Springer, T.A., 1987. Leukocyte adhesion deficiency: an inherited defect in the Mac-1, LFA-1, and p150,95 glycoproteins. *Annual Review of Medicine*, 38, pp.175–94.

Bahra, P. *et al*., 1998. Each step during transendothelial migration of flowing neutrophils is regulated by the stimulatory concentration of tumour necrosis factor-alpha. *Cell adhesion and communication*, 6(6), pp.491–501.

Bottini, N. & Firestein, G.S., 2013. Duality of fibroblast-like synoviocytes in RA: passive responders and imprinted aggressors. *Nature reviews. Rheumatology*, 9(1), pp.24–33.

Burton, V.J. *et al*., 2011. Delay of migrating leukocytes by the basement membrane deposited by endothelial cells in long-term culture. *Experimental Cell Research*, 317(3), pp.276–92.

Campioni, D. *et al*., 2008. Loss of Thy-1 (CD90) antigen expression on mesenchymal stromal cells from hematologic malignancies is induced by in vitro angiogenic stimuli and is associated with peculiar functional and phenotypic characteristics. *Cytotherapy*, 10(1), pp.69–82.

Coelho, F.M. *et al*., 2008. The chemokine receptors CXCR1/CXCR2 modulate antigen-induced arthritis by regulating adhesion of neutrophils to the synovial microvasculature. *Arthritis and rheumatism*, 58(8), pp.2329–2337.

Cooke, B.M. *et al*., 1993. A simplified method for culture of endothelial cells and analysis of adhesion of blood cells under conditions of flow. *Microvascular Research*, 45(1), pp.33–45.

Corada, M. *et al*., 2005. Junctional adhesion molecule-A-deficient polymorphonuclear cells show reduced diapedesis in peritonitis and heart ischemia-reperfusion injury. *Proceedings of the National Academy of Sciences of the United States of America*, 102(30), pp.10634–9.

Croft, A.P. *et al*., *Synovial fibroblasts differentiate into distinct functional subsets in the presence of cytokines and cartilage*, Birmingham.

Djouad, F. *et al*., 2005. Reversal of the immunosuppressive properties of mesenchymal stem cells by tumor necrosis factor alpha in collagen-induced arthritis. *Arthritis and Rheumatism*, 52(5), pp.1595–603.

Dominici, M. *et al*., 2006. Minimal criteria for defining multipotent mesenchymal stromal cells. The International Society for Cellular Therapy position statement. *Cytotherapy*, 8(4), pp.315–7.

Duchene, J. *et al*., 2007. A novel inflammatory pathway involved in leukocyte recruitment: role for the kinin B1 receptor and the chemokine CXCL5. *Journal of Immunology*, 179(7), pp.4849–4856.

El-Jawhari, J.J. *et al*., 2014. Mesenchymal Stem Cells, Autoimmunity & Rheumatoid Arthritis. *QJM: monthly journal of the Association of Physicians*.

Engelhardt, B. & Wolburg, H., 2004. Mini-review: Transendothelial migration of leukocytes: through the front door or around the side of the house? *European Journal of Immunology*, 34(11), pp.2955–63.

Feng, D. *et al*., 1998. Neutrophils emigrate from venules by a transendothelial cell pathway in response to FMLP. *The Journal of Experimental Medicine*, 187(6), pp.903–15.

Haniffa, M.A. *et al*., 2009. Mesenchymal stem cells: the fibroblasts' new clothes? *Haematologica*, 94(2), pp.258–63.

Hemeda, H. *et al*., 2010. Interferon-gamma and tumor necrosis factor-alpha differentially affect cytokine expression and migration properties of mesenchymal stem cells. *Stem Cells and Development*, 19(5), pp.693–706.

Iso, Y. *et al*., 2007. Multipotent human stromal cells improve cardiac function after myocardial infarction in mice without long-term engraftment. *Biochemical and Biophysical Research Communications*, 354(3), pp.700–6.

Jeffery, H.C. *et al*., 2013. Analysis of the effects of stromal cells on the migration of lymphocytes into and through inflamed tissue using 3-D culture models. *Journal of Immunological Methods*, 400-401, pp.45–57. Available at: http://www.pubmedcentral.nih.gov/articlerender.fcgi?artid=3878567&tool=pmcentrez&rendertype=abstract [Accessed February 28, 2014].

Johnson-Léger, C., Aurrand-Lions, M. & Imhof, B.A., 2000. The parting of the endothelium: miracle, or simply a junctional affair? *Journal of Cell Science*, 113, pp.921–33.

Kemp, K. *et al*., 2010. Inflammatory cytokine induced regulation of superoxide dismutase 3 expression by human mesenchymal stem cells. *Stem Cell Reviews*, 6(4), pp.548–59.

Khandoga, A. *et al*., 2005. Junctional adhesion molecule-A deficiency increases hepatic ischemia-reperfusion injury despite reduction of neutrophil transendothelial migration. *Blood*, 106(2), pp.725–33.

Koh, B.I. & Kang, Y., 2012. The pro-metastatic role of bone marrow-derived cells: a focus on MSCs and regulatory T cells. *EMBO Reports*, 13(5), pp.412–22.

Krampera, M., 2011. Mesenchymal stromal cell “licensing”: a multistep process. *Leukemia*, 25(9), pp.1408–14.

Krampera, M. *et al*., 2006. Role for interferon-gamma in the immunomodulatory activity of human bone marrow mesenchymal stem cells. *Stem Cells*, 24(2), pp.386–98.

Kuzuya, M. & Kinsella, J.L., 1994. Induction of endothelial cell differentiation in vitro by fibroblast-derived soluble factors. *Experimental Cell Research*, 215(2), pp.310–8.

Lally, F. *et al*., 2005. A novel mechanism of neutrophil recruitment in a coculture model of the rheumatoid synovium. *Arthritis and Rheumatism*, 52(11), pp.3460–9.

Langer, H.F. & Chavakis, T., 2009. Leukocyte-endothelial interactions in inflammation. *Journal of Cellular and Molecular Medicine*, 13(7), pp.1211–20.

Laranjeira, M.S., Fernandes, M.H. & Monteiro, F.J., 2012. Reciprocal induction of human dermal microvascular endothelial cells and human mesenchymal stem cells: time-dependent profile in a co-culture system. *Cell Proliferation*, 45(4), pp.320–34.

Ley, K. *et al*., 2007. Getting to the site of inflammation: the leukocyte adhesion cascade updated. *Nature reviews. Immunology*, 7(9), pp.678–89.

Ley, K. *et al*., 1995. Sequential contribution of L- and P-selectin to leukocyte rolling in vivo. *The Journal of Experimental Medicine*, 181(2), pp.669–75.

Luo, B.-H., Carman, C. V & Springer, T.A., 2007. Structural basis of integrin regulation and signaling. *Annual Review of Immunology*, 25, pp.619–47.

Luu, N.T. *et al*., 2003. CD31 regulates direction and rate of neutrophil migration over and under endothelial cells. *Journal of Vascular Research*, 40(5), pp.467–79.

Luu, N.T. *et al*., 2013. Crosstalk Between Mesenchymal Stem Cells and Endothelial Cells Leads to Down-Regulation of Cytokine-Induced Leukocyte Recruitment. *Stem Cells*, 31, pp.2690–702.

Luu, N.T. *et al*., 2010. Responses of endothelial cells from different vessels to inflammatory cytokines and shear stress: evidence for the pliability of endothelial phenotype. *Journal of Vascular Research*, 47(5), pp.451–61.

Luu, N.T., Rainger, G.E. & Nash, G.B., 2000. Differential ability of exogenous chemotactic agents to disrupt transendothelial migration of flowing neutrophils. *Journal of Immunology*, 164(11), pp.5961–9.

Luu, N.T., Rainger, G.E. & Nash, G.B., 1999. Kinetics of the different steps during neutrophil migration through cultured endothelial monolayers treated with tumour necrosis factor-alpha. *Journal of Vascular Research*, 36(6), pp.477–85.

Marmon, S., Hinchey, J., *et al*., 2009. Caveolin-1 expression determines the route of neutrophil extravasation through skin microvasculature. *The American Journal of Pathology*, 174(2), pp.684–92.

Marmon, S., Cammer, M., *et al*., 2009. Transcellular migration of neutrophils is a quantitatively significant pathway across dermal microvascular endothelial cells. *Experimental Dermatology*, 18(1), pp.88–90.

Mayadas, T.N. *et al*., 1993. Leukocyte rolling and extravasation are severely compromised in P selectin-deficient mice. *Cell*, 74(3), pp.541–54.

McGettrick, H.M. *et al*., 2009. Fibroblasts from different sites may promote or inhibit recruitment of flowing lymphocytes by endothelial cells. *European Journal of Immunology*, 39(1), pp.113–25.

McGettrick, H.M. *et al*., 2012. Tissue stroma as a regulator of leukocyte recruitment in inflammation. *Journal of Leukocyte Biology*, 91(3), pp.385–400.

McGettrick, H.M., Butler, L.M. & Nash, G.B., 2007. *Methods in Molecular Biology, vol. 370: Adhesion Protein Protocols* Second. A. S. Coutts, ed., Totowa, New Jersey: Humana Press Inc.

Nabah, Y.N.A. *et al*., 2004. Angiotensin II induces neutrophil accumulation in vivo through generation and release of CXC chemokines. *Circulation*, 110(23), pp.3581–3586.

Nash, G.B., Buckley, C.D. & Ed Rainger, G., 2004. The local physicochemical environment conditions the proinflammatory response of endothelial cells and thus modulates leukocyte recruitment. *FEBS letters*, 569(1-3), pp.13–17.

Parsonage, G. *et al*., 2003. Global gene expression profiles in fibroblasts from synovial, skin and lymphoid tissue reveals distinct cytokine and chemokine expression patterns. *Thrombosis and Haemostasis*, 90(4), pp.688–97.

Phillipson, M. *et al*., 2006. Intraluminal crawling of neutrophils to emigration sites: a molecularly distinct process from adhesion in the recruitment cascade. *The Journal of Experimental Medicine*, 203(12), pp.2569–75.

Prasanna, S.J. *et al*., 2010. Pro-inflammatory cytokines, IFNgamma and TNFalpha, influence immune properties of human bone marrow and Wharton jelly mesenchymal stem cells differentially. *PloS One*, 5(2), p.e9016.

Prockop, D.J., 2009. Repair of tissues by adult stem/progenitor cells (MSCs): controversies, myths, and changing paradigms. *Molecular Therapy: the journal of the American Society of Gene Therapy*, 17(6), pp.939–46.

Raffaghello, L. *et al*., 2008. Human mesenchymal stem cells inhibit neutrophil apoptosis: a model for neutrophil preservation in the bone marrow niche. *Stem Cells*, 26(1), pp.151–62.

Ren, G. *et al*., 2008. Mesenchymal stem cell-mediated immunosuppression occurs via concerted action of chemokines and nitric oxide. *Cell Stem Cell*, 2(2), pp.141–50.

Saalbach, A., Haustein, U.F. & Anderegg, U., 2000. A ligand of human thy-1 is localized on polymorphonuclear leukocytes and monocytes and mediates the binding to activated thy-1-positive microvascular endothelial cells and fibroblasts. *The Journal of Investigative Dermatology*, 115(5), pp.882–8.

Sanz, M.-J. & Kubes, P., 2012. Neutrophil-active chemokines in in vivo imaging of neutrophil trafficking. *European Journal of Immunology*, 42(2), pp.278–83.

Schenkel, A.R., Chew, T.W. & Muller, W.A., 2004. Platelet endothelial cell adhesion molecule deficiency or blockade significantly reduces leukocyte emigration in a majority of mouse strains. *Journal of Immunology*, 173(10), pp.6403–8.

Schmitz, K. *et al*., 2011. Reoxygenation attenuates the adhesion of neutrophils to microvascular endothelial cells. *Angiology*, 62(2), pp.155–62.

Sheikh, S. *et al*., 2005. Differing mechanisms of leukocyte recruitment and sensitivity to conditioning by shear stress for endothelial cells treated with tumour necrosis factor-alpha or interleukin-1beta. *British Journal of Pharmacology*, 145(8), pp.1052–61.

Smith, E. *et al*., 2008. Duffy antigen receptor for chemokines and CXCL5 are essential for the recruitment of neutrophils in a multicellular model of rheumatoid arthritis synovium. *Arthritis and Rheumatism*, 58(7), pp.1968–73.

Springer, T.A., 1995. Traffic signals on endothelium for lymphocyte recirculation and leukocyte emigration. *Annual Review of Physiology*, 57, pp.827–72.

Sumagin, R. & Sarelius, I.H., 2010. Intercellular adhesion molecule-1 enrichment near tricellular endothelial junctions is preferentially associated with leukocyte transmigration and signals for reorganization of these junctions to accommodate leukocyte passage. *Journal of Immunology*, 184(9), pp.5242–52.

Tull, S.P. *et al*., 2009. Omega-3 fatty acids and inflammation: Novel interactions reveal a new step in neutrophil recruitment. *PLoS Biology*, 7(8).

Tyndall, A., 2014. Mesenchymal stem cell treatments in rheumatology-a glass half full? *Nature reviews. Rheumatology*, 10(2), pp.117–24.

Uccelli, A., Moretta, L. & Pistoia, V., 2008. Mesenchymal stem cells in health and disease. *Nature reviews. Immunology*, 8(9), pp.726–36.

Vora, M., Romero, L.I. & Karasek, M.A., 1996. Interleukin-10 Induces E-Selectin on Small and Large Blood Vessel Endothelial Cells. *The Journal of Experimental Medicine*, 184(9), pp.821–9.

Waterman, R.S. *et al*., 2010. A new mesenchymal stem cell (MSC) paradigm: polarization into a pro-inflammatory MSC1 or an immunosuppressive MSC2 phenotype. *PloS One*, 5(4), p.e10088.

Watkins, N.A. *et al*., 2009. A HaemAtlas: characterizing gene expression in differentiated human blood cells. *Blood*, 113(19), pp.e1–9.

Williams, M.R. *et al*., 2011. Emerging mechanisms of neutrophil recruitment across endothelium. *Trends in Immunology*, 32(10), pp.461–9.

Zarbock, A. & Ley, K., 2008. Mechanisms and consequences of neutrophil interaction with the endothelium. *The American Journal of Pathology*, 172(1), pp.1–7.